PRODUCTION OF NITRILE HYDROLYSING BIOCATALYSTS FROM *RHODOCOCCUS RHODOCHROUS*

by

Marushka Soobben

(1129969)

A dissertation

Submitted in fulfilment of the requirements for the degree

Master of Science

in

Molecular and Cell Biology

in the Faculty of Science, University of the Witwatersrand, Johannesburg, South Africa

Supervisor: Professor Karl Rumbold

Co-Supervisor: Professor Dean Brady

February 2020

DELCARATION

University of the Witwatersrand, Johannesburg

School of **MOLECULAR AND CELL BIOLOGY (MCB)**

SENATE PLAGIARISM POLICY

Declaration by Students

I **MARUSHKA SOOBBEN** (Student number: **1129969**) am a student registered for **MSC IN MICROBIOLOGY AND BIOTECHNOLOGY** in the year **2020**.

I hereby declare the following:

- I am aware that plagiarism (the use of someone else's work without their permission and/or without acknowledging the original source) is wrong.
- I confirm that ALL the work submitted for assessment for the above course is my own unaided work except where I have explicitly indicated otherwise.
- I have followed the required conventions in referencing the thoughts and ideas of others.
- I understand that the University of the Witwatersrand may take disciplinary action against me if there is a belief that this is not my own unaided work or that I have failed to acknowledge the source of the ideas or words in my writing.

Signature: 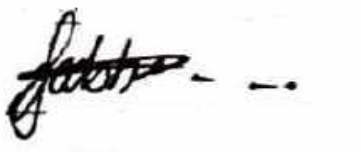

Date: _____17 August 2020_____

ABSTRACT

Biocatalysis plays an important role in initiating environmentally-friendly processes during chemical synthesis. This involves the utilisation of enzymes from various biological systems during the synthesis of chemicals. The use of biocatalysts provides a sustainable alternative to metal catalysts when manufacturing pharmaceuticals and chemicals. Members of the genus *Rhodococcus* have been found to host many enzymes that can be utilised in biocatalysis due to their highly diverse physiological and metabolic functions. *Rhodococcus rhodochrous* is able to code for both a nitrilase and a nitrile hydratase which are necessary for the bioconversion of nitriles to carboxylic acids. Here, dimethylformamide successfully induced nitrilases from *R. rhodochrous* A29, A99 and ATCC BAA-870. These strains were cultured using a benchtop bioreactor. Benzonitrile was used as a substrate for an activity assay where benzoic acid was successfully produced. This was shown by using TLC, FT-IR and NMR spectroscopy. Next, *Escherichia coli* BL21 (DE3) containing two plasmids encoding a cobalt nitrile hydratase from *R. rhodochrous* ATCC BAA-870 was cultured in a bioreactor and induced with IPTG. Protein quantification showed an increase in total cellular proteins after induction. Benzamide was successfully produced by using benzonitrile as the substrate during an activity assay indicating successful heterologous expression of a nitrile hydratase. In addition, 100 % conversion rate was observed with a minimum of 32 U of enzyme activity for both enzymes. In future, the process whereby these enzymes are produced should be optimised and various substrates should be tested to determine the substrate specificity of nitrile hydrolysing enzymes from these strains.

ACKNOWLEDGEMENTS

To begin, I would like to thank my supervisor **Professor Karl Rumbold** for introducing me to the world of biocatalysis and for granting me an opportunity to be a part of his lab and to contribute the field.

I would like to thank my co-supervisor **Professor Dean Brady** for assisting me in every aspect of my project and for the constant guidance whenever it was required.

A special thanks goes to **my family** for their love, encouragement and their financial support throughout.

I express my deepest thanks to **Rishelan Naidu** for the endless love and support, keeping me company during late nights in the lab and for the constant faith my in abilities whenever I was doubtful.

I am grateful to **Mudzuli Maphupha** for the constant help regarding organic chemistry, the late night questions and for the new found friendship that made my year more enjoyable.

I am also grateful for **Lindelo Mguni** for the his support throughout, the late night questions, never hesitating to help me in the lab when necessary and for always being there to calm me and aid me when stressful situations arose.

Thank you to **Refilwe Moepya** and **Thapelo Mbhele** for helping me run HPLC-MS/MS.

Thank you to the **Wits Postgraduate Merit Award** for the for the financial aid.

Lastly, thank you to Wits School of Molecular and Cell Biology as well as Wits School of Chemistry for granting me the opportunity to work in their labs.

TABLE OF CONTENTS

LIST OF ABBREVIATIONS AND ACRONYMS

AIDS: Acquired Immunodeficiency Syndrome

Ar: Aromatic

B-PER: Bacterial Protein Extraction Reagent

cDNA: Complementary Deoxyribonucleic Acid

DMF: Dimethylformamide

DMSO: Dimethyl Sulfoxide

DNA: Deoxyribonucleic Acid

ESI: Electrospray Ionisation

FSH: Follicle-Stimulating Hormone

FT-IR: Fourier-Transform Infrared

HCl: Hydrochloric Acid

HDL: High-Density Lipoprotein

His: Histidine

HIV: Human Immunodeficiency Virus

HPLC: High-Performance Liquid Chromatography

HRMS: High Resolution Mass Spectroscopy

IPTG: Isopropyl β-D-1-thiogalactopyranoside

J: Coupling Constant

lac: Lactose

LDL: Low-Density Lipoprotein

LH: Luteinizing Hormone

Luria Bertani: LB

MCS: Multiple Cloning Sites

mRNA: Messenger Ribonucleic Acid

Mp: Melting point

MS: Mass Spectroscopy

MSG: Monosodium Glutamate

NHase: Nitrile Hydratase

NMR: Nuclear Magnetic Resonance

OD: Optical Density

PCR: Polymerase Chain Reaction

R_f: Retention Factor

RNA: Ribonucleic Acid

Rpm: Revolutions Per Minute

TCE: Trichloroethene

TLC: Thin-Layer Chromatography

TMG: Thiomethyl Galactosidase

trp: Tryptophan

TSA: Tryptone Soy Agar

TSB: Tryptone Soy Broth

UV: Ultraviolet

LIST OF CHEMICAL FORMULAE

Acetamide: C_2H_5NO

Acetic Acid: CH_3COOH

Acrylamide: C_3H_5NO

Acrylic Acid: $C_3H_4O_2$

Benzamide: C_7H_7NO

Benzoic Acid: $C_7H_6O_2$

Benzonitrile: C_7H_5N

Chloroform: $CDCl_3$

Cobalt Chloride: $CoCl_2$

Dipotassium Phosphate: K_2HPO_4

Ethylene Cyanohydrin: C_3H_5NO

Hydrochloric Acid: HCl

Magnesium Sulphate: $MgSO_4$

Monopotassium Phosphate: KH_2PO_4

Nicotinamide: $C_6H_6N_2O$

Nicotinic Acid: $C_6H_5NO_2$

Nitrilotrispropionamide: $C_9H_{18}N_4O_3$

Sodium Benzoate: C_6H_5COONa

Sodium Chloride: NaCl

Sodium Hydroxide: NaOH

LIST OF FIGURES

LIST OF SCHEMES

LIST OF TABLES

CHAPTER 1:

LITERATURE REVIEW

1.1 BIOCATALYSIS

There is an increasing inclination towards the utilisation of environmentally friendly and sustainable processes driven by current economical and sustainability concerns (De Regil & Sandoval, 2013; Truppo, 2017). However, both pharmaceutical and industrial sectors currently rely on traditional synthetic methods. This requires metal catalysts that are costly to obtain and unsustainable (Turner & Truppo, 2013). For example, the metal catalyst rhodium is highly useful in asymmetrical transformations but is costly and unsustainable due to its scarcity (Truppo, 2017). Therefore, green chemistry attempts to reduce the environmental impact caused by the synthesis and application of chemicals (Saleh & Koller, 2018).

Biocatalysis comprises of the utilisation of enzymes from various biological systems in order for chemicals to be synthesised (Turner & Truppo, 2013). These enzymes can be used for reactions in various forms such as native whole cells, recombinant cells and isolated enzymes. This is determined by the process or enzyme required (Truppo, 2017). Currently, biocatalysis is a substantial part of environmentally-friendly production of chemicals, pharmaceuticals, food preservatives and cosmetics (De Regil & Sandoval, 2013).

Environmental and economic advantages are present when converting chemocatalytic processes into biocatalytic methods. Firstly, enzymes have the ability to biodegrade. Secondly, they are produced using low-cost renewable resources. Thirdly, a large supply of the enzyme can be produced and stored (De Regil & Sandoval, 2013). However, certain limitations need to be conquered before relying solely on biocatalysts. These include low reaction yields when placed in a non-aqueous environment, high enzyme selectivity, inhibition of products and substrates as well as instability, by denaturing, *in vitro* when faced with an extreme pH or high temperatures (Glazer & Nikaido, 2007; Kaul & Asano, 2012). However, there are several approaches in place to tackle these issues such as protein and genetic engineering, chemical modifications and the use of enzymes from extremophiles enabling them to survive in extreme conditions (De Carvalho, 2017; Osbon & Kumar, 2019). Therefore, the research of biological

enzymes is pivotal in order to comprehend their potential applications and abilities. Enzymes proven to have potential value in chemical synthesis are important in the industrial sector and have to be studied when devising appropriate production systems and formulations to ensure optimal processes are employed while pursuing environmentally friendly initiatives (Heinrich *et al.*, 2002). Furthermore, systems to mass-produce both whole cells and isolated enzymes are required to commercialise biocatalysts with economic potential (Lin & Tao, 2017).

1.2 BIOREACTORS

Up-scaling certain processes and biomass for microbial cultures, has become important over the years in order to meet global demands. For instance, when Fleming (1929) discovered penicillin from the *Penicillium* fungus, the need for this antibiotic was high in demand in the pharmaceutical industry. In order to meet these demands, large scale production was undertaken in a bioreactor (Mandenius, 2016). In addition, up-scaling enzyme production in the industrial sector is both financially and commercially beneficial (Crater & Lievense, 2018).

Bioreactors, also known as fermenters, are used to create a biosphere to maintain an optimum biological environment for an array of microbial growth or processes that produce commercial products, such as ethanol and penicillin (Obom *et al.*, 2013). Bioreactors have innovative methods of dealing with factors that affect microbial growth compared to the shake flask system. Bioreactors are able to maintain precise temperature and pH of microbial cultures whereas shake flasks are incapable due to incubators having a range of ~ 5 ºC from the set temperature (Obom *et al.*, 2013).

In a bioreactor, the cooling jacket (Fig. 1.1) provides temperature control when the culture overheats or cools down. The temperature inside the culture is measured with a temperature probe to ensure the appropriate temperature is controlled between ~ 0.1 ºC from the intended setpoint. The pH is an essential factor in microbial growth, shake flasks run the risk of pH changes depending on the acidity or basic levels of their products from their metabolic pathways (Obom *et al.*, 2013). Bioreactors are attached to acid and base reservoirs where when a change in pH is detected by the pH probe, the bioreactor will add either acid or base to maintain the intended pH. In a shake flask, the oxygen uptake and gas exchange are limited whereas a bioreactor has a polarographic probe where the oxygen levels are monitored and adjusted when necessary, by either pumping sterile air into the culture via the sparger (Fig. 1.1) or by increasing the speed of the impeller (Obom *et al.*, 2013). However, if the impeller is too

fast, the cells can be damaged due to the force of the blades. This system has a vast number of benefits compared to the shake flask method. Therefore, a large biomass of microbial cultures as well as a high yield of proteins can be obtained when using a bioreactor for microbial growth and enzyme production.

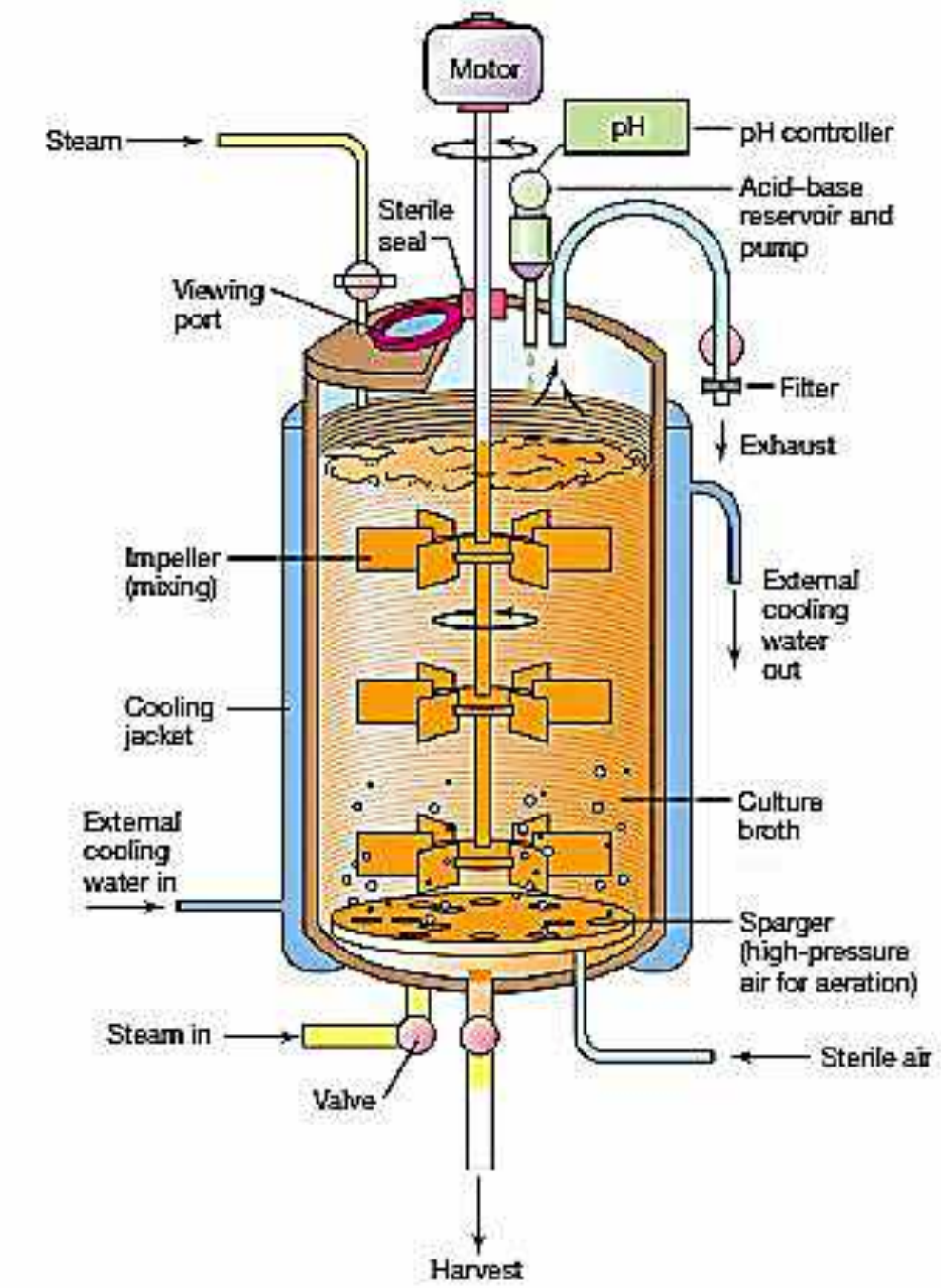

Figure 1.1: Industrial Aerobic Bioreactor. An internal view of the construction of a general industrial aerobic bioreactor (Madigan & Martinko, 2006).

1.3 RHODOCOCCUS

Species belonging to the *Rhodococcus* genus are exceedingly valuable in the industrial, clinical and environmental fields as they are highly diverse, both genetically and physiologically. Zopf first introduced the genus *Rhodococcus* belonging to the Norcardiaceae family in 1891. These obligate anaerobes are Gram-positive, catalase-positive, oxidase-negative and partially acid-fast bacteria (Goodfellow & Alderson, 1977). They are incapable of forming endospores and are non-motile due to their lack of flagella (Majidzadeh & Fatahi-Bafghi, 2018). However, pili can be found in small numbers (Yanagawa & Honda, 1976). When cultured, a salmon-pink or red pigment is observed, caused by carotenoids, accompanied by filamentous branching coccobacilli (Zopf, 1891; Takaichi *et al.*, 1989; Finnerty, 1992). Moreover, DNA of this genus is found to be rich in guanine and cytosine thereby increasing their DNA stability (Alvarez, 2019). *Rhodococcus* can be isolated from diverse environmental niches such as soil, plants, the blood of *Rhodococcus*-infected and *Rhodococcus*-exposed healthy animals, marine sediments and within insects (Larkin *et al.*, 2006). The larger portion of *Rhodococcus* species is known to be harmless. However, some species are able to cause infections by presenting pathogenic properties to some plants and animals. For example, the leafy-gall disease in plants caused by *Rhodococcus fascians* and pneumonia in foals caused by *Rhodococcus equi* (Busch *et al.*, 2019).

Rhodococcus spp. are exceedingly versatile in their metabolic pathways and functions which increases their biocatalytic potential (Chen *et al.*, 2013). Chen and co-workers (2013) discovered that *R. rhodochrous* ATCC 17895 hosts a full nitrile degradation operon which comprises of nitrile hydratase, amidase, aldoxime dehydratase and the necessary regulators. A total of 27 distinct monooxygenases and dioxygenases, 10 phosphatases and two ureases have also been found. However, the ability of *R. rhodochrous* to produce nitrile degradation enzymes, such as nitrilases or nitrile hydratases, is dependent on the media used (Nagasawa *et al.*, 1991b). In addition, for commercial purposes, isolation and extraction of the selected gene from *R. rhodochrous* and ligating it into a vector for expression in a heterologous host such as *Escherichia coli* can produce considerable amounts of an isolated enzyme which has the potential for commercial value in the chemical, pharmaceutical and environmental industries (Fakruddin *et al.*, 2012; Rosano & Ceccarelli, 2014).

1.3.1 Environmental Applications

Bioremediation requires micro-organisms to aid in the clean-up of environmental pollutants. Members of the genus *Rhodococcus* play a large role in the degradation of certain hazardous pollutants. *Rhodococcus corallinus* B-276 is able to degrade the highly volatile, hazardous, industrial solvent trichloroethene (TCE) (Saeki *et al.*, 1999). This solvent is used in a variety of applications and is known to contaminate aquifers. *Rhodococcus corallinus* B-276 degrades TCE when induced with propene, by forcing the bacteria to solely use propene as a carbon and energy source; this induces the alkene mono-oxygenase gene which catalyses the oxidation of TCE (Saeki *et al.*, 1999). In order to confirm that the alkene mono-oxygenase gene catalyses the reaction, Saeki and co-workers (1999) used heterologous protein expression. This resulted in transformed *E. coli* exhibiting the same degradation of TCE as *R. corallinus* B-276.

The contamination of soil and aquifers by petroleum hydrocarbons needs to be remediated as they are toxic to organisms (Namkoong *et al.*, 2002). Hydrocarbon contaminated sites are common due to oil spillages and the emission of oily waste (Kis *et al.*, 2017). Contaminated sites will usually contain bacterial strains that are able to metabolise these hydrocarbons (Kis *et al.*, 2017). However, since hydrocarbons are insoluble in water, many micro-organisms do not possess the required pathway for metabolising this pollutant. Kis and co-workers (2017) discovered that *Rhodococcus* sp. MK1, isolated from an industrially contaminated site, is capable of degrading diesel oil components. Inadequate information is available about the exact pathways present in *Rhodococcus* sp. However, there are possibly several enzymes responsible for the degradation of these aliphatic and aromatic compounds (Kis *et al.*, 2017).

Haloalkanes are pollutants of aquifers and ecosystems in the biosphere. The degradation of haloalkanes requires the carbon – halogen bond to be cleaved (Curragh *et al.*, 1994). There are three methods in which this can occur: 1) Oxidative dehalogenation where the reaction is catalysed by monooxygenases resulting in gem-halohydrins or halogenated epoxides (Curragh *et al.*, 1994). This will then decompose into aldehydes whereby a halide ion is released. 2) Reductive dehalogenation methanogenic, sulphate reducing and denitrifying bacteria. 3) Hydrolytic dehalogenation which forms an alcohol and releases a halide ion. Curragh and co-workers (1994) found that *R. rhodochrous* NCIMB 13064 isolated from an industrial site, is able to activate several pathways to use 1-haloalkanes as a carbon source. This bacteria codes for a type of dehalogenase enzyme which converts long-chain haloalkanes into lipids, thereby

removing the pollutant from the affected soil. This shows the importance of the *Rhodococcus* species in bioremediation.

1.3.2 Industrial Applications

Rhodococcus species show great value in synthesising compounds important to the industry as well as pharmaceuticals. For instance, *Rhodococcus* sp. 124 is able to use three independent enzymatic pathways in order to oxygenate indene which is used in the production of pharmaceutical drugs and industrial products (Chartrain *et al.*, 1998; Buckland *et al.*, 1999). First, naphthalene is used to induce a mono-oxygenase enzyme to allow an epoxide derivative of indene to be produced, which is resolved to *cis*-(1*S*, 2*R*)-indandiol or *trans*-(1*R*, 2*R*)-indandiol (Chartrain *et al.*, 1998). Secondly, naphthalene also induces a dioxygenase enzyme that produces *cis*-(1*R*, 2*S*)-indandiol (Chartrain *et al.*, 1998). Thirdly, toluene is added and induces dioxygenase which produces the *cis*-(1*S*, 2*R*) enantiomer (Chartrain *et al.*, 1998). This is possible due to the array of oxygenases present in the *Rhodococcus* species, that are able to catalyse a stereoselective reaction wherein oxygen is incorporated into hydrocarbons. *Rhodococcus* sp. I24 enzymes are able to oxygenate indene to form indandiols which is utilised in the production of the drug indinavir used as a protease inhibitor in the treatment of HIV/AIDS (Buckland *et al.*, 1999). Therefore, *Rhodococcus* sp. I24 is highly beneficial to chemical synthesis in the pharmaceutical industry.

Another useful group of enzymes produced by members of the genus *Rhodococcus* is epoxide hydrolase. These enzymes catalyse the hydrolysis of epoxides which are highly reactive (Van der Werf *et al.*, 1998). The ability to degrade epoxides is crucial for organisms, as epoxides are carcinogenic, mutagenic and toxic to living cells (Van der Werf *et al.*, 1998). Epoxide hydrolases are currently able to perform three essential functions in biological systems (Swaving & de Bont, 1998). First, in bacteria, they are able to degrade hydrocarbons. Second, in mammals, they are involved in detoxifying the body from epoxides formed during P450 dependent mono-oxygenase pathways (Armstrong, 1987). Third, they are able to synthesise hormones in plants and insects, for example: leukotrienes which aid in immune reactions and juvenile hormones which ensure the growth of larvae (Samuelsson & Funk, 1989; Czarnetzk *et al.*, 1990; Touhara & Prestwich, 1993). Van der Werf and co-workers (1998) showed that *R. erythropolis* DCL14 has the ability to utilise limonene as the sole carbon source which resulted in the induction of limonene-1,2-epoxide hydrolase. This enzyme then converts limonene-1,2-

epoxide to limonene-1,2-diol epoxide hydrolase. This gives additional value to *Rhodococcus* species in biocatalysis.

A highly sought-after group of enzymes are those which possess the ability to hydrolyse nitriles, such as nitrilases, amidases and nitrile hydratases. They are exceedingly valuable in the industry for their ability to convert nitriles to their corresponding amides and carboxylic acids. Several *Rhodococcus* strains are able to encode either one or all of these enzymes, such as *R. rhodochrous* J1, *R. rhodochrous* ATCC BAA-870, *R. erythropolis* 3843 *R. rhodochrous* tg1-A6 *R. ruber* NCIMB 40757 *R. rhodochrous* PA-34 *Rhodococcus* sp. NDB 1165 (Busch *et al.*, 2019). The bioconversion of nitriles allows for the synthesis of products such as acrylamide, nicotinamide, acrylic acid and nicotinic acid (Busch *et al.*, 2019).

The first generation of acrylamide production in industry started in 1985, which utilised *Rhodococcus* sp. N-774 (Watanabe *et al.*, 1987a; Watanabe *et al.*, 1987b). This was then replaced by *Pseudomonas chlororaphis* B23 during the second generation approach (Nagasawa & Yamada, 1989; Nagasawa *et al.*, 1989). This change brought about an improvement in acrylamide productivity. However, the co-factor of both these bacterial strains used ferric ions which were found to be less efficient when compared to a strain encoding nitrile hydratase with a non-corrinoid cobalt (III) centre at the active site (Nagasawa *et al.*, 1986; Sugiura *et al.*, 1987; Endo & Watanabe, 1989). This cobalt nitrile hydratase was discovered in *R. rhodochrous* J1 and produced optimum results when induced with urea and supplemented with cobalt ions (Nagasawa *et al.*, 1988a; Nagasawa *et al.*, 1991a). This resulted in *R. rhodochrous* J1 becoming the most efficient producer of acrylamide compared to other acrylamide-forming bacterial strains. This represents the third-generation process where Nagasawa and co-workers (1993) discovered that *R. rhodochrous* J1 produced a more heat-stable nitrile hydratase which is able to tolerate higher concentrations of acrylonitrile and acrylamide compared to nitrile hydratase from *P. chlororaphis* B23 and *Brevibacterium* R312. *R. rhodochrous* J1 is highly tolerant and was able to catalyse the breakdown of acetonitrile even when 50 % (*w/v*) of acrylamide was present (Nagasawa *et al.*, 1993). Various temperatures were evaluated during bioconversion and a 6 % level of acrylonitrile was continuously fed for 10 hours. The total acrylamide present was 65.6 % (*w/v*) at 10 ºC, 56.7 % (*w/v*) at 15 ºC and 56.0 (*w/v*) at 20 ºC. This portrays a highly stable enzyme that is able to continue converting acrylonitrile in high concentrations of acrylamide. Therefore, high yields can be manufactured at an optimal rate. The production of

nitrile hydrolysing enzymes increases the biocatalytic potential of the *Rhodococcus* genus in the pharmaceutical and industrial sectors.

1.4 NITRILE HYDROLYSING ENZYMES

Nitriles are widespread in the environment where many various plants have the ability to produce them (Howden & Preston, 2009). Since a cyano (CN) functional group is present in nitriles, they are considered to host toxic properties (Yamada & Kobayashi, 1996). Nonetheless, various bacteria and fungi are able to degrade nitriles (Kobayashi *et al.*, 1992). During nitrile degradation, micro-organisms that encode nitrilases convert nitriles to their corresponding carboxylic acids (Scheme 1.1) (Yamada & Kobayashi, 1996). By contrast, micro-organisms that encode nitrile hydratases will convert nitriles to their corresponding amides (Asano *et al.*, 1982). Amidases are responsible for degrading the resultant amide into the corresponding carboxylic acid (Scheme 1.1) (Asano *et al.*, 1982).

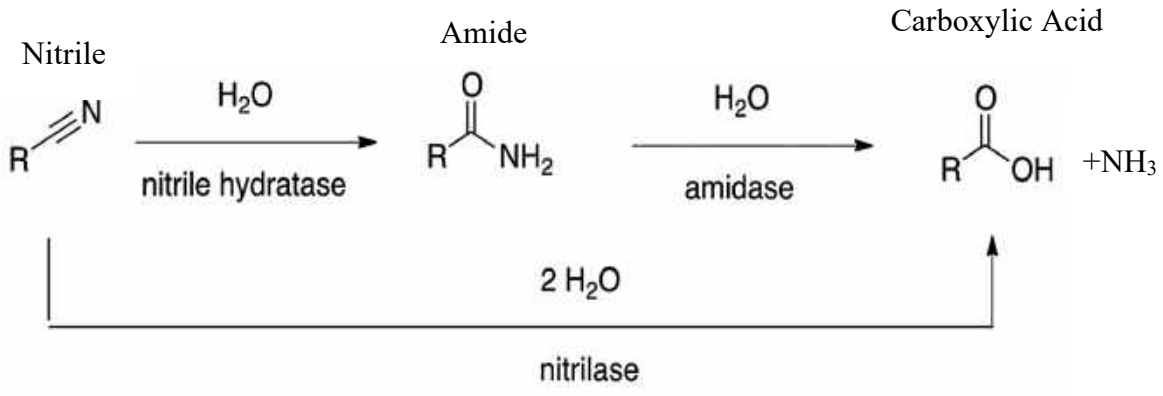

Scheme 1.1: Nitrile Degradation Pathways. At the top: Nitriles are hydrolysed by enzymes a two-step pathway whereby a nitrile hydratase hydrolyses the nitrile into its corresponding amide. This amide is then hydrolysed, by an amidase, into its corresponding carboxylic acid with the release of ammonia. **At the bottom**: The single reaction whereby nitriles are hydrolysed directly into their carboxylic acid derivatives by a nitrilase enzyme. Ammonia is released during this pathway. (Adapted from Angelini *et al.*, 2015).

1.4.1 Nitrilases

Nitrilases are thiol enzymes belonging to the first branch of its superfamily called nitrilase and can be located in many plants, animals, yeasts and prokaryotes (Pace & Brenner, 2001. These enzymes are utilised as biocatalysts for the production of carboxylic acids such as acrylic acid and nicotinic acid. Thimann and Mahadevan (1964) were the first to describe the nitrilase

enzyme mechanism. After extraction and isolation from the leaves of barley, the enzyme was tested on 27 different nitriles which were all converted to their corresponding carboxylic acid (Thimann & Mahadevan, 1964). This was due to a nucleophilic attack by a thiol group, on the nitrile carbon within the active site of the nitrilase enzyme resulting in thioimidate. Subsequently, hydrolysis of thioimidate occurs to form a thioester with the release of ammonia, after which, the acyl-enzyme is hydrolysed forming a carboxylic acid (Thimann & Mahadevan, 1964).

Soil isolated *Pseudomonas* sp. was the first bacterium from which a nitrilase was isolated and purified. This enzyme was induced by solely using ricinine (N-methyl-3-cyano-4-methoxy-2-pyridone) as a carbon source (Hook & Robinson, 1964; Robinson & Hook, 1964). Over 23 organisms, including bacteria, fungi, yeasts and plants have well-characterised nitrilase activity (O'Reilly & Turner, 2003). A single polypeptide with a size range of 25 – 45 kDa is the most general characteristic for the majority of nitrilases (O'Reilly & Turner, 2003). In addition, nitrilases have a catalytic triad of amino acid residues, namely glutamate-lysine-cysteine with the enzymes representing a α-β-β-α sandwich fold (Pace *et al.*, 2000). This is a highly conserved motif that is present in a majority of members belonging to the nitrilase family (Pace & Brenner, 2001).

1.4.1.1 Factors Affecting Nitrilase Activity

The activity and formation of these enzymes are dependent on its environment, such as the inducer, metal ions present, pH, carbon source, temperature, nitrogen source in the culture and bioconversion conditions (Gong, *et al.*, 2012). For *Rhodococcus* species, the best nitrogen sources in the culture medium are yeast extract, casamino acid and peptone; while the best carbon sources are: starch, glucose, mannitol and sodium acetate (Gong, *et al.*, 2012). Metal ions are not essential as a co-factor for nitrilase activity (Nagasawa *et al.*, 1988a). Nitrilases can be induced using a wide variety of nitriles, amides, carboxylic acids as well as their analogues (Gong, *et al.*, 2012). For example, in order to induce the nitrilase gene from *R. rhodochrous* J1, ε-Caprolactam was used and proved to be a potent inducer in many rhodococcal strains (Prasad *et al.*, 2007).

During bioconversion, it is vital that the most favourable conditions are maintained to ensure optimal nitrilase activity and preservation of the enzymatic structure. For most organisms hosting a nitrilase gene, a pH between 7.0 – 8.0 and a temperature between 30 ºC – 55 ºC should

be maintained (Gong, *et al.*, 2012). Enzyme modifiers have a potent effect on the activity of nitrilases, especially thiol-binding reagents. These affect the thiol-containing cysteine residue, which has a pivotal role in the catalytic activity of nitrilases (Gong, *et al.*, 2012). Examples of these reagents are copper (Cu^{2+}), silver (Ag^{+}), mercury (Hg^{2+}), 2-nitrobenzoic acid, iodoacetamide and iodoacetic acid (Gong, *et al.*, 2012). Carbonyl reagents did not affect the nitrilase from *R. rhodochrous* PA-34 but had an inhibitory effect on the *R. rhodochrous* J1 nitrilase (Bhalla *et al.*, 1992; Kobayashi *et al.*, 1989).

During the biotransformation process, a high concentration of nitriles as substrates exhibit inhibitory effects on nitrilase enzymes (Yamada & Kobayashi, 1996). However, a high concentration of the substrate in the medium can also enhance the reaction rate (Costes *et al.*, 2001). Furthermore, organic solvents are used during a reaction in order to increase the solubility of products or substrates such as nitriles(Gong, *et al.*, 2012). These solvents can also have a positive or negative effect on the catalytic activity of nitrilases. For example, methanol was found to increase the rate of the reaction with a nitrilase from *Synechocystis* sp. PCC6803 (Heinemann *et al.*, 2003). However, high concentrations of organic solvents can suppress conversion activity (Bauer *et al.*, 1999). Therefore, it is important to ensure that all the factors are optimal when using nitrilases for catalytic reactions. Furthermore, it is essential to take into account from which organism the enzyme was derived (Yamada & Kobayashi, 1996).

1.4.2 Nitrile Hydratases

Nitrile hydratases are metalloenzymes utilised in biocatalytic processes for the production of amides as well as in bioremediation for the removal of toxic nitriles from waste streams (Huang *et al.*, 1997). Asano and co-workers (1982) were the first to isolate a nitrile hydratase from *Arthrobacter* sp. J1, which was later recognised as *R. rhodochrous* J1 by Kato and co-workers (2000). Nitrile hydratases can be isolated from bacteria in the phyla, Cyanobacteria, Proteobacteria, Firmicutes and Actinobacteria as well as a few yeasts and moulds (Prasad & Bhalla, 2009). However, the eukaryotic choanoflagellate *Monosiga brevicollis* was found to possess a gene encoding a nitrile hydratase (Foerstner *et al.*, 2008).

Huang and co-workers (1997) were the first to determine the crystal structure of an iron-containing nitrile hydratase from *Rhodococcus* sp. R312. Bacterial nitrile hydratases fall into one of two groups (Yamada & Kobayashi, 1996). The first group comprises of iron-containing nitrile hydratases where the centre of the protein is a non-haem iron (III) at the active site which

provides them with a grey-green hue (Yamada & Kobayashi, 1996; Mascharak, 2002). The second group includes the cobalt-containing nitrile hydratases with a non-corrinoid cobalt(III) centre at the active site (Mascharak, 2002). The cobalt-containing nitrile hydratases have been found to be more robust and possess broader substrate specificity (Mascharak, 2002). These enzymes are comprised of an α and a β subunit existing as a heterodimer of αβ that is 46 kDa in size or a tetramer of $\alpha_2\beta_2$ that is 92 kDa in size whereby each αβ dimer is bound to one metal atom (Mascharak, 2002).

1.4.2.1 Factors Affecting Nitrile Hydratase Activity

Optimal conditions are required to culture bacteria, encoding nitrile hydratases in order for the enzyme to have optimal activity. A neutral pH range of 7.0 – 8.0 is required with a temperature ranging from 20 ºC – 35 ºC. The incubation time bacteria require to produce the highest amount of a nitrile hydratase, depends on the bacterial species. For instance, *R. rhodochrous* J1 takes 76 – 80 hours to produce optimum levels of the enzyme whereas *R. rhodochrous* NHB-2 requires 24 hours (Nagasawa *et al.*, 1988a; Sankhian *et al.*, 2003). Since bacteria produce a nitrile hydratase from the beginning of the exponential phase to the stationary phase, it is essential to understand the growth parameters of the bacteria being used to produce a nitrile hydratase and to adhere to its optimal parameters (Singh *et al.*, 2018).

The immobilisation of cells has an advantageous effect on the activity of nitrile hydratases as there is more stability in cells that are immobilised compared to free cells (Singh *et al.*, 2018). Furthermore, immobilised cells can be reused (Singh *et al.*, 2018). There are various processes to immobilise free cells, such as cross-linking, entrapment, adsorption and immobilisation of the cellular membrane (Singh *et al.*, 2018). The addition of specific metal ions such as Fe^{3+} or Co^{2+}, in the culture medium, is vital for the formation of nitrile hydratases (Prasad & Bhalla, 2010). Lavrov and co-workers (2019) discovered that the cobalt-containing nitrile hydratase promoter can be activated by nickel ions in several *Rhodococcus* strains. However, the presence of cobalt ions was essential for the production of the nitrile hydratase.

1.4.3 Industrial Applications

Organic compounds such as amides and carboxylic acids are essential in chemical synthesis and the pharmaceutical industry (Brady *et al.*, 2004). The conversion of nitriles can be used to

synthesise these compounds by utilising the hydrolysing biocatalytic properties of nitrile hydratases, amidases and nitrilases.

1.4.3.1 Products from the Hydrolysis of Acrylonitrile

The production of acrylamide (C_3H_5NO), from acrylonitrile (Scheme 1.2), is an important industrial process. Acrylamide is utilised in various processes such as the treatment of paper and the production of coagulators, adhesive, paper sizing, paint and soil conditioners (Yamada & Kobayashi, 1996). Traditionally, hydrolysis of acrylonitrile depended on copper salts to catalyse the reaction when forming acrylamide (Yamada & Kobayashi, 1996). This process was rendered as unnecessarily problematic as first, acrylic acid was formed at a higher rate compared to the rate of acrylamide. Second, polymerisation occurred at the double bond of the substrate and product. Lastly, the formation of nitrilotrispropionamide (3-[bis(3-amino-3-oxopropyl)amino] propanamide, $C_9H_{18}N_4O_3$) and ethylene cyanohydrin (3-hydroxypropanenitrile, C_3H_5NO) as by-products (Yamada & Kobayashi, 1996). Therefore, this increased the need to search for alternative catalysts such as nitrile hydratases encoded by micro-organisms. Members of the genus *Rhodococcus* encode nitrile hydratases which have the ability to synthesise acrylamide by hydrolysing acrylonitrile and additionally reducing the environmental risks posed by chemical synthesis. However, when using whole cells, a possible hinderance is the hydrolysis of acrylamide if an amidase gene is present, thereby resulting in low acrylamide yields (Yamada & Kobayashi, 1996).

The production of acrylic acid ($C_3H_4O_2$) from acrylonitrile (Scheme 1.2), is in demand in the industrial sector as it serves as an important substrate for the synthesis of acrylic esters (Tsukamoto *et al.*, 2008). These esters are pivotal for the production of textile products, resin, paper, adhesives and polyacrylic acid. A biocatalytic approach by Kamal and co-workers (2010) found that using both a pure form of a nitrilase from *Rhodococcus ruber* AKSH-8 as well as the whole cells acrylonitrile was hydrolysed directly to acrylic acid. In order to extract acrylic acid from the mixture, ethyl acetate extraction was performed (Kamal *et al.*, 2010). This provides acrylic acid which can be used in industrial processes.

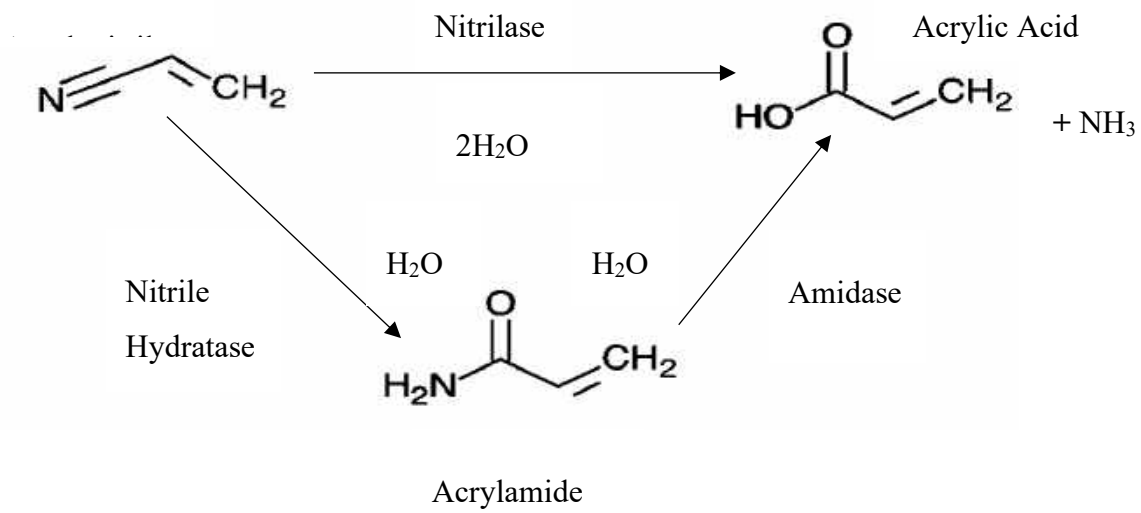

Scheme 1.2: Bioconversion of Acrylonitrile by Nitrile Hydrolyzing Enzymes. Acrylonitrile is converted to acrylic acid by a nitrilase. Acrylonitrile is then converted, by a nitrile hydratase, into acrylamide which can be subsequently converted to acrylic acid by an amidase.

1.4.3.2 Products from the Hydrolysis of 3-Cyanopyridine

Nicotinamide ($C_6H_6N_2O$), also known as niacinamide, is a variation of vitamin B_3 which is important in combatting the effects of neurodegenerative disorders, injury or strokes, by aiding in the protection of neurons and the central nervous system (CNS) (Fricker *et al.*, 2018). Nitrile hydratases can hydrolyse 3-cyanopyridine to form nicotinamide. Nagasawa and co-workers (1988b) were able to form nicotinamide by utilising a nitrile hydratase from *R. rhodochrous* J1 (Scheme 1.3). When resting *R. rhodochrous* J1 cells were utilised at optimum conditions, there was a 100% conversion of 3-cyanopyridine to nicotinamide with no conversion to nicotinic acid.

Nicotinic acid ($C_6H_5NO_2$) also known as Niacin, is a variation of vitamin B_3 much like nicotinamide. However, nicotinic acid is able to lower the level of all atherogenic lipoproteins (low-density lipoproteins) and raises the level of high-density lipoproteins (Carlson, 2005). This acid has great importance in the pharmaceutical industry where it is a powerful lipid-modifying drug and vitamin (Carlson, 2005). Meat and legumes are natural sources of nicotinic acid (Çatak, 2019). However, in order to biologically synthesise this acid, nitrilases or the two-step reaction can be used (Scheme 1.3). Mathew and co-workers (1988) successfully used *R. rhodochrous* J1 for the bioconversion of 3-cyanopyridine, using the nitrilase pathway, into nicotinic acid.

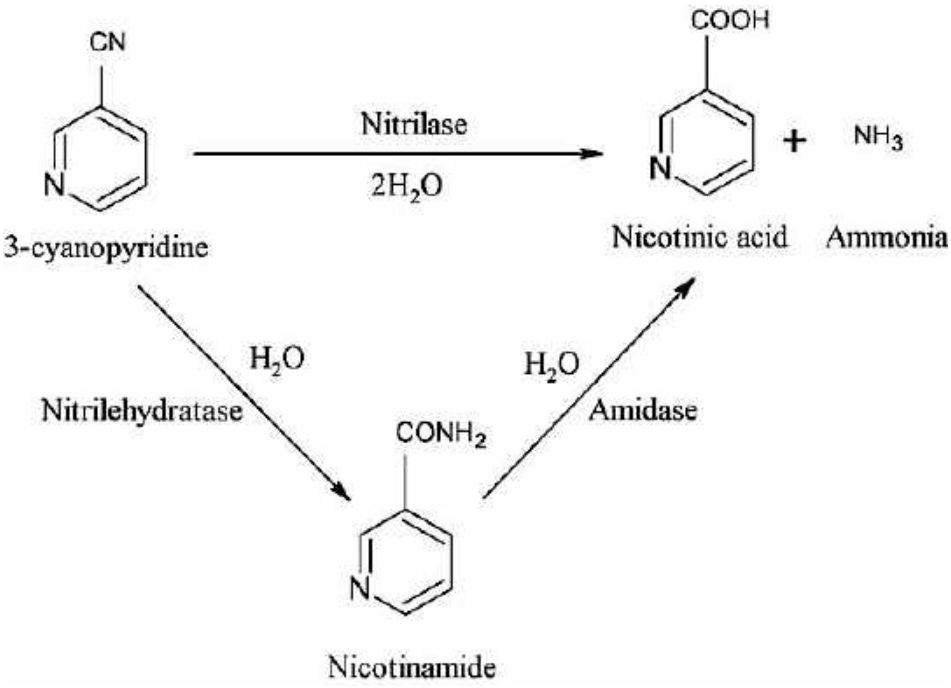

Scheme 1.3: Bioconversion of 3-Cyanopyridine by Nitrile Hydrolyzing Enzymes. 3-cyanopyridine is hydrolysed by a nitrilase forming nicotinic acid. 3-cyanopyridine is converted, by a nitrile hydratase, into nicotinamide which is then converted to nicotinic acid by an amidase (Sharma *et al.*, 2006).

1.4.3.3 Products from the Hydrolysis of Benzonitrile

Benzamide (C_7H_7NO) and its analogues are highly important in the medical field as they exhibit anti-microbial, pain-relieving, anti-inflammatory anti-depressant, anti-tumour and various other pharmacological activities (Asif, 2016). Hydrolysis of benzonitrile by nitrile hydratases produce benzamide (Scheme 1.4) which can be used to produce its analogues such as sulpiride, amisulpride, parsalmide and numerous others (Frederick *et al.*, 2006; Asif, 2016). Furthermore, these analogues are used as drugs to treat medical issues. *R. rhodochrous* ATCC BAA-870 exhibits a constitutive production of a nitrile hydratase that is capable of converting benzonitrile to benzamide without an inducer (Frederick *et al.*, 2006).

Benzoic acid ($C_7H_6O_2$) is produced in two ways when using biocatalytic enzymes (Scheme 1.4). It can be used in a multitude of different ways, for example, its antifungal and antimicrobial properties can be used in food preservatives, cosmetic, hygiene products, medicines such as topical and oral ointments (De Olmo *et al.*, 2017). However, it is mostly used in nylon production by producing phenol and caprolactam (De Olmo *et al.*, 2017). Therefore, it is crucial to produce this with the least amount of negative environmental effects. Nitrilase from *R. rhodochrous* J1 induced by isovaleronitrile displayed the ability to convert

benzonitrile without the formation of benzamide suggesting that the nitrile hydratase/amidase two-step pathway did not have a role in the formation of benzoic acid (Kobayashi *et al.*, 1989).

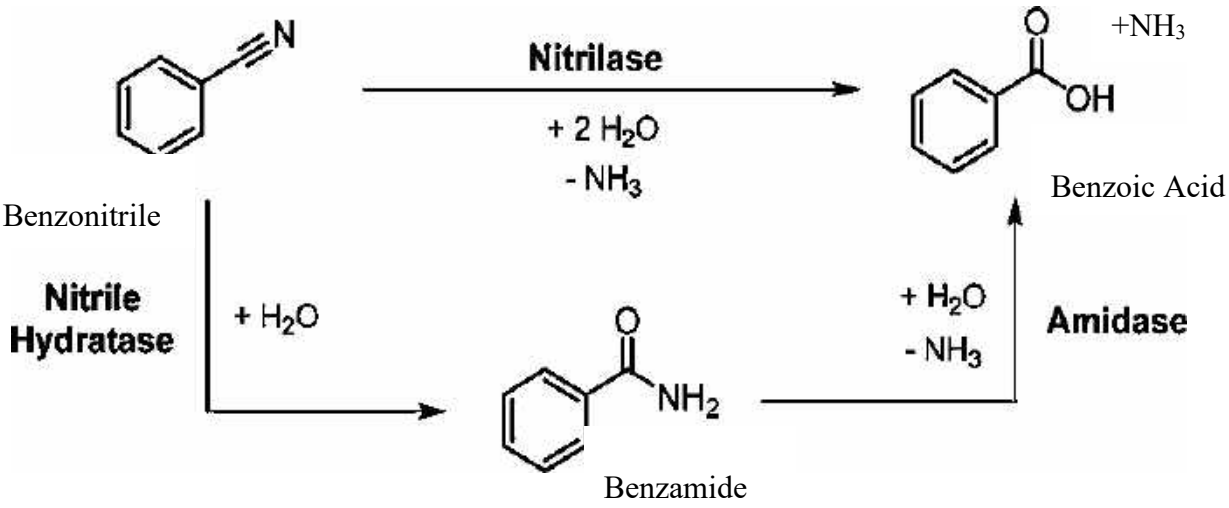

Scheme 1.4: Bioconversion of Benzonitrile by Nitrile Hydrolyzing Enzymes. Benzonitrile is hydrolysed to benzoic acid by a nitrilase. Benzonitrile is converted, by a nitrile hydratase, into benzamide which is subsequently converted to benzoic acid by an amidase. (Scheme modified from Fisk *et al.*, 2017).

1.5 HETEROLOGOUS PROTEIN EXPRESSION

The ability to express sufficient amounts of a protein from specific genes used to be costly process where difficulty in accessing the gene of interest and producing vast amounts of pure protein proved to be arduous (Devasahayam, 2007). The discovery of recombinant DNA technology helped remedy this process. Genes are able to be placed and expressed in cells where the gene is not naturally found. This process is termed heterologous gene expression (Fakruddin *et al.*, 2012). This process is exceedingly beneficial for pharmaceutical and industrial processes when producing isolated biocatalytic enzymes such as nitrilases and nitrile hydratases.

Generally, bacterial or yeast systems can be used to host a gene of interest from an organism by using specific restriction enzymes to extract the desired gene from the native cell (Hoseini & Sauer, 2015). Next, DNA ligase is used to insert the gene into the cloning vector thereby forming recombinant DNA (Fig. 1.2). Subsequently, bacterial cells, for example, *Escherichia coli*, are transformed to host the vector thereby forming competent bacteria (Fig. 1.2) (Hoseini & Sauer, 2015). This gene can then be regulated by a native or an inducible promotor (Rosano & Ceccarelli, 2014). Afterwards, the desired gene will be expressed by using the new host's

cellular machinery (Rosano & Ceccarelli, 2014). In order to mass-produce the desired protein, competent bacteria can be cultured in a bioreactor and induced if necessary (Crater & Lievense, 2018).

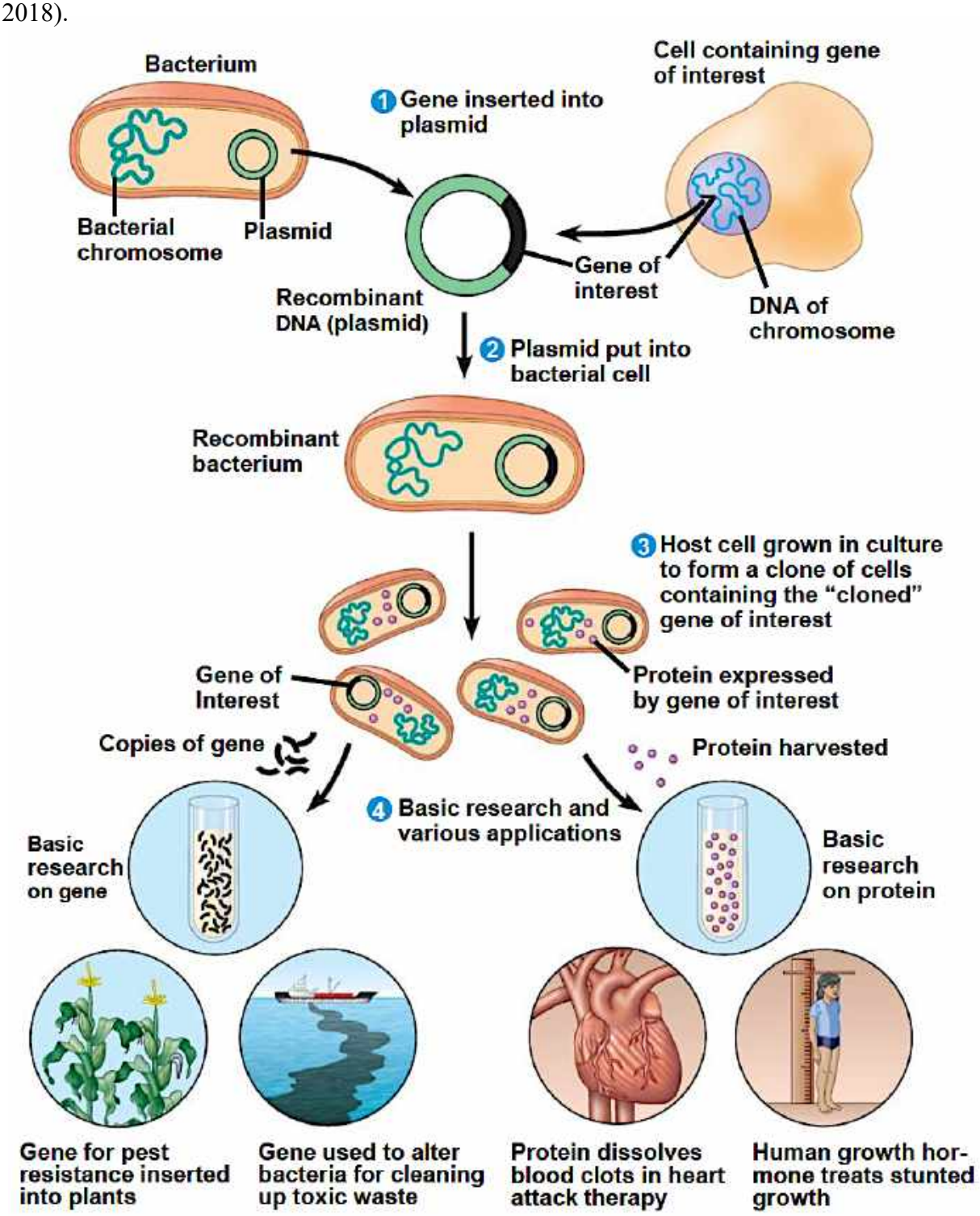

Figure 1.2: Introduction of a Selected Foreign Gene into a Bacterial Cell. Step one shows the ligation of the isolated gene of interest into the plasmid forming recombinant DNA. Step two is the transformation of bacterial cells to form a competent bacterium. Step three is the replication and mass production of competent bacterial cells. Step four depicts the potential various applications of these cells (Campbell *et al.*, 2008).

In the food industry, lysozymes play a vital role in eliminating bacteria (Khan *et al.*, 2016). This increases the shelf-life of foods by inhibiting food spoilage which prevents colonisation of bacteria on foods such as, vegetables, cheese, meat and fish (Khan *et al.*, 2016). Lysozymes from egg whites and humans possess antimicrobial properties which can be used against food spoilage, as anti-tumour drugs and as a treatment for HIV (Cao *et al.*, 2015). However, human lysozyme has been found to have a specific activity three times higher than lysozymes in egg whites (Cao *et al.*, 2015). Therefore, recombinant DNA technology has helped develop methods that allow transgenic plants, microorganisms and animals such as chickens and cows to produce human lysozyme (Cao *et al.*, 2015; Ercan & Demirci, 2016).

Vaccines produced by recombinant DNA technology have been found to have a higher efficacy and specificity than conventional vaccines (Khan *et al.*, 2016). Encoding pathogen antigens into adenovirus vectors allowing for vaccinations through a painless, non-invasive nasal spray which is used against mucosal pathogens (Zhang *et al.*, 2011). This vaccination method is not limited to humans, animals can also be mass immunized with these vectors (Zhang *et al.*, 2011). Recombinant DNA technology enables mass production of vaccines at low costs as the required vectors can be mass-produced in serum-free suspension cells (Zhang *et al.*, 2011). Recombinant hormones such as the Follicle-Stimulating Hormone (FSH) and Luteinizing Hormone (LH) are complex proteins from eukaryotes. With the use of recombinant DNA technology these proteins, from humans, can now be expressed *in vitro* (Fan & Hendrickson, 2005; Assidi *et al.*, 2008). This has enhanced both ovulation and pregnancy in patients being treated with LH and r-FSH (Fan & Hendrickson, 2005; Assidi *et al.*, 2008).

Genetically engineered microbes play a pivotal role in the environment as bio-remediators. *Pseudomonas fluorescens* HK44 engineered to contain a naphthalene catabolic plasmid (pUTK21) including a *lux* gene with a promoter produced by a transposon-based bioluminescence successfully degraded naphthalene with a bioluminescent effect. This effect allows for *in situ* monitoring of the bio-remedial process (King *et al.*, 1990; Chatterjee & Meighen, 1995; Sayler *et al.*, 1999; Ripp *et al.*, 2000). In the industrial sector, recombinant DNA technology is useful for mass production of a required enzyme such as lipases, proteases, amylases or metabolites such as ethanol or anti-biotics (Waegeman & De Mey, 2012). The *E. coli* bacterium is a popular host in recombinant protein expression as it mass produces proteins efficiently at a low cost.

1.5.1 Advantages of Using *Escherichia coli*

Escherichia coli is the most commonly utilised bacteria for heterologous protein production (Schumann & Ferreira, 2004). This is due to its ability to produce large quantities of the required protein in a short span of time due to its fast growth rate (Fakruddin *et al.*, 2012; Rosano & Ceccarelli, 2014). In addition, a bioreactor is able to yield high amounts of protein by culturing large volumes of bacteria which results in an increase of final biomass in a short time frame (Fakruddin *et al.*, 2012). No complex equipment is needed when using *E. coli* in the laboratory thereby increasing its appeal from an economic standpoint (Brown, 1995; Fakruddin *et al.*, 2012). Since this bacterial system has been well studied, a wide variety of vectors and optimal strains exist and are already optimised for the expression of specific genes; thereby saving valuable time (Makino *et al.*, 2011). Furthermore, the ideal composition of media and temperature ranges have already been identified for *E. coli*. A vast amount of knowledge pertaining to physiological and genetic aspects of this bacterium is already present thereby providing an exceptional understanding of the organism compared to other bacterial systems (Alteri & Mobley, 2012). Furthermore, various strains are utilised to optimise production such as *E. coli* BL21 which has low amounts of acetate production when glucose is present and has a protease deficiency (Kim *et al.*, 2017). Lastly, many expression vectors are commercially accessible with various N and C terminal tags which adds to the list of benefits as to why *E. coli* is the ideal bacterial system for heterologous protein expression (Gomes *et al.*, 2016).

1.5.2 Limits of Using *Escherichia coli*

The use of *E. coli* for gene expression exhibits certain limitations. The resulting protein may be insoluble if the cell is incapable of folding the protein correctly which may form inclusion bodies (Leonhartsberger, 2006 ;Fakruddin *et al.*, 2012). This can occur when eukaryotic genes are expressed in an *E. coli* bacterial system as *E. coli* has a limited capacity for certain post-translational modifications such as fatty acid acylation and the formation of disulphide bonds essential for adequate folding of certain proteins (Leonhartsberger, 2006; Fakruddin *et al.*, 2012; Tokmakov *et al.*, 2012; Gomes *et al.*, 2016). In addition, incorrect glycosylation can affect the protein's activity, structure, function and stability (Jung & Williams, 1997). The expression of recombinant protein can also be affected by the nucleotide sequence of the gene of interest. If introns are present in the gene, *E. coli* will be unable to remove them as it does

not possess the required machinery. This can be remedied by utilising complementary DNA (cDNA) obtained from messenger RNA (mRNA) which does not possess introns (Gomes *et al.*, 2016). Further complications can arise such as premature termination if the gene of interest possess nucleotide sequences acting as a termination signal for *E. coli* resulting in a lack of gene expression (Brown, 2006). Amino acid coding differences between prokaryotes and eukaryotes pose a problem during translation of eukaryotic proteins. When this occurs the term codon usage bias is used (Brown, 1995). However, *in vitro* mutagenesis could be conducted in order to modify potential termination sequences and to replace unfavourable codon biases with those supported by *E. coli* (Brown, 2006; Gomes *et al.*, 2016).

1.5.3 Factors Affecting Heterologous Expression

There are several factors that can affect recombinant protein expression when placed under the control of an *E. coli* system. When protein synthesis occurs in the cytoplasm at a fast rate, inclusion bodies can be formed (Betts & King, 1999). These insoluble, spherical aggregates are formed when the cell fails to repair or remove proteins that are incorrectly folded (Blackwell & Horgan, 1991). The build-up in the cytoplasm can be avoided by using a secretion vector to relocate recombinant protein synthesis to another area, such as the periplasm (Fahnert *et al.*, 2004). Moreover, proteins are protected from degradation by proteases when synthesised in the periplasmic space (Hoffman & Wright, 1985). In order to prevent inclusion bodies from forming, the process of recombinant protein production must be slowed (Schumann & Ferreira, 2004). This can be done by 1) having a low plasmid copy number. 2) Decreasing the temperature during recombinant protein synthesis. 3) The co-expression of chaperone proteins. 4) Using solubility partners. 5) The use of extreme pH values during fermentation (Schumann & Ferreira, 2004). This results in the synthesis of soluble recombinant proteins.

After the addition of a plasmid in *E. coli* cells, it is vital to ensure that the plasmid is stable, as instability can result in the loss of the plasmid. Instability can occur due to a multitude of reasons 1) cells that are grown for many generations can cause instability, particularly during large scale productions (Pierce & Gutteridge, 1985). 2) It is essential to take into account which hosts work best with certain plasmids as this can have both positive and negative effects on the overall stability of the plasmid (Rai & Padh, 2001). 3) The size and origin of the DNA inserted into the vector has an effect on stability (Rai & Padh, 2001). 4) Plasmid loss can also occur due to plasmid-free *E. coli* cells in the culture, outcompeting plasmid-containing cells (Ashby

& Stacey, 1984). This is due to the growth rate of the plasmid-free cells being significantly higher than plasmid-free cells. This can be remedied by adding an antibiotic resistance gene into the plasmid for selection of plasmid-containing cells (Pierce & Gutteridge, 1985). 5) The physiological parameters such as temperature, pH, recombinant protein build-up, aeration and the growth medium, can affect the stability (Rai & Padh, 2001). 6) An error during the replication of an individual cell can affect the end population (Ashby & Stacey, 1984). 7) The increase in metabolic energy for plasmid function and maintenance may also cause instability (Aiba *et al.*, 1982). This can be remedied by utilising runaway-replication plasmid vectors whereby the plasmid copy number is directly proportional to the temperature (Bittner & Vapnek, 1981). Therefore, high temperatures can be used for only a portion of the time during the growth cycle resulting in high expression levels of the gene of interest (Bittner & Vapnek, 1981).

The strength of a promotor has an effect on the expression of the gene whereby genes controlled by strong transcriptional promotors have an increase in expression levels (Carrier & Nugent, 1983). Therefore, many vectors for both bacteriophages and plasmids, are specifically designed to station the gene of interest directly downstream from a strong promotor (Carrier & Nugent, 1983). However, it is essential that the promotor for the gene of interest is highly regulated by either a change in temperature or a particular metabolite being added to the growth medium (Swartz, 2001). This ensures that there is no constitutive production of recombinant protein which has the potential to affect regular cellular functions when produced at a basal level. When the promotor is not strictly regulated it causes "leaky" expression of the promotor and the resulting genes which can result in losing the plasmid or constitutive expression which can cause cellular death (Ringquist *et al.*, 1992). In *E. coli* the tryptophan (*trp*) and the lactose (*lac*) are the most widely used operons containing strong transcriptional promotors (Glick & Whitney, 1987).

1.5.4 The Lactose Operon System

A widely used operon system in *E. coli,* is the lactose operon system. This operon is responsible for expressing β-galactosidase, lactose permease and thiogalactoside transacetylase with structural genes for these enzymes called *lacZ*, *lacY* and *lacA,* respectively (Fig. 1.3) (Ullmann, 2001). The promotor upstream of the genes regulates their expression using an upstream gene (*lacI*) coding for the Lac repressor which has the ability to bind to the operator (encoded by

lacO) (Fig 1.3a). This blocks RNA polymerase from binding to the promotor thereby inhibiting expression of the genes (Yildirim, & Mackey, 2003). However, when an inducer is present, such as allolactose, it is able to bind to the allosteric or active site of the Lac repressor. Inhibiting its ability to bind to the operator by causing a conformational change (Yildirim, & Mackey, 2003). RNA polymerase is then free to bind to the promotor which allows expression of the genes as depicted in Fig. 1.3b.

This operon is commonly used for the expression of exogenous genes, in *E. coli*. The gene of interest is inserted into the *lac* operon on the plasmid which is introduced into *E. coli*. Restriction enzymes are used to cut the DNA of the plasmid at the sites of interest and DNA ligase is used to join DNA. This allows the gene of interest to be placed on the *lac* operon which is then controlled by its promotor. Next, it is vital to ensure that an inducer is present or the gene will not be expressed. The most commonly used chemical inducer is isopropyl β-D-1-thiogalactopyranoside (IPTG). Lactose can also be used as an inducer, however, a constant supply needs to be present as the cell will degrade the compound. In addition, IPTG will not be metabolised by the cell and is, therefore the preferred option.

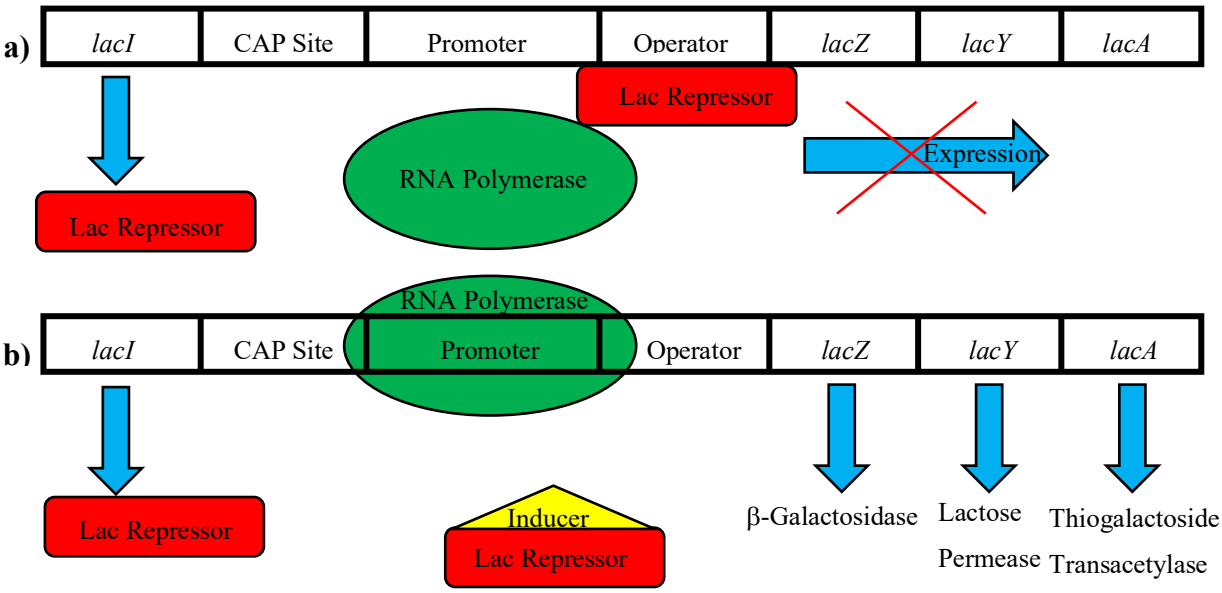

Figure 1.3: a) Negative Regulation of the *lac* Operon. When the Lac repressor (red) is encoded by the *lacI* gene, it is able to bind to the operator which blocks the binding of RNA polymerase (green). This results in lack of expression (blue) of *lacZ*, *lacY* and *lacA* genes. **b) Presence of an Inducer on the *lac* Operon.** If an inducer (yellow) is present, it will bind to the repressor (red) which will cause a conformational change. This decreases the ability of the repressor to bind to the operator. RNA polymerase (green) is then able to freely bind to the promotor which allows for the expression (blue) of *lacZ*, *lacY* and *lacA* genes which express β-galactosidase, lactose permease and thiogalactoside transacetylase, respectively.

1.6 RATIONALE

The use of biocatalysts affords cheaper, sustainable alternatives compared to unsustainable, costly metal catalysts when chemically synthesising pharmaceuticals and other chemicals. Therefore, the production of biological enzymes required for bioconversion can prove to be of high value both commercially and environmentally. *Rhodococcus* spp. have also been found to host to numerous enzymes with biocatalytic potential, due to their highly diverse physiological and metabolic functions. The first section of the study includes the production of nitrilases from three *Rhodococcus rhodochrous* strains, namely A29, A99 and ATCC BAA-870, by induction through the addition of dimethylformamide. The next section of the study comprised the expression of a cobalt nitrile hydratase from *R. rhodochrous* ATC BAA-870 in an *Escherichia coli* BL21 (DE3) host. This cell line was cultured and induced with IPTG. In order to establish whether the enzyme of interest is present after induction of *R. rhodochrous* A29, A99 and ATCC BAA-870 as well as *E. coli* BL21 (DE3), activity assays using benzonitrile as the substrate, were performed and the presence of resulting product was confirmed to ensure enzyme production and enzyme activity.

CHAPTER 2:

PRODUCTION OF NITRILASES

2.1 INTRODUCTION

Organisms that do not possess the constitutive production of nitrilases are required to be induced in order for nitrilase expression to occur. This can be done by introducing nitriles into the growth medium. However, if other nitrile-degrading enzymes are present, they may also be induced. Nitrile-containing inducers such as benzonitrile, acrylonitrile and 3-cyanopyridine managed to induce a nitrilase from *Alcaligenes faecalis* MTCC 10757 (Nageshwar *et al.*, 2011) In addition, acrylonitrile was found to be the best inducer in this strain. A nitrilase from *Stenotrophomonas maltophilia* AC21 was successfully induced by acetonitrile in 2016 by Badoei-Dalfard and co-workers. As a nitrilase inducer, 2-cyanopyridine was shown to be effective in the filamentous fungus *Fusarium solani* IMI96840 (Vejvoda *et al.*, 2010). Tetrachloroterephthalonitrile showed the best induction ability in *Rhodococcus* sp. CCZU10-1 when compared to the induction ability of benzonitrile and phenylacetonitrile, (He *et al.*, 2014). The nitrilase of *Rhodococcus* sp. NDB 1165 proved to be inducible by propionitrile (Prasad *et al.*, 2007). Isovaleronitrile allowed the induction of the nitrilase in *Rhodococcus rhodochrous* J1 (Kobayashi *et al.*, 1989) and *Nocardia globerula* NHB-2 was successfully induced by short-chain aliphatic nitriles such as butyronitrile, valeronitrile, isobutyronitrile as well as propionitrile (Sharma *et al.*, 2011).

A risk of using nitriles as an inducer is the hydrolysis of the inducer by a nitrilase. Therefore, in order to prevent this, other inducers are an interest of study. For instance, ε-Caprolactam, has the ability to successfully induce nitrilase expression in *Fusarium proliferatum* AUF-2 (Yusuf *et al.*, 2013), *Rhodococcus* sp. *CCZU10-1*(He *et al.*, 2014) and *A. faecalis* MTCC 10757 (Nageshwar *et al.*, 2011). However, it was found to be ineffective in *N. globerula* NHB-2 (Sharma *et al.*, 2011). In *R. rhodochrous* J1 ε-Caprolactam, γ-Butyrolactam and δ-valerolactam all proved to be effective as nitrilase inducers (Nagasawa *et al.*, 1990). In addition, ε-Caprolactam was highly successful in this strain due to the nitrilase making up 30 % of all soluble proteins produced when the culturing medium was infused with 0.5 % (*w/v*) of ε-Caprolactam.

The expression of nitrilases in plants is caused by the presence of isothiocyanates and nitriles from glucosinolates (Miller & Conn, 1980). Since these compounds are toxic, plants express nitrilases in order to detoxify cells (Miller & Conn, 1980). It is predicted that expression of nitrilase when exposed to dimethylformamide (DMF), may be part of a cell detoxification pathway as DMF is known to be toxic to cells (Chhiba-Govindjee *et al.*, 2018). Initially, DMF was used to boost both nitrilase and nitrile hydratase activity. However, Chhiba-Govindjee and co-workers (2018) were the first to successfully induced nitrilase expression in *Pimelobacter sim*plex PPPPB BD-1781, *R. rhodochrous* ATCC BAA-870 and PPPB BD-1780 with DMF. Therefore, a different class of inducers, such as ε-Caprolactam, can be utilised instead of nitriles (Nagasawa *et al.*, 1990). DMF also falls into this group as it has been found to share structural similarities, as ε-Caprolactam, which indicates that they may share the same mechanism of induction (Chhiba-Govindjee *et al.*, 2018). Since DMF costs are cheaper than ε-Caprolactam, it is found to be more commercially appealing (Chhiba-Govindjee *et al.*, 2018). In this work, DMF was used as an inducer of nitrilase in *Rhodococcus rhodochrous* A29, A99 and ATCC BAA-870.

2.2 AIM AND OBJECTIVES

2.2.1 Aim

1) To establish whether nitrilase activity is present in DMF induced *R. rhodochrous* A29, A99 and ATCC BAA-870 cells.

2.2.2 Objectives

1) To culture and induce *R. rhodochrous* A29, A99 and ATCC BAA-870 in a bioreactor.

2) To test for nitrilase activity in *R. rhodochrous* A29, A99 and ATCC BAA-870.

2.3 METHODS AND MATERIALS

2.3.1 Organisms

2.3.1.1 Rhodococcus rhodochrous Isolates

Three *R. rhodochrous* strains were used in this study. *R. rhodochrous* A29 and A99 strains were isolated from agricultural soil samples by Rapheela and co-workers (2017). *R. rhodochrous* ATCC BAA-870, also known as Ismall, was isolated from industrial soil samples in Modderfontein, Johannesburg by Brady and co-workers (2004) using an enrichment method by Layh and co-workers (1997). These cells were formerly cryopreserved in 100mM phosphate buffer with a 20 % (*v/v*) glycerol concentration at a pH of 7.2 and temperature of – 80 ºC (Chhiba-Govindjee *et al.*, 2018).

2.3.2 Biomass Production and Induction

2.3.2.1 Pre-Culture

The three *R. rhodochrous* strains were individually streaked on tryptone soy agar (TSA), containing 30 g/L of tryptone soy broth (TSB) (biolab®, Batch # 1043963) and 1 % (*w/v*) agar, (VWR Chemicals®, Batch # 16B180001) and incubated at 28 ºC for 72 hours. Afterwards, a single salmon-pink colony was selected and streaked on another TSA Petri dish and incubated at the previous conditions. A single salmon-pink colony, from the latter culture, was used to inoculate 5 mL of TSB. This was placed on a shaker at 180 rpm for 72 hours at 28 ºC. Afterwards, 3 mL of the previous culture was used to inoculate 200 mL of TSB in a 2 L Erlenmeyer flask and incubated on a rotary shaker at 180 rpm for 72 hours at 28 ºC. All steps were performed using aseptic techniques and required a control to ensure no contamination occurred. In addition, *R. rhodochrous* has a distinct salmon/red pigmentation (Zofp, 1891) which was observed in order to ensure that the appropriate bacterium was grown for each strain (Fig. 2.2).

2.3.2.2 Biomass Production

Once each strain was cultured, a 2 L aerobic benchtop bioreactor, with a BIOSTAT® B-plus benchtop controller (Sartorius Stedim Biotech, Fig. 2.1), was used to increase the biomass to a volume of 1.2 L. Minimal media was composed of 1 L distilled water, 15 g/L glucose (Sigma-

Aldrich®, Batch # SZBF0200V), 7.5 g/L monosodium glutamate (MSG) (Merck Chemicals®, Batch # MF9M591241), 1 g/L yeast extract (Sigma-Aldrich®, Batch # BCBV8725), 0.5 g/L $MgSO_4$ (Promark Chemicals®, Batch # 40900) anhydrous, 0.5 g/L KH_2PO_4 (Merck Chemicals®, Batch # 1034582) and 0.5 g/L K_2HPO_4 anhydrous (Merck Chemicals®, Batch # MB0M593278). This media was placed in the bioreactor and was sterilized by autoclaving at 121 ºC for 20 minutes. For the inoculum, the shake flask seed culture of each strain was separately centrifuged at 3,836 × g (5,000 rpm) for five minutes at 4 ºC in a Sorvall™ RC 6+ Centrifuge. The supernatant was cast-off and the pellet was re-suspended in 200 mL minimal media. This was then aseptically pumped into the bioreactor (Fig. 2.1). In order to induce nitrilase production, 0.5 % (*v/v*) DMF was aseptically pumped into the bioreactor. The following parameters were set for biomass production: 72 hours incubation, pH of 7.2, 28 ºC incubation temperature, agitation at 600 rpm and a gas flow of 3.0 L/m. Biomass production for each strain required a control not induced with DMF. The absorbance, with a wavelength of 600 nm, was measured every 12 hours for each strain using a Beoco Germany S-20 spectrophotometer.

Figure 2.1: Industrial Aerobic Bioreactor containing *Rhodococcus rhodochrous*. *Rhodococcus rhodochrous* was grown in a 2.0 L bioreactor with the following parameters: 72 hours incubation, pH of 7.2, 28 ºC incubation temperature, agitation at 600 rpm and a gas flow of 3.0 L/m. The distinct salmon-pink pigmentation of *R. rhodochrous* confirms its presence.

2.3.3 Cell harvesting and Storage

Once biomass production and induction were completed, the cells were harvested by centrifuging the culture broth at 3,836 × g (5,000 rpm) for five minutes at 4 ºC in a Sorvall™ RC 6+ Centrifuge. The resulting pellet was stored at –20 ºC in sterile Falcon tubes in 200 mg aliquots.

2.3.4 Nitrilase Activity Assay

Benzonitrile (Sigma-Aldrich Chemicals®, Batch # STBC7761V) was used as a substrate to confirm the presence of nitrilase activity in induced *R. rhodochrous* strains. A volume of 1 µL of benzonitrile and 180 µL of 50 mM Tris buffer (ACE chemicals, Batch # 32165), at a pH of 7.6, was added per milligram of wet cell paste. The assay was incubated for 30 minutes at 30 ºC on a 180 rpm rotary shaker. The resulting product was expected to be benzoic acid. However, in *R. rhodochrous* ATCC BAA-870, benzamide is also expected to be produced. This is due to the constitutive production of a nitrile hydratase from *R. rhodochrous* ATCC BAA-870 (Chhiba-Govindjee *et al.*, 2018). Moreover, uninduced *R. rhodochrous* strains were also tested as a control, to confirm the absence of nitrilase production.

2.3.4.1 Thin-Layer Chromatography

Thin-layer chromatography is an analytical technique that separates compounds in a mixture based on compounds varying in solubility and adsorption in the stationary and mobile phase (Fried & Sherma, 1999). This allows for the identification of compounds, their purity and to chart the advancement of a reaction. R_f (retention factor) is determined by the distance travelled by the spot divided by the distance travelled by the solvent.

In this study aluminium thin-layer chromatography (TLC) sheets (Merck Chemicals ®, Batch # 040425002) were utilised in order to monitor the reaction to determine if a product was synthesised during the nitrilase activity assay. Negative controls contained 50 mM Tris buffer and induced *R. rhodochrous* cells to ensure no product was present before the addition of benzonitrile. Acrylamide, benzonitrile and 2-bromo-5-cyanobenzoic acid were used as positive controls (Fig. 2.2) to determine where on the TLC plate the amide, carboxylic acid and undegraded nitrile would be located. The TLC plates were spotted after the 30-minute incubation. These plates were run using 60 % hexane and 40 % ethyl acetate as the solvent.

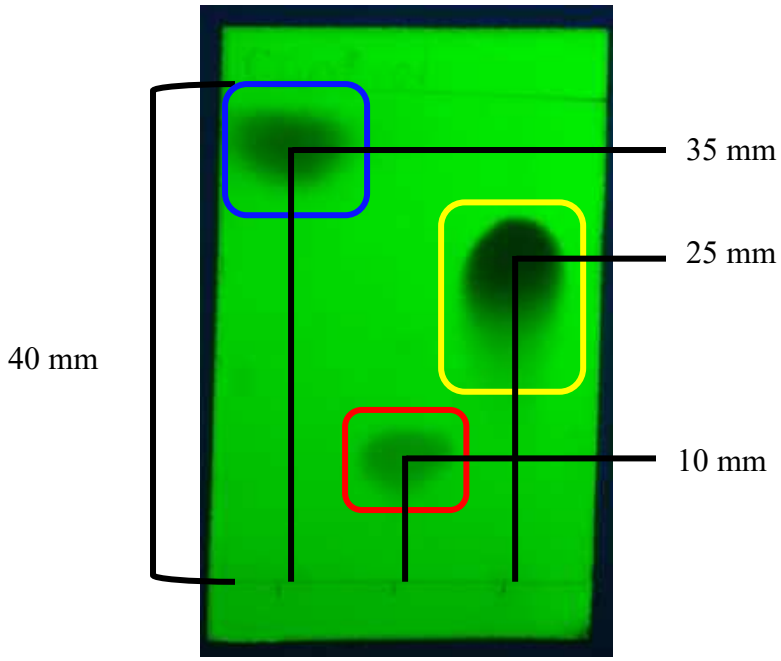

Figure 2.2: Positive Control TLC Plate Under UV Light. The solvent, 40 % ethyl acetate/hexane, travelled 40 mm up the TLC plate. **Spot 1** represents benzonitrile (Blue) with an R_f = 0.875 as it travelled 35 mm. **Spot 2** represents acrylamide (Red) with an R_f = 0.25 which travelled 10 mm. **Spot 3** represents 2-bromo-5-cyanobenzoic acid (Yellow) with an R_f = 0.625 which travelled 25 mm.

2.3.4.2 Liquid-Liquid Extraction

In order to extract the synthesised product, the reaction mixture after the nitrilase activity assay was mixed with dH_2O to a final volume of 20 mL. This was then placed in a 100 mL separation column and 20 mL of ethyl acetate was added. The column was vigorously shaken in order to extract benzoic acid from the aqueous phase by allowing it to dissolve in the solvent phase (Fig. 2.3).

The products of *R. rhodochrous* ATCC BAA-870 nitrile degradation included both benzoic acid and benzamide and had to be separated in order to obtain pure products. This was done using acid-base extraction, by adding 2 M of sodium hydroxide (NaOH) to the separation column before the mixture was shaken. Once shaken, the benzoic acid reacted with the NaOH, to form sodium benzoate (C_6H_5COONa), which remained in the aqueous phase while benzamide was extracted to the solvent phase. These phases could then be separated. Thereafter, benzoic acid was extracted from the aqueous phase by adding 2 M of hydrochloric acid (HCl) to the separation column before the mixture was shaken. This then caused sodium

benzoate to be protonated thereby forming benzoic acid. This returned benzoic acid to the solvent phase after vigorously shaking the separating column (Nichols, 2017).

Once the aqueous phase was separated from the solvent phase, for all strains and products of *R. rhodochrous*, one teaspoon (approximately 3 – 5 g) of $MgSO_4$ anhydrous was added to the solvent phase as a drying agent. This was then filtered by means of a paper filter (Boeco Germany, Batch # 16-020) and the products were collected in a round bottom flask. Furthermore, a Büchi Rotavapor® R II was used to remove the remaining ethyl acetate in order to concentrate the product.

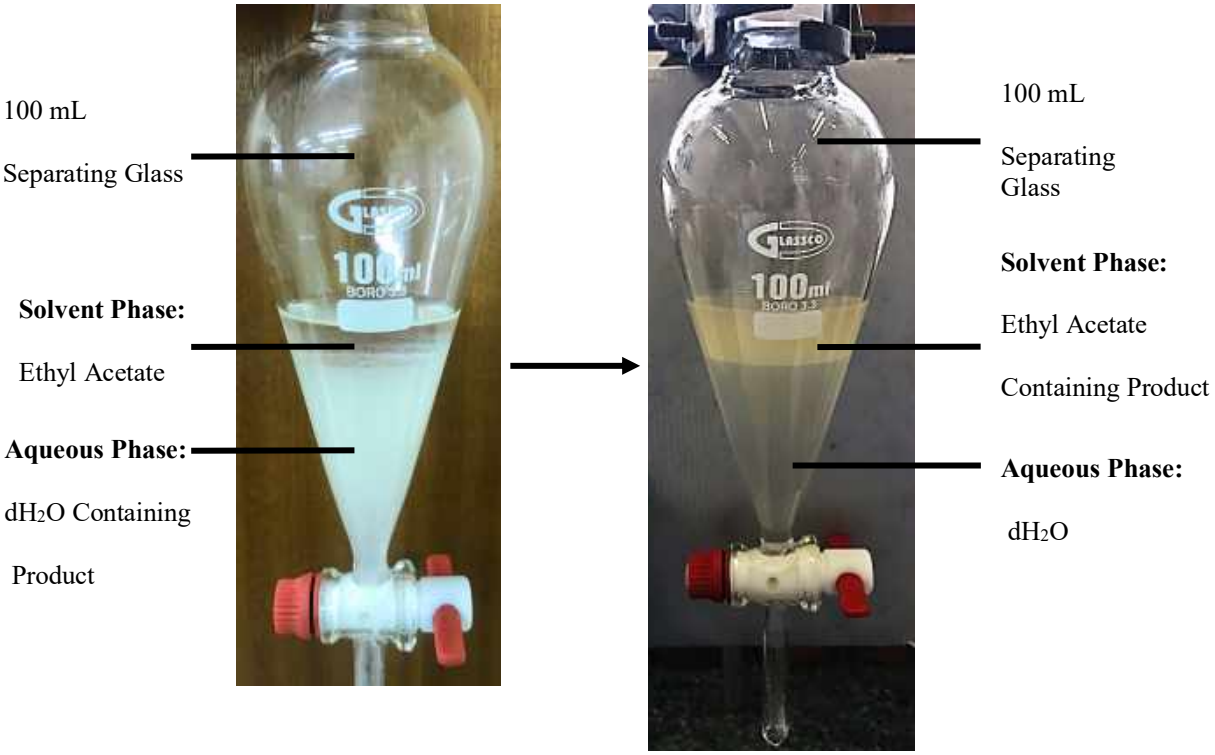

Figure 2.3: Aqueous and Solvent phases in a 100 mL Separating Column. After vigorous shaking of the column, the product enters the solvent phase from the aqueous phase.

2.3.4.3 Melting point

Melting point is the temperature at which a compound or substance melts at atmospheric pressure. In order to attain fundamental physiochemical characteristics of organic compounds, it is vital to know the melting point (Yalkowsky *et al.*, 1994). This is due to its relationship with vapour pressure and aqueous solubility. The purity of the compound can be established by the melting point range at which the compound begins to melt and when it is entirely melted.

Therefore, a shorter range depicts a purer compound than a longer range (Allen, 1942). Furthermore, a range narrower than 5 ºC is considered short and a range larger than 5 ºC is considered broad (Dent, 2006). In addition, melting points can also be depressed if the compound is impure (Dent, 2006). In order to establish the melting point of the synthesised product, a Stuart® SMP10 Melting Point Apparatus was used. The temperature was logged once the solid had started to melt and when the solid was completely melted.

2.3.4.4 Fourier-Transform Infrared Spectroscopy

Fourier-Transform Infrared (FT-IR) spectroscopy uses vibrations caused by infrared radiation absorption by molecular bonds to determine the structural properties and functional groups of specific compounds (Mollaoglu *et al.*, 2018). The spectrum produced depicts the molecular structure of a compound with peaks and bands in specific positions which translate to a type of molecular bond. This is vital in portraying which functional group a compound possesses (Mollaoglu *et al.*, 2018). FT-IR spectroscopy was conducted using the Bruker Tensor 27 FT-IR system & OPUS data collection program (Version 6.5). This was conducted to confirm if the carboxylic acid functional group and the aromatic bonds of benzoic acid were present in the samples.

2.3.4.5 Nuclear Magnetic Resonance Spectroscopy

Nuclear magnetic resonance (NMR) spectroscopy is a vital analytical technique which aids in confirming and identifying the purity and molecular structure of a compound. In order to fully confirm that benzoic acid is present NMR was performed. Since the desired product is soluble in deuterated chloroform ($CDCl_3$) (Sigma-Aldrich®, Batch # MKBP4908V), it was used as the solvent. Afterwards, 256 proton scans and 2048 carbon scans were run using a Bruker 400MHz NMR for both proton and carbon scans. Moreover, the resultant spectra were used to confirm if nitrilase activity was present in DMF induced *R. rhodochrous* strains.

2.3.5 Calculations

2.3.5.1 Growth Rate

The exponential growth phase determines the growth rate of each bacterial strain. A line of best fit (Log Absorbance (OD_{600}) vs Time) was used to calculate the growth rate (μ) for the

exponential growth portion of each strain. The following equation by Widdel (2007) was used for the calculation of the growth rates.

$$\mu = \frac{2.303\ (Log10(OD_2) - Log10(OD_1))}{(Time_2 - Time_1)}$$

2.3.5.2 Statistical Analysis

The growth rate of each uninduced strain was compared to the growth rate of the corresponding induced strain in order to determine if the presence of DMF has a significant effect on the growth rate. Levene's test (F-Test: Two-Sample for Variances) was performed for the Absorbance (OD_{600}) data of each strain (Table A1 & Table A2, Appendix A). This test is essential in statistics as it aids in selecting the appropriate test when analysing the data. Since the null hypothesis was accepted for Levene's test, a t-test: Two-Sample Assuming Equal Variances was conducted to determine if the growth rates were significantly different. A significance level of 0.05 ($\alpha = 0.05$) was used for all statistical tests. A single asterisk (*) is used in order to denote a P-value where $P \leq 0.05$. This implies a significant difference in the growth rate. All statistical analyses were performed using the Analysis ToolPak in Microsoft® Excel (Version 16.37).

2.3.5.3 Number of Moles

During the nitrilase activity assay, 100 mg of wet cell paste was used with 100 µL of 99 % benzonitrile in 18 mL of Tris buffer with a pH of 7.6. The number of moles converted, of benzonitrile, was calculated using the following equation:

$$Moles\ (mol) = \frac{Mass\ (g)}{Molar\ Mass\ (g/mol)}$$

2.3.5.4 Enzyme Activity

The minimum enzyme activity present during the nitrilase activity assay was determined using the following equation:

$$Enzyme\ Activity\ (U) = \frac{\mu mol}{Minutes}$$

2.4 RESULTS

2.4.1 Growth Curves

All *R. rhodochrous* strains were cultured for a total of 72 hours (Fig. 2.4; Table A1, Appendix A). All three strains reached an exponential growth phase 24 hours post-incubation. Each stained experienced exponential growth for a total of 36 hours after which a stationary growth phase occurred at 60 hours lasting 12 hours before the cultures were removed from the bioreactor and stored. The wet cell weight produced by each strain, from 1.2 L of media, was: 8.74 g for *R. rhodochrous* A99, 6.87 g for *R. rhodochrous* ATCC BAA-870 and 6.13 g for *R. rhodochrous* A29.

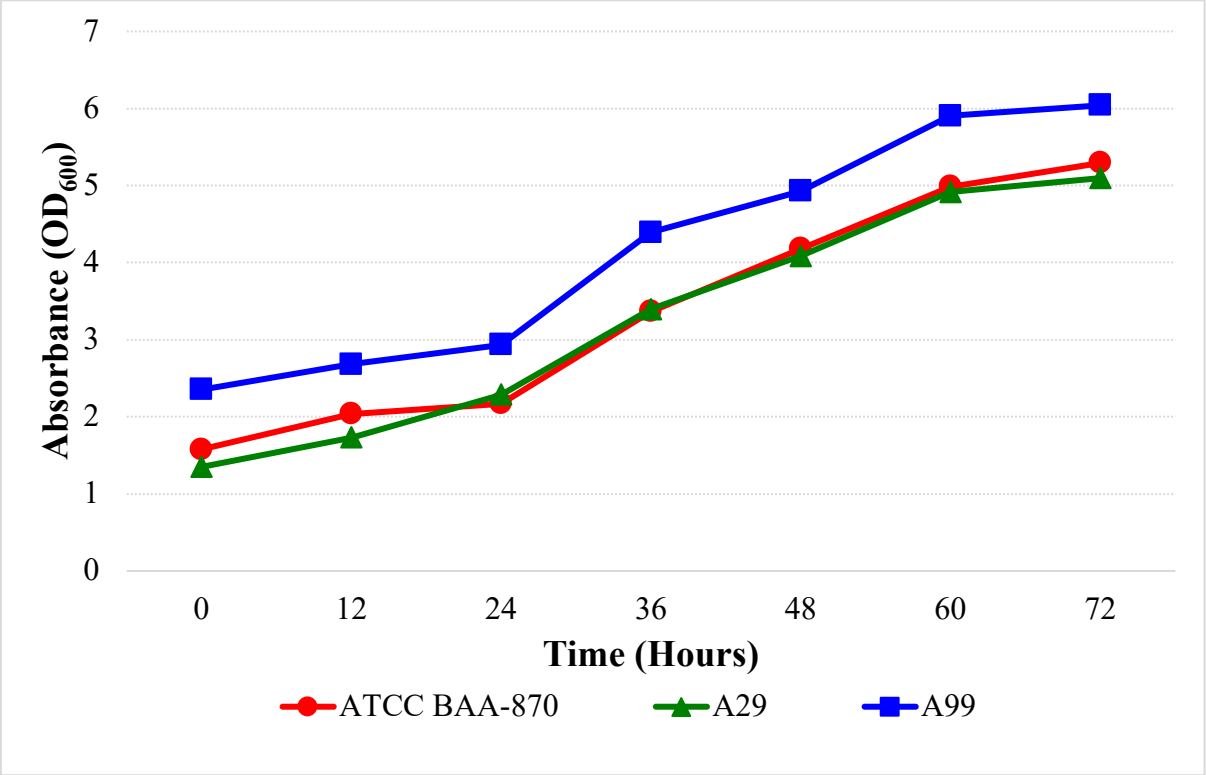

Figure 2.4: Growth Curve of *Rhodococcus rhodochrous* A29, A99 and ATCC BAA-870. *R. rhodochrous* A29 (Green) started with the least number of cells followed by *R. rhodochrous* ATCC BAA-870 in the middle (Red) and *R. rhodochrous* A99 (Blue) starting with the most cells. All three strains endured a lag phase of 24 hours followed by an exponential phase of 36 hours and a stationary phase of 12 hours before removal from the bioreactor.

All three strains remained in the lag phase for 24 hours post-incubation (Fig. 2.5; Table A2, Appendix A). The subsequent exponential phase lasted for 24 hours in *R. rhodochrous* A29 and ATCC BAA-870 and lasted for 36 hours in *R. rhodochrous* A99. The cultures were removed from the bioreactor 72 hours post-incubation which was approximately 12 – 24 hours into the stationary growth phase. The wet cell weight produced by each strain, from 1.2 L of media, was: 9.64 g for *R. rhodochrous* A99, 4.93g for *R. rhodochrous* ATCC BAA-870 and 4.26 g for *R. rhodochrous* A29.

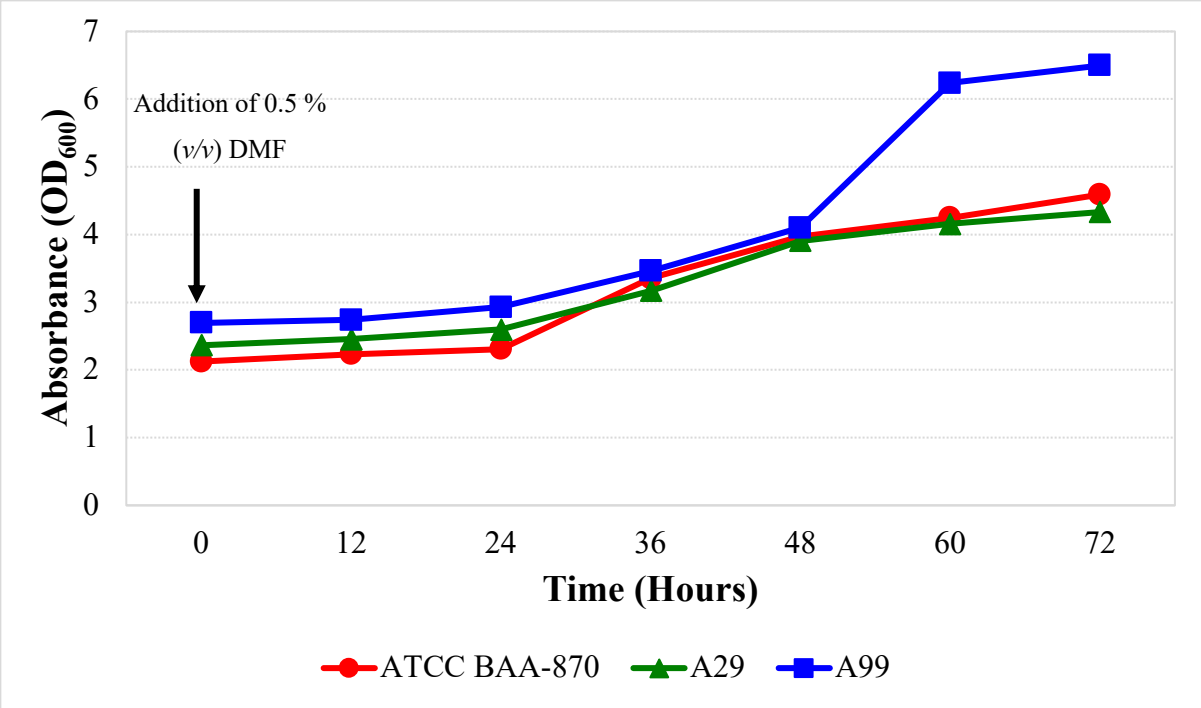

Figure 2.5: Growth Curve of DMF Induced *Rhodococcus rhodochrous* A29, A99 and ATCC BAA-870. An addition of 0.5 % (*v*/*v*) DMF was added to each strain at the start of biomass production (zero hours). *R. rhodochrous* ATCC BAA-870 (Red) started with the least number of cells followed by *R. rhodochrous* A29 (Green) in the middle and *R. rhodochrous* A99 (Blue) starting with the most cells. All three strains endured a lag phase of 24 hours followed by an exponential phase of 24 for *R. rhodochrous* ATCC BAA-870 and A29 and 36 hours for *R. rhodochrous* A99. Followed by a stationary phase of 24 hours for *R. rhodochrous* ATCC BAA-870 and A29 and 12 hours for *R. rhodochrous* A99 before removal from the bioreactor.

Levene's Test for all three strains accepted the null hypothesis which represents data with equal variances. There was no significant difference in the growth rates, presented in Table 2.1, before and after the addition of DMF according to the resulting P-values (P(T<=t) = 0,41, P(T<=t) = 0,64, P(T<=t) = 0,48) for *R. rhodochrous* A29, A99 and ATCC BAA-870,

respectively. Therefore, the addition of 0.5 % DMF as a nitrilase inducer has no significant effect on the growth rate of induced *R. rhodochrous* A29, A99 and ATCC BAA-870 strains.

Table 2.1: Growth Rate of Uninduced and Induced *R. rhodochrous* Strains per Hour and % per Hour

***Rhodococcus rhodochrous* Strain**	**Growth Rate ($hour^{-1}$)**	**Growth Rate (%/hour)**
Uninduced *R. rhodochrous A29*	0.2478	24.78
DMF Induced *R. rhodochrous A29*	0.2043	20.43
Uninduced *R. rhodochrous A99*	0.2215	22.25
DMF Induced *R. rhodochrous A99*	0.2440	24.40
Uninduced *R. rhodochrous ATCC BAA-870*	0.2714	27.24
DMF Induced *R. rhodochrous ATCC BAA-870*	0.2720	27.20

2.4.2 Benzoic Acid Synthesis

2.4.2.1 Thin-Layer Chromatography

After the nitrilase activity assay, the products synthesised by uninduced strains of *R. rhodochrous* A29, A99 and ATCC BAA-870 were spotted at one, two and three, respectively on a TLC plate (Fig. 2.6). A product was not synthesised from *R. rhodochrous* A29 and A99 strains, as only the substrate was present after the nitrilase activity assay. This indicates that no nitrilase enzyme was present in these uninduced strains. However, no benzonitrile was present in the reaction containing *R. rhodochrous* ATCC BAA-870. Instead, benzamide was produced due to the presence of a nitrile hydratase. On the TLC plate, benzonitrile from both *R. rhodochrous* A29 and A99 reactions had an R_f = 0.80 and the benzamide from the *R. rhodochrous* ATCC BAA-870 reaction had an R_f = 0.36.

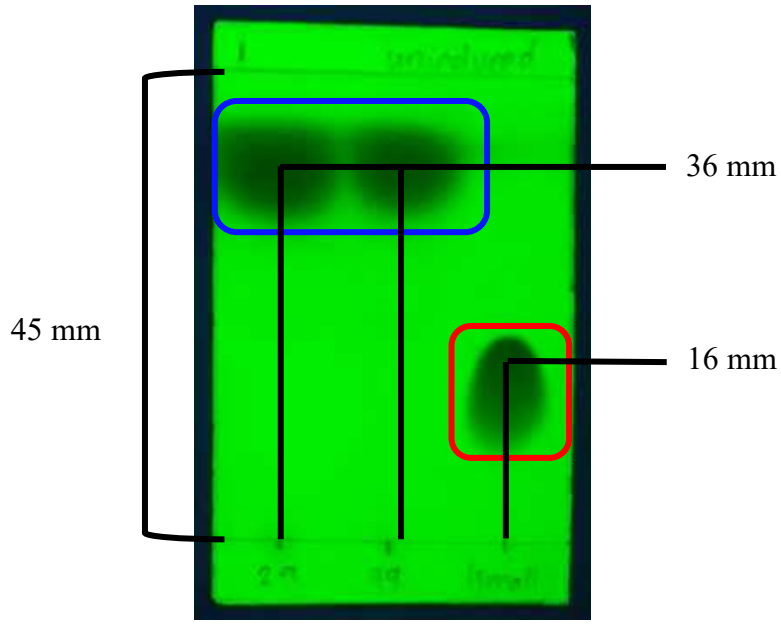

Figure 2.6: Nitrilase Activity Assay Products from Uninduced *R. rhodochrous* A29, A99 and ATCC BAA-870, on a TLC Plate Under UV Light. The solvent, 40 % ethyl acetate/hexane, travelled 45 mm up the TLC plate. **Spot 1** represents benzonitrile (Blue), from *R. rhodochrous* A29, with an R_f = 0.80 as it travelled 36 mm. **Spot 2** represents benzonitrile (Blue), from *R. rhodochrous* A99, with an R_f = 0.80 which travelled 36 mm. **Spot 3** represents benzamide (Red), *R. rhodochrous* ATCC BAA-870, with an R_f = 0.36 which travelled 16 mm.

Identical products were synthesised by all three DMF induced strain of *R. rhodochrous*, after the nitrilase activity assay. The reaction was spotted on a TLC plate at one, two and three for each strain, respectively (Fig. 2.7). All three *R. rhodochrous* strains displayed a production benzoic acid. Benzamide was again synthesised by a nitrile hydratase expressed by *R. rhodochrous* ATCC BAA-870.

A TLC plate (Fig. 2.8) was used to ensure that pure products were obtained after the acid-base extraction from *R. rhodochrous* ATCC BAA-870, as both benzamide and benzoic acid were present in the reaction after the nitrilase assay. Benzamide and benzoic acid were successfully separated and extracted from the mixture.

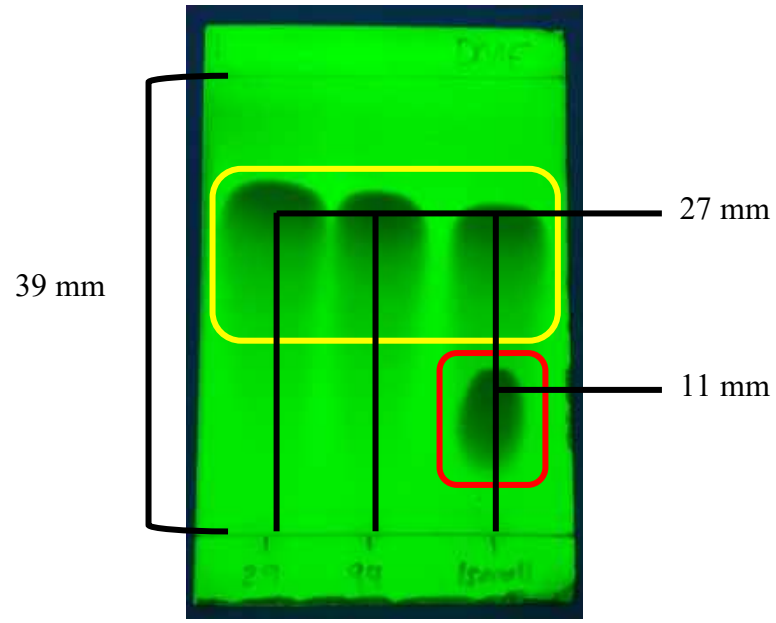

Figure 2.7: Nitrilase Activity Assay Present Products from DMF Induced *R. rhodochrous* A29, A99 and ATCC BAA-870, on a TLC Plate Under UV Light. The solvent, 40 % ethyl acetate/hexane, travelled 39 mm up the TLC plate. **Spot 1** represents benzoic acid (yellow), *R. rhodochrous* A29, with an R_f = 0.69 as it travelled 27 mm. **Spot 2** represents benzoic acid (yellow), *R. rhodochrous* A99, with an R_f= 0.69 which travelled 27 mm. **Spot 3** represents benzamide (Red) and benzoic acid (yellow), *R. rhodochrous* ATCC BAA-870,with an R_f = 0.28 which travelled 11 mm and R_f = 0.69 which travelled 27 mm, respectively.

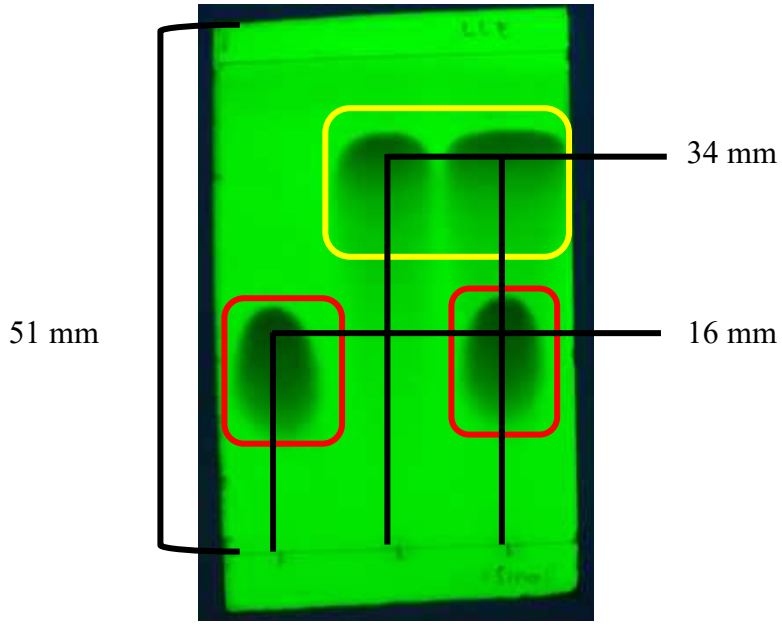

Figure 2.8: Acid-Base Extraction Products from *R. rhodochrous* ATCC BAA-870, TLC Plate Under UV Light. The solvent, 40 % ethyl acetate/hexane, travelled 51 mm up the TLC plate. **Spot 1** represents benzamide (Red) with an R_f = 0.14 as it travelled 16 mm. **Spot 2** represents benzoic acid (yellow) with an R_f= 0.67 which travelled 34 mm. **Spot 3** represents benzamide (Red) and benzoic acid (yellow) with an R_f = 0.31 which travelled 16 mm and R_f = 0.67 and which travelled 34 mm, respectively.

2.4.2.2 Chemical Analytical Data for Benzoic Acid (Strain A29)

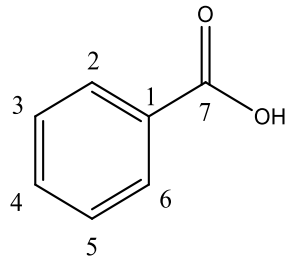

The desired product was extracted and concentrated and was afforded as a white solid. **Rf:** 0.69 (40 % Ethyl Acetate/Hexane); **Mp =** 119 – 123 °C; **IR(v_{max}/cm^{-1}):** 3300-2300 (O–H); 1677 (C=O); 3017 (**Ar**C–H); 1601, 1582 (**Ar**C=C); **^{1}H NMR (400 MHz, Chloroform-*d*):** δ 12.51 (s, 1H, OH), 8.21 – 8.11 (m, 2H, H2&H6), 7.63 (t, *J* = 7.4 Hz, 1H, H4), 7.50 (t, *J* = 7.7 Hz, 2H, H3&H5); **^{13}C NMR (101 MHz, Chloroform-*d*):** δ 172.68 (C7), 133.86 (C4), 130.25 (C2&C6), 129.38 (C1), 128.51(C3&C5).

2.4.2.3 Chemical Analytical Data for Benzoic Acid (Strain A99)

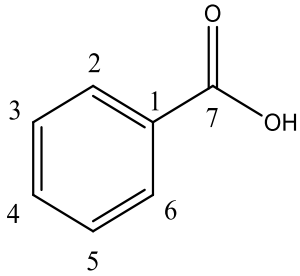

The desired product was extracted and concentrated and was afforded as a white solid. **Rf:** 0.69 (40 % Ethyl Acetate/Hexane); **Mp =** 119 – 123 °C; **IR(v_{max}/cm^{-1}):** 3300-2300 (O–H); 1678 (C=O); 3017 (**Ar**C–H); 1601, 1582 (**Ar**C=C); **^{1}H NMR (400 MHz, Chloroform-*d*):** δ 12.65 (s, 1H, OH), 8.22 – 8.11 (m, 2H, H2&H6), 7.63 (t, *J* = 7.4 Hz, 1H, H4), 7.49 (t, *J* = 7.6 Hz, 2H, H3&H5); **^{13}C NMR (101 MHz, Chloroform-*d*):** δ 172.72 (C7), 133.86 (C4), 130.26 (C2&C6), 129.40 (C1), 128.52 (C3&C5).

2.4.2.4 Chemical Analytical Data for Benzoic Acid (Strain ATCC BAA-870)

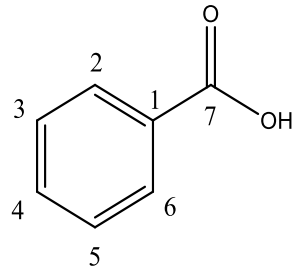

The desired product was extracted and concentrated and was afforded as a white solid. **Rf:** 0.69 (40 % Ethyl Acetate/Hexane); **Mp =** 118 – 123 °C; **IR(ν_{max}/cm^{-1}):** 3300-2300 (O–H); 1681 (C=O); 3017 (**Ar**C–H); 1601, 1583 (**Ar**C=C); **^{1}H NMR (400 MHz, Chloroform-*d*):** δ 10.72 (s, 1H, OH), 8.25 – 7.95 (m, 2H, H2&H6), 7.55 (t, *J* = 7.4 Hz, 1H, H4), 7.42 (t, *J* = 7.8 Hz, 2H, H3&H5); **^{13}C NMR (101 MHz, Chloroform-*d*)**: δ 171.73 (C7), 133.61 (C4), 130.14 (C2&C6), 129.67 (C1), 128.42 (C3&C5).

2.4.3 Benzonitrile Conversion

The TLC plate (Fig. 2.7), ^{1}H NMR (Fig. A1, A3, A5, Appendix A), ^{13}C NMR (Fig. A2, A4, A6, Appendix A), and FT-IR (Fig. A7, A8, A9, Appendix A) showed no signs of benzonitrile left in the reaction after 30 minutes. Therefore, 100 % of the benzonitrile substrate was converted to benzoic acid by a nitrilase expressed by all three strains. Therefore, 960 µmol of benzonitrile was fully converted to 960 µmol of benzoic acid in 30 minutes by a nitrilase enzyme with a minimum enzyme activity of 32 U. Since this was produced from 100 mg of cell paste then one gram of cell paste can afford 19.2 mmol of benzoic acid in an hour. Therefore, 1 kg of wet cell paste would produce 19.2 mol/kg/h (*w/w*) whereby a molecular mass of 122.12 g/mol would allow for the productivity of 2.34 kg/kg/h (*w/w*). Furthermore, 1 µmol of benzonitrile is converted every minute by 32 U of nitrilase.

2.5 DISCUSSION

The addition of 0.5 % DMF was shown to have no effect on the growth rate of *R. rhodochrous* A29, A99 and ATCC BAA-870. Previous studies show that nitrile-based inducers such as isovaleronitrile, exhibit a reduction in cell growth when concentrations were increased. Since isovaleronitrile is metabolised by the cell, a high concentration is required in the culture for adequate induction. However, in *R. rhodochrous* J1 cells, isovaleronitrile was deemed toxic to its growth when present in high concentrations (Nagasawa *et al.*, 1990). Studies done by Nagasawa and co-workers (1990) show similar findings when inducing *R. rhodochrous* J1 with 0.75 % (*w/v*) ε-Caprolactam whereby the bacterial growth rate was found to decrease significantly. However, concentrations of 0.3, 0.4 and 0.5 % (*w/v*) were able to yield high specific activities of the nitrilase enzyme without the inhibition of cell growth. Since a concentration of 0.5 % (*w/v*) ε-Caprolactam produced the highest specific activity without growth rates decreasing, it was deemed the best concentration for nitrilase induction. Therefore,

increasing the concentration of DMF may also cause a decrease in cell growth. In addition, Bromley-Challenor and co-workers (2000) found that an increase in DMF concentration inhibited the growth of their bacterial consortium. When compared to nitrile-based inducers, ε-caprolactam was found to be the most powerful nitrilase inducer in *R. rhodochrous* J1 as it not metabolised by the cell while still providing a nitrilase with a high specific activity (Nagasawa *et al.*, 1990). Since DMF is a cheaper alternative to ε-Caprolactam and has no effect on cell growth, it provides cause to further study the effects and induction properties of DMF in various organisms hosting the nitrilase pathway.

During TLC analysis of the uninduced *R. rhodochrous* strains, benzonitrile was identified to be the sole compound present in both uninduced *R. rhodochrous* A29 and A99 due to the lack of the nitrilase enzyme. This suggests that uninduced *R. rhodochrous* A29 and A99 do not constitutively express nitrile hydrolysing enzymes. Therefore, they require an inducer to produce nitrile hydrolysing enzymes. Studies by Chhiba-Govindjee and co-workers (2018) corroborate this observation. By contrast, uninduced *R. rhodochrous* ATCC BAA-870 converted benzonitrile into benzamide suggesting that this strain constitutively expresses a nitrile hydratase enzyme (Chhiba-Govindjee *et al.*, 2018). Therefore, due to the lack of benzoic acid, it can be deduced that no constitutive nitrilase activity was present in *R. rhodochrous* A29, A99 and ATCC BAA-870.

The TLC analysis conducted after DMF induction shows that all three *R. rhodochrous* strains produced the same compound as they have the same R_f value. After comparison to the positive control, it suggests that this product is benzoic acid. Thereby suggesting that DMF has induced nitrilase production in all three strains. When induced, *R. rhodochrous* ATCC BAA-870, once again, showed the production of benzamide along with benzoic acid.

Charsley and co-workers (2006) determined the melting point of several organic compounds, with near-equilibrium conditions, including benzoic acid which was found to have a melting point of 122.41 °C. Barati and co-workers (2013) acquired a melting point of 121-123 °C for benzoic acid and Epishina and co-workers demonstrated that benzoic acid begins to melt at 121 °C and completely melts at 122 °C. The melting point of the benzoic acid produced by both *R. rhodochrous* A29 and A99 was 119 – 123 °C and that of *R. rhodochrous* ATCC BAA-870 was 118 – 123 °C. The previous research shows a smaller melting range meaning they obtained a reasonably pure form of benzoic acid. All three strains produced benzoic acid which had a range equal to or less than 5 °C. Small traces of impurities, such as ethyl acetate or the red

pigment in *R. rhodochrous* may account for the greater divergences observed here (Tao *et al.*, 2009). These impurities can be avoided by allowing the products to be dried completely by a vacuum pump for several hours after concentrating the product with the Büchi Rotavapor® R II. The red pigmentation can be avoided by lysing the cells and extracting the protein instead of using whole cells (Tao *et al.*, 2009).

The benzoic acid synthesised by *R. rhodochrous* A29, A99 and ATCC BAA-870 had similar FT-IR spectra as all the specific bond types fell within the same range of each other in all three spectra. The O–H bonds fell between 3300-2300 cm^{-1} in all three spectra. This is the expected range for an O–H bond in a carboxylic acid. The aromatic (C–H) bonds were located in the O–H bond region, as a small peak at 3017 cm^{-1}. Aromatic C–H bonds and C–H bonds for non-aromatic compounds have a peak in different regions on the spectra due to hybridisation (Gable, 2006). Therefore, aromatic C – H bonds can be identified. The aromatic C=C bonds had two small peaks at 1601 cm^{-1} and 1582 cm^{-1} for *R. rhodochrous* A29 and A99 spectra (Fig. A7 & A8) but 1601 cm^{-1} and 1583 cm^{-1} for benzoic acid from *R. rhodochrous* ATCC BAA-870. The C=O bond had a long, sharp peak at 1677 $cm^{-1}$for *R. rhodochrous* A29, 1678 for *R. rhodochrous* A99 and 1681 for *R. rhodochrous* ATCC BAA-870. All the required bonds for benzoic acid are present and fall within the correct regions according to Gable (2019). These results portray the compound present in all three spectra as aromatic with a carboxylic acid functional group. This confirmed a benzoic acid structure which indicated the presence of nitrilases after DMF induction.

Benzoic acid has six protons and seven carbons in total. Therefore, NMR spectra must display six protons and seven carbons in the correct chemical shift regions in order to confirm the synthesis of benzoic acid by a nitrilase in all three *R. rhodochrous* strains. The ^{1}H NMR spectra for benzoic acid produced by a nitrilase from *R. rhodochrous* A29, *R. rhodochrous* A99 and *R. rhodochrous* ATCC BAA-870 presented similar peaks. However, the exact chemical shift values differed for each spectrum. All three spectra displayed the OH group as a singlet which was more downfield than the other peaks. This is due to the O atom de-shielding the H atom by reducing the electron density around the nucleus. This occurs as the electronegativity of O is greater than H and therefore attracts the electrons from the H atom. Therefore, the nucleus has an increased chemical shift compared to other H atoms present in benzoic acid. However, the chemical shift for benzoic acid from both *R. rhodochrous* A29 and *R. rhodochrous* A99 fell in the 12.5 – 12.7 ppm region whereas benzoic acid from *R. rhodochrous* ATCC BAA-870

was observed at a chemical shift of 10. 72 ppm. Fortunately, it remains in the range where OH protons are expected to be located on an NMR spectrum.

The rest of the H atoms were found in their respective chemical shift regions for all three spectra. The two protons (H2 and H6) accounted for appeared as a multiplet with a chemical shift ranging between 7.95 – 8.25 ppm. This is due to the interference of their neighbouring protons. A triplet occurred which represented one proton (H4) with a coupling constant (*J* value) of 7.4 Hz and a chemical shift falling in the range of 7.55 – 7.63ppm. This is due to the signal interference of neighbouring protons causing coupling to occur (Diehl, 2008). The last two protons (H3 and H5) appeared as a triplet with peaks occurring with a chemical shift falling in the range of 7.42 – 7.50. However, the *J* values differed for each spectrum. A *J* value of 7.7, Hz, 7.6 Hz and 7.8 Hz were observed for benzoic acid from *R. rhodochrous* A29, *R. rhodochrous* A99 and *R. rhodochrous* ATCC BAA-870, respectively. These triplets occur when the signals of H3 are affected by H2 and H4 and when the signal of H5 is affected by H4 and H6. These ^{1}H NMR spectra confirm the presence of six protons. These chemical shift values correspond with the work done by Nikishin and co-workers (2009) as well as Matsusaki and co-workers (2012). Furthermore, the chloroform-*d* solvent is indicated by a singlet peak and has a chemical shift of 7.26 ppm in all three spectra. This is peak was observed in the correct chemical shift region (Yuan *et al.*, 2017).

The ^{13}C NMR spectra show the present C atoms from benzoic acid produced by a nitrilase from *R. rhodochrous* A29, *R. rhodochrous* A99 and *R. rhodochrous* ATCC BAA-870. All three spectra displayed peaks with extremely similar chemical shifts respective to the appropriate C atom. The C atom in the carbonyl group (C7) was observed at a chemical shift of ~172 ppm. This down-field location is due to the de-shielding effect of O. This carbonyl group location agrees with the range (160 – 220 ppm) where carbonyls are generally located (Diehl, 2008). A peak with a chemical shift of 171.45 ppm was present on the ^{13}C NMR spectrum for *R. rhodochrous* ATCC BAA-870. However, this can be attributed to the presence of ethyl acetate. The short single peak represents the next carbon (C4), in the para-position of the carbonyl group, was observed at a chemical shift of ~133 ppm. A single tall peak with a chemical shift of ~ 130 ppm represents two carbons (C2 and C6) as they share the same environment. This is due to the taller height of the peak compared to shorter peaks. This is also the case for C3 and C5 which have a tall single peak with a chemical shift of ~ 128 ppm. Lastly, one short peak, representing one C atom (C1) has a chemical shift of ~ 129 ppm. Therefore, ^{13}C NMR showed

that a total of seven carbons were present in all three spectra with chemical shifts that correspond with the work done by Scott (1972), Nikishin and co-workers (2009) and Novak and co-workers (1995). Furthermore, the three chloroform-*d* solvent peaks present have a chemical shift of 77.39, 77.08, 76.76 ppm; 77.42, 77.10, 76.79 ppm and 77.48, 77.16 and 76.84 ppm. According to Yuan (2017), the chemical shift for chloroform-*d* solvent in ^{13}C NMR spectra should fall at ~ 77 ppm. Therefore, these chemical shifts fall within the correct range. These NMR results confirm the presence of benzoic acid synthesised by a nitrilase in all three strains.

During the synthesis of benzoic acid 1 kg of wet cell paste could produce ~19.2 mol/kg/h (*w/w*) giving a productivity of 2.34 kg/kg/h (*w/w*). Since ~ 6 – 7 g of wet cell paste can be produced in a 1.2 L benchtop bioreactor in 72 hours then large quantities of benzoic acid can be produced and extracted for commercial use when produced in an industrial size bioreactor. However, in *R. rhodochrous* ATCC BAA-870, not all 960 µmol of benzonitrile was converted to benzoic acid as benzamide was formed due to the presence of a nitrile hydratase. Therefore, further studies, such as HPLC, could be performed to determine the specific activity and the rate of conversion of the nitrilase from this strain. Furthermore, heterologous expression could be used to increase the rate of enzyme production thereby allowing larger amounts of enzyme production in a shorter time frame.

2.6 CONCLUSION

Dimethylformamide was confirmed to induce nitrilase expression in *Rhodococcus rhodochrous* strains A29, A99 and ATCC BAA-870. The TLC analyses indicated that no nitrilase was expressed in uninduced *R. rhodochrous* A29, A99 and ATCC BAA-870 suggesting that nitrilases are not constitutively synthesised by these strains. Further, TLC analyses detected the presence of a synthesised compound by DMF-induced *R. rhodochrous* A29, A99 and ATCC BAA-870. This compound was determined to be an aromatic carboxylic acid by FT-IR spectroscopy. The NMR spectra showed that the compound has six protons and seven carbons present, thereby confirming the presence of benzoic acid as the product formed from benzonitrile. In addition, a 100 % bioconversion of benzonitrile (960 µmol) to benzamide was observed as well as a minimum enzyme activity of 32 U. Therefore, the results of TLC, FT-IR spectroscopy and NMR spectra all indicate the bioconversion of benzonitrile to benzoic acid by nitrilases from DMF-induced *R. rhodochrous* A29, A99 and ATCC BAA-870. Since

DMF is commercially appealing, it can be studied further as a nitrilase inducer for alternative organisms hosting the nitrilase pathway.

2.7 RECOMMENDATIONS

In future, high-performance liquid chromatography (HPLC) can be performed to determine the exact concentration of benzoic acid synthesised after the bioconversion of benzonitrile as well as the rate of conversion. This will indicate the specific enzyme activity of the nitrilase. Transformation of *E. coli* BL21 (DE3) can be executed for heterologous protein expression. Optimisation of nitrilase expression should be studied and implemented in order to produce high levels of nitrilase efficiently using DMF as an inducer. In addition, various substrates should be tested to determine the substrate range of the nitrilase produced by each strain.

CHAPTER 3:

HETEROLOGOUS EXPRESSION OF A NITRILE HYDRATASE

3.1 INTRODUCTION

Virtually every division of the biological field uses recombinant-DNA technology whereby genes of interest are expressed using the cellular machinery of an alternative host (Lodish *et al.*, 2000). The end goals are to 1) perform reverse genetics where novel genes are identified from proteins with products that have not yet been isolated. 2) Use known gene products in order to study their regulation and functions. 3) Study and amend genetic defects. 4) Use heterologous expression of foreign genes, such as disease-resistance genes, to aid in disease-susceptible hosts. 5) Produce vast quantities of a product of interest, for example, antibiotics and enzymes for bioconversion as well as for bioremediation (Carroll, 1993). These goals are met by extracting a gene of interest using restriction enzymes. This gene can then be modified after which it is amplified using polymerase chain reaction (PCR). This gene is then inserted into a vector which is placed into another host such as *E. coli* which will express the required gene (Lodish *et al.*, 2000; Li *et al.*, 2013; Hoseini & Sauer, 2015; Khan *et al.*, 2016). Additionally, *E. coli* BL21 (DE3) strain is most commonly used in heterologous expression due to its lack of proteases which would degrade the protein of interest if it were produced, and it is used with the T7-pET system whereby induction occurs by using IPTG (Hausjell *et al.*, 2018).

The production of nitrile hydratases via heterologous protein expression was successfully undertaken by Pei and co-workers (2014). The iron-containing nitrile hydratase gene from *Pseudomonas putida* F1 was expressed when cloned in *E. coli* BL21 (DE3) with an activator protein. The resulting iron-containing nitrile hydratase enzyme demonstrated a broad substrate specificity where the degradation of aromatic-nitriles, such as 3-cyanopyridine, 4-cyanopyridine and benzonitrile, was effective. Furthermore, the presence of the activator was paramount for effective, soluble nitrile hydratase expression and activity. However, some chaperone proteins can be used when the activator gene is absent (Pei *et al.*, 2014).

The α and β subunits of the iron-containing nitrile hydratase from *Rhodococcus equi* TG328-2 were cloned and expressed in *E. coli* BL21 (DE3) by Rzeznicka and co-workers (2010). The IPTG inducible vectors pET21a and pET28a were used with a T7-RNA polymerase expression system instead of rhamnose inducible vectors (Rzeznicka *et al.*, 2010). This was due to the lack of nitrile hydratase expression when using rhamnose inducible vectors. This resulted in high levels of the nitrile hydratase being produced. However, a two-construct system had to be employed as the activator protein was not detected when the genes were cloned in the same plasmid as the protein subunits (Rzeznicka *et al.*, 2010). Therefore, the activator was cloned onto a separate plasmid and the *E. coli* BL21 (DE3) was transformed using both plasmids which resulted in the maximum amount of a nitrile hydratase, as a soluble protein, and maximum nitrile hydratase activity compared to previous attempts (Rzeznicka *et al.*, 2010).

Frederick (2013) designed a two-construct system to heterologously express cobalt-containing nitrile hydratase from *Rhodococcus rhodochrous* ATCC BAA-870 in *E. coli* BL21 (DE3) by using pRSFDuet-1 and pET21a (+) as expression vectors. The alpha subunit of the nitrile hydratase was cloned with the chaperone protein on a pRSFDuet-1 vector and the beta subunit of the nitrile hydratase was cloned onto the pET21a (+) vector. This two-construct system proved to be successful for the expression of nitrile hydratase from *R. rhodochrous* ATCC BAA-870. Therefore, this method was used by Schmid (2020) to transform *E. coli* BL21 (DE3) which are used in this study.

3.2 AIM AND OBJECTIVES

3.2.1 Aim

1) To heterologously express a nitrile hydratase from transformed *E. coli* cells.

3.2.2 Objectives

1) To culture and induce transformed *E. coli* BL21 (DE3) cells hosting a cobalt nitrile hydratase gene, in a bioreactor.

2) To quantify the total proteins present in each culture.

3) To test that the nitrile hydratase was expressed.

3.3 METHODS AND MATERIALS

3.3.1 Organisms

The transformed *E. coli* BL21(DE3) cells used in this study were transformed using a heat shock method by Schmid (2020). The *E. coli* BL21(DE3) cells were used to host both plasmids (pRSFDuet-1 and pET-21a(+)), containing the chaperone protein, alpha and beta subunits, using a two-construct system. The gene coding for the alpha subunit and the chaperone protein were inserted into the second multiple cloning site (MCS) of the pRSFDuet-1 plasmid as a single construct. These genes were placed in between the *Nde*l and *Pac*l restriction sites. The gene coding for the beta subunit was inserted into the pET-21a (+) plasmid at the MCS between the *Nde*l and *Xho*l restriction sites. In addition, a carboxyl-terminal (C-terminal) His-tag was incorporated as the native stop codon from the gene was removed.

The plasmid maps are presented in Fig. 3.1 and Fig. 3.2. In order to optimise expression, the ribosome binding site (RBS) was removed from both the alpha and beta subunits (Frederick, 2013; Schmid, 2020). Therefore, these sequences were inserted into the plasmid from their start codon. However, since the chaperone coding sequence is within the alpha subunit, its RBS was not removed. In addition, these plasmids also contained the gene for kanamycin and ampicillin resistance as a selectable marker (Schmid, 2020).

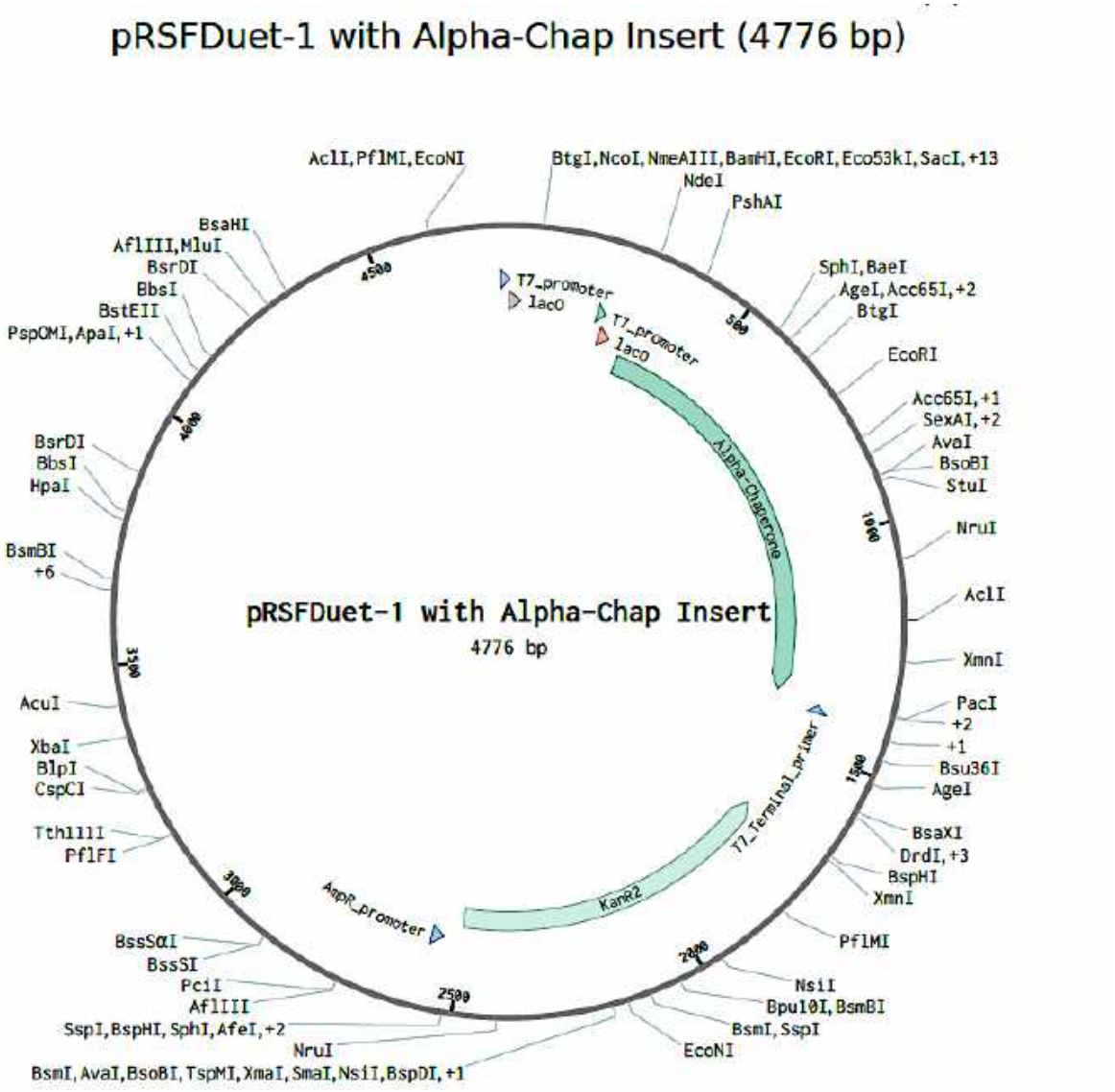

Figure 3.1: Plasmid Map of pRSFDuet-1. This map depicts the pRSFDuet-1 plasmid containing both genes coding for the alpha subunit of the nitrile hydratase and its chaperone protein. They were inserted into the plasmid at the second MCS between the *Nde*I and *Pac*I restriction sites (Schmid, 2020).

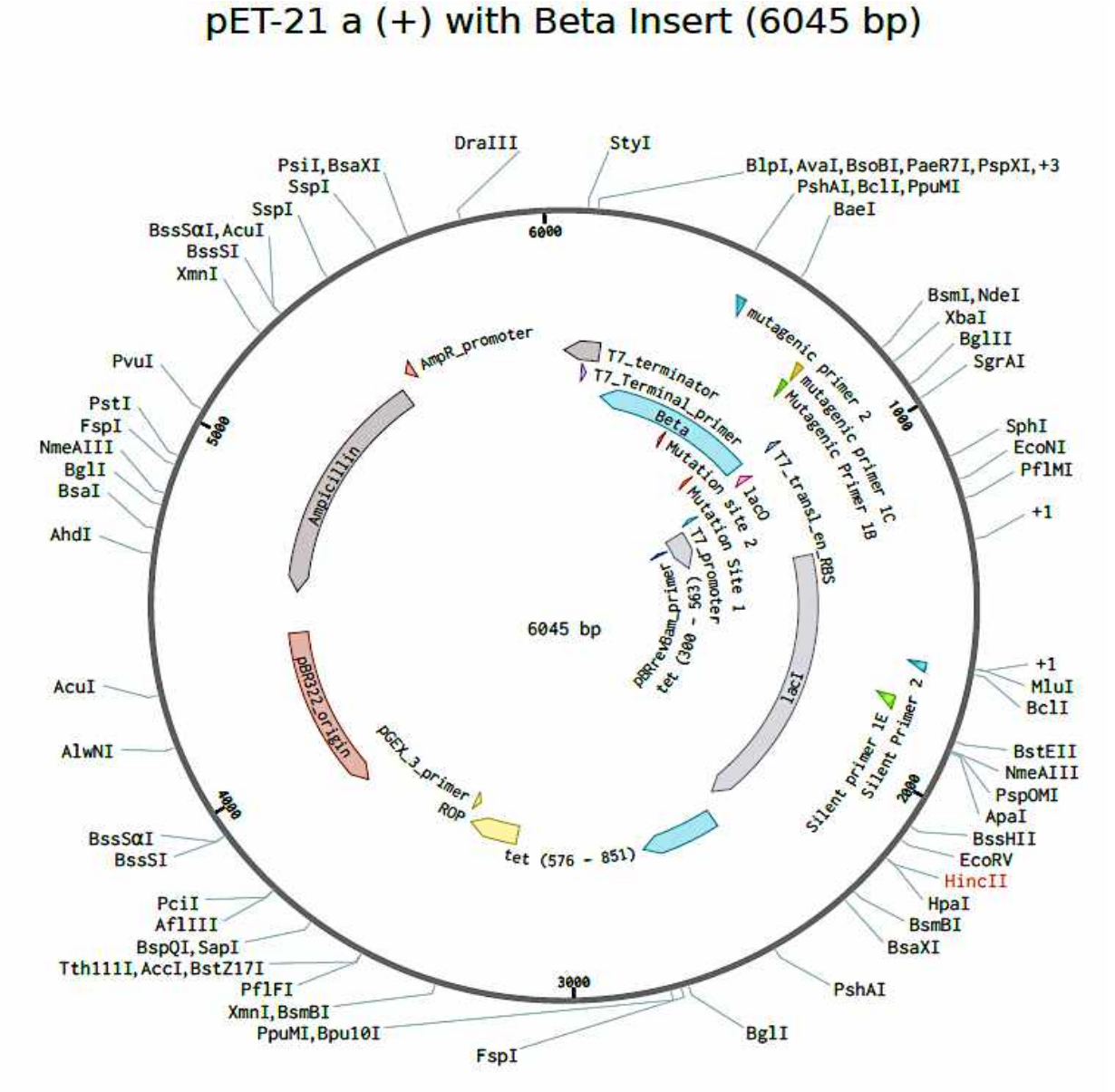

Figure 3.2: Plasmid Map of pET-21a(+). This map depicts the pET-21a(+) plasmid containing genes coding for the beta subunit of the nitrile hydratase. They were inserted into the plasmid at the MCS between the *Nde*I and *Xho*I restriction sites (Schmid, 2020).

3.3.2 Biomass Production and Induction

3.3.2.1 Pre-Culture

Cryopreserved *E. coli* BL21(DE3), containing the nitrile hydratase encoding plasmids, were streaked on a Petri dish containing Luria Bertani (LB) agar (5 g/L of NaCl (Merck Chemicals

®, Batch # 1026871), 5 g/L of yeast extract, 10 g/L tryptone (Sigma-Aldrich®, Batch # SLBR3816V) and 1 % (*w/v*) agar) amended with 50 µg/mL kanamycin and 100 µg/mL ampicillin and incubated at 37 ºC overnight (approximately 16 hours). Next, a single colony was used to re-streak a new LB agar plate amended with 50 µg/mL kanamycin and 100 µg/mL ampicillin. This was incubated under the same conditions. A single colony was used to inoculate 5 mL of LB broth containing 50 µg/mL kanamycin and 100 µg/mL ampicillin. This was then left on a shaker at 180 rpm overnight at 37 ºC. Once the *E. coli* BL21(DE3) was grown, 3 mL of the latter culture was used to inoculate 200 ml of LB broth containing 50 µg/mL kanamycin and 100 µg/mL ampicillin, in a 2 L Erlenmeyer flask and incubated at 180 rpm at 37 ºC overnight. Each step was aseptically performed and included a control to ensure no contamination occurred. A control of *E. coli* BL21(DE3) was pre-cultured at the same conditions, excluding antibiotics.

3.3.2.2 Biomass Production

In order to increase the biomass to 1.2 L, a 2 L bioreactor with 1 L of LB broth was employed. Once the LB broth was placed in the bioreactor, it was autoclaved at 121 ºC for 20 minutes. The 200 mL culture from the pre-culturing phase was aseptically pumped into the bioreactor with the following parameters for biomass production: pH of 7.0, 37 ºC incubation temperature, agitation at 600 rpm and a gas flow of 3.0 L/m. The absorbance (OD_{600}) was measured every hour using a Boeco Germany S-20 Spectrophotometer. The culture was grown to an absorbance (OD_{600}) of ~ 0.3 after which the cells were induced and grown until the stationary growth phase was reached. A separate batch of transformed *E. coli* BL21(DE3) was cultured under the same conditions excluding cellular induction. As a control, *E. coli* BL21(DE3) was grown using the same bioreactor parameters without the use of antibiotics or induction.

3.3.2.3 Induction

In order to induce protein expression from the *lac* operon, 0.1 mM IPTG and 0.1 mM cobalt chloride ($CoCl_2$) were added when the cells reached an absorbance (OD_{600}) of ~ 0.3. The following bioreactor conditions were selected for biomass production after induction: pH of 7.0, 25 ºC incubation temperature, agitation at 600 rpm and a gas flow rate of 3.0 L/m in. The absorbance was measured every hour and the cells were removed once the stationary growth phase was reached. When inducing the *lac* operon, several inducers such as thiomethyl galactosidase (TMG), IPTG, lactose and allolactose can be used to bind to the *lac* repressor.

Here, IPTG is used at a concentration of 0.1 mM to ensure that enough IPTG is present for the induction of protein expression without inhibiting cellular growth (Larentis *et al.*, 2014). $CoCl_2$ was also added during induction as a metal source for the cobalt-containing nitrile hydratase (Nojiri *et al.*, 2000).

At the end of these procedures three types of biomass were obtained:

1) Uninduced *E. coli* BL21 (DE3) cells lacking the nitrile hydratase coding plasmids (control).

2) Uninduced-transformed *E. coli* BL21 (DE3) cells containing the nitrile hydratase coding plasmids.

3) Induced-transformed *E. coli* BL21 (DE3) cells containing the nitrile hydratase coding plasmids.

3.3.3 Cell harvesting and Storage

Once the stationary phase was reached, the cells were harvested by centrifuging at 3,836 × g (5,000 rpm) for five minutes at 4 ºC in a Sorvall™ RC 6+ Centrifuge. Approximately 4 – 6 g of wet cell paste was harvested for the plasmid-free uninduced *E. coli* BL21(DE3), uninduced-transformed *E. coli* BL21(DE3) and induced-transformed *E. coli* BL21(DE3). The wet cell paste was then stored at – 4 ºC in sterile Falcon tubes in 1 g aliquots.

3.3.4 Cell Lysis

In order to ensure lysis of the cell wall, bacterial protein extraction reagent (B-PER™) and a QSonica Sonicator ($Model_{CL-18}$; Serial Number: 2016080399) were used in conjunction. A 4 mL volume of B-PER™ (Thermo Fisher Scientific®, Batch # UCZ279161) was used per gram of wet cell paste. In this study, 0.5 g for each biomass was used. The cells were repeatedly pipetted up and down until a homogenous mixture was achieved. Subsequently, this mixture was sonicated under the following parameters: 20 % amplification, 5 seconds pulse on followed by 10 seconds pulse off run for 30 cycles. This was repeated twice with a 30-second rest in between. Once the cells were lysed, the lysate was immediately centrifuged at 15,000 × g (9,900 rpm) for 5 minutes at 4 ºC in a Sorvall™ RC 6+ Centrifuge.

3.3.5 Protein Quantification

A Qubit™ 2.0 fluorometer (Invitrogen, USA) was used to establish the concentration of total proteins present. A volume of 20 uL of the sample was added to a working solution of Qubit reagent (Thermo Fisher Scientific®, Batch # 2018269) diluted at a 1:200 ratio in Qubit buffer (Thermo Fisher Scientific®, Batch # 2018269) solution in Qubit assay tubes (cat. # Q32856). This mixture was then vortexed for 2 – 3 seconds and incubated at 25 ºC for 15 minutes. The tubes were then inserted in the Qubit™ 2.0 fluorometer and readings of the stock concentration were recorded.

3.3.6 Nitrile Hydratase Activity Assay

Benzonitrile was used as a substrate to determine if nitrile hydratase activity is present in the untransformed-uninduced *E. coli* BL21 (DE3) control, uninduced-transformed *E. coli* BL21 (DE3) and induced-transformed *E. coli* BL21 (DE3). A volume of 1 µL of benzonitrile and 180 µL of 50 mM Tris buffer (pH of 7.6) was added for every mg of wet cell paste and µL of the cell lysate used. In this experiment, 100mg wet cell paste and 100 uL of cell lysate were used. The mixture was then incubated for 30 minutes at 25 ºC on a shaker rotating at 180 rpm. This experiment was performed for both the whole cells before lysis and the cell lysate procured after lysis to ensure the presence of a nitrile hydratase both before and after lysis.

3.3.6.1 Thin-Layer Chromatography

In order to determine how many compounds are present in a mixture the TLC method is used. Each functional group determines the polarity of a compound which affects the R_f depending on the solvent used. Here, both a nitrile and an amide are run on the plate, which are both polar molecules. Therefore, 60 % hexane (non-polar) and 40 % ethyl acetate (polar) was found to be a good solvent ratio. After the nitrile hydratase activity assay was complete, thin-layer chromatography (TLC) was performed to determine if a product had been synthesised by a nitrile hydratase. Acrylamide and benzonitrile were used as positive controls (Fig. 3.3) to determine where an amide and benzonitrile would be present on the TLC plates when using 60 % hexane and 40 % ethyl acetate as the solvent. This was performed for nitrile hydratase activity assay with cells before lysis and the cell lysate.

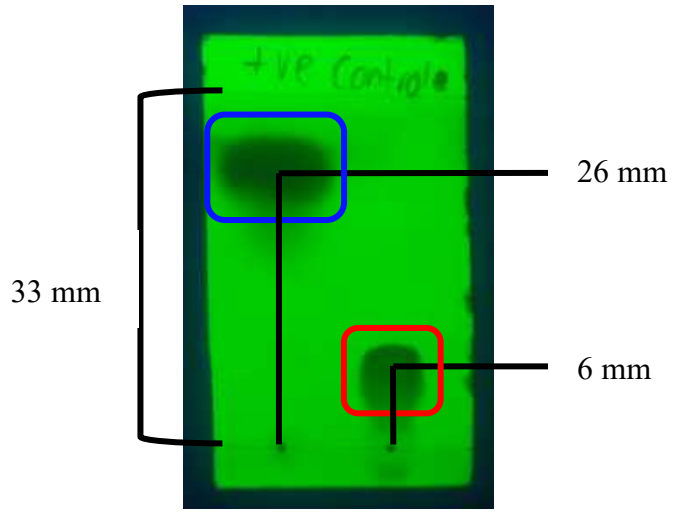

Figure 3.3: Positive Control TLC Plate Under UV Light. The solvent, 40 % ethyl acetate/hexane, travelled 33 mm up the TLC plate. **Spot 1** represents benzonitrile (Blue) with an R_f= 0.79 as it travelled 26 mm**. Spot 2** represents acrylamide (Red) with an R_f = 0.18 which travelled 6 mm.

3.3.6.2 Liquid-Liquid Extraction

In order to extract the synthesised benzamide from the reaction, an ethyl acetate/water extraction was performed. The nitrile hydratase assay reaction was mixed with dH_2O until a total volume of 20 mL had been reached. A 100 mL separation column was then used which contained 20 mL of ethyl acetate and the dH_2O mixed with the reaction. The separation column was shaken in order to allow benzamide to dissolve in the solvent phase. The aqueous phase and the solvent phase were then separated. Afterwards, one teaspoon (approximately 3 – 5 g) of $MgSO_4$ anhydrous was mixed into the solvent phase as a drying agent. In order to remove the $MgSO_4$ anhydrous, the mixture was filtered by using a paper filter (Boeco Germany, Batch # 16-020) while the remains were collected in a round bottom flask. Furthermore, a Büchi Rotavapor® R II was used to concentrate the product by eliminating all traces of ethyl acetate.

3.3.6.3 Melting Point Analysis

A Stuart® SMP10 Melting Point Apparatus was used to determine the melting point of the benzamide product synthesised during the nitrile hydratase assay. The temperature was recorded once the solid had started to show signs of melting and when the solid was entirely liquid. This is done to obtain a temperature melting range in order to determine the purity of the compound.

3.3.6.4 Fourier-Transform Infrared Spectroscopy

Fourier-Transform Infrared (FT-IR) spectroscopy was performed using the Bruker Tensor 27 FT-IR system & OPUS data collection program (version 6.5) in order to confirm the presence of benzamide. This was done by establishing the present functional groups as this technique aids in the identification of compounds (Mollaoglu *et al.*, 2018). For benzamide, aromatic bonds, a carbonyl group and NH_2 bonds were expected to be found.

3.3.6.5 Nuclear Magnetic Resonance Spectroscopy

Nuclear magnetic resonance spectroscopy was used to determine the structure of the product as well as its purity. Since the synthesised product was soluble in dimethyl sulfoxide (DMSO-d_6) DMSO (Merck Chemicals ®, Batch # 91624522), it was used as the solvent. Next, 256 proton scans and 2048 carbon scans were run by employing a Bruker 400 MHz NMR for proton and carbon scans. The benzamide compound is expected to have seven protons and seven carbons in total.

3.3.6.6 High Resolution-Mass Spectroscopy

HPLC is used to separate the compound with (Mass Spectroscopy/ Mass Spectroscopy) MS/MS acting as the detector. This method is preferred over other detectors due to its high sensitivity and specificity (Pitt, 2009). Electrospray ionisation is used to ionise the compounds. Therefore, compounds are detected at their molar mass + H (positive mode). In this work, High Resolution-Mass Spectroscopy (HRMS) was performed, in positive mode, to determine the exact mass of the product. Since benzamide has a molar mass of 121.14 g/mol a peak of ~ 122 g/mol was expected. This was performed on a Bruker compact 8255754.20116 using the Bruker Compass Data Analysis (Version 4.3) software package.

3.3.6.7 High-Performance Liquid Chromatography

An HPLC-MS/MS apparatus was used in order to establish the exact concentrations of benzamide and benzonitrile in the reaction. First, a nitrile hydratase assay was performed with the cell lysate, as described in section 3.3.6, and the reaction was stopped after 15 minutes using 0.2 mL of 1.0 M HCl. The resultant products were then run through two available reverse phase columns (50 x 2.10 mm Phenomenex and Thermo Scientific C18 2.1 x 50 mm). After ionisation, benzamide is expected to be identified at a peak of ~ 122 g/mol and benzonitrile at

~ 104 g/mol. The mobile phase consisted of HPLC gradient grade acetonitrile (VWR Chemicals®, Batch # 17J301493) and sterilised distilled water. In addition, formic acid was added in order to aid with the ionisation of benzonitrile. Various flow rates and ratios of the mobile phase were evaluated during method development.

3.3.7 Calculations

3.3.7.1 Growth Rate

The exponential growth phase of each culture was used to create a line of best fit in a log absorbance OD_{600} vs time graph in order to calculate the growth rate (μ). The growth rate for each resultant biomass was calculated using the following equation by Widdel (2007).

$$\mu = \frac{2.303\ (Log10(OD_2) - Log10(OD_1))}{(Time_2 - Time_1)}$$

3.3.7.2 Statistical Analysis

The growth rates of both cultures containing the plasmid coding for a nitrile hydratase were compared in order to determine if the addition of 0.1mM $CoCl_2$, during induction, hindered the growth rate of the culture in a significant manner. Using the exponential portion of the recorded absorbance (OD_{600}) for both cultures (Table B1, Appendix B) both Levene's test (F-Test: Two-Sample for Variances) and well as a t-Test (Two-Sample Assuming Equal Variances) were conducted using the Analysis ToolPak in Microsoft® Excel (Version 16.37). A significant P-value ($P \leq 0.05$) is indicated by the use of an asterisk (*). In addition, the significance level used is 0.05 ($\alpha = 0.05$).

3.3.7.3 Number of Moles

The number of moles present in 100 μL of benzonitrile (99 %) used during the nitrile hydratase assay was calculated using the following equation:

$$Moles\ (mol) = \frac{Mass\ (g)}{Molar\ Mass\ (g/mol)}$$

3.3.7.4 Enzyme Activity

Once µmol of the substrate was determined, the minimum enzyme activity could be calculated with the following equation:

$$Enzyme\ Activity\ (U) = \frac{\mu mol}{Minutes}$$

3.3 RESULTS

3.4.1 Growth Curve

Uninduced-untransformed *E. coli* BL21 (DE3) was grown in a bioreactor for a total of 16 hours at a constant temperature of 37 ºC (Fig. 3.3, Table B1). Exponential growth began at approximately one-hour post-incubation and lasted for eight hours. The cells were then removed after 16 hours when the stationary phase had been reached. Both the induced and uninduced transformed *E. coli* BL21 (DE3) were grown, for a total of 24 hours. Once these cultures reached an absorbance of OD_{600} ~ 0.3 the temperature was decreased to 25 ºC. For the uninduced-transformed *E. coli* BL21 (DE3) a lag phase of six hours and exponential phase of 11 hours were observed. The other batch of transformed *E. coli* BL21 (DE3) was induced with 0.1 mM of IPTG and $CoCl_2$ when the temperature was decreased to 25 ºC. A lag phase of seven hours was observed for the latter culture followed by an exponential phase of 10 hours. The death phase was not reached for any batch cultures. The wet cell weight produced by each culture, from 1.2 L of LB media, was: 4.78 g of *E. coli* BL21 (DE3), 6.65 g of transformed-uninduced *E. coli* BL21 (DE3) and 6.34 g of transformed-induced *E. coli* BL21 (DE3).

The null hypothesis was accepted for Levene's test thereby representing homogenous data. No significance (P(T<=t) = 0.63) was found between the growth rates of cultures containing the nitrile hydratase coding plasmids (Table 3.1). Therefore, the addition of 0.1mM of IPTG and $CoCl_2$ has no significant effect on the growth rate.

Table 3.1: Growth Rate *Escherichia coli* BL21 (DE3) Cultures per Hour and % per Hour

Bacteria	Contain Plasmids	Induced	Growth Rate ($hour^{-1}$)	Growth Rate (%/hour)
***E. coli* BL21 (DE3)**	No	No	0.2871	28.71
	Yes	No	0.1850	18.50
	Yes	Yes	0.2185	21.85

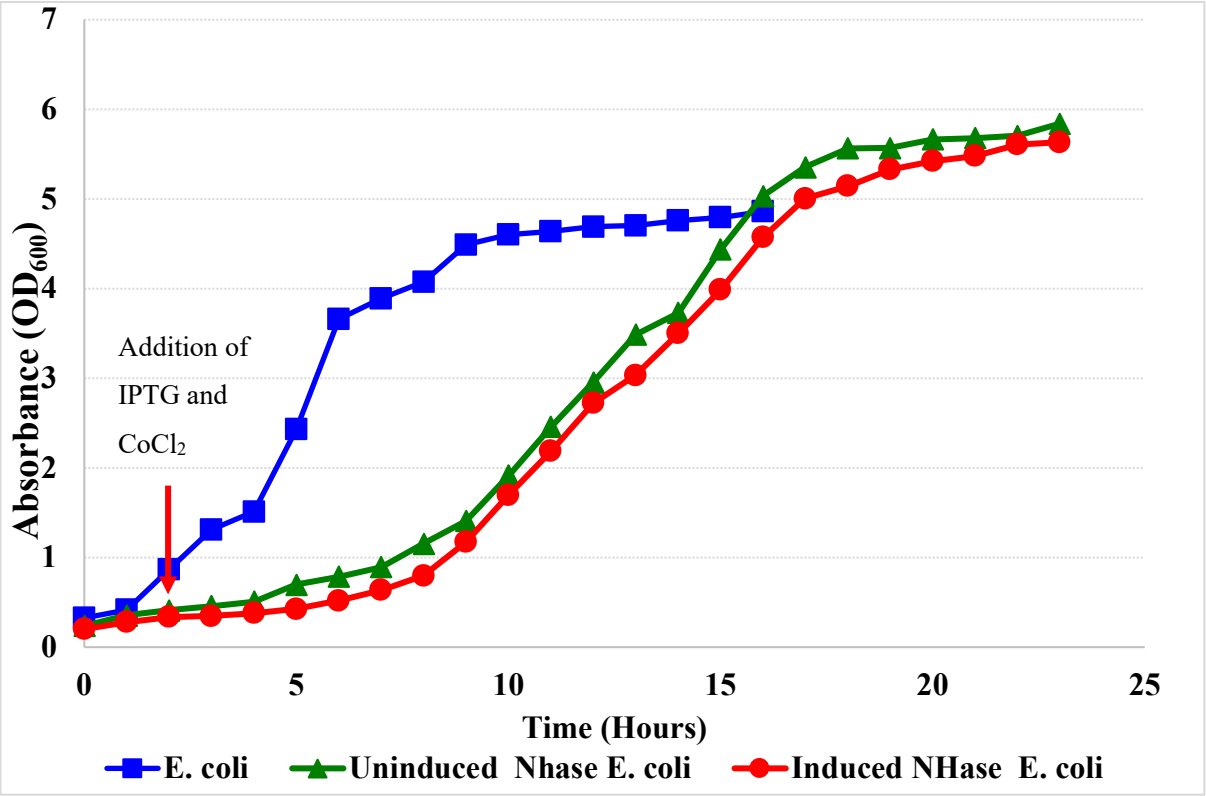

Figure 3.4: Growth Curve for the Differently Treated *Escherichia coli* BL21(DE3) Cultures used in the Study. The absorbance (OD_{600}) was recorded every hour for each culture. For the transformed-induced *E. coli* BL21 (DE3) induction took place after two hours (OD_{600} = 0.336) (red arrow) and the temperature was decreased to 25 ºC for the next 21 hours.

3.4.2 Benzamide Synthesis

3.4.2.1 Thin-Layer Chromatography

Before cell lysis, a nitrile hydratase activity assay was performed for *E. coli* BL21 (DE3), transformed-uninduced *E. coli* BL21 (DE3) and transformed-induced *E. coli* BL21 (DE3). The products were spotted on a TLC plate (Fig. 3.5). Only the substrate was present after the nitrile hydratase assay from both untransformed-uninduced *E. coli* BL21 (DE3) and transformed-uninduced *E. coli* BL21 (DE3). Since this represents benzonitrile it suggests that no nitrile hydratase was present as the substrate was not converted. A product was synthesised by transformed-induced *E. coli* BL21 (DE3) as no substrate was present after the assay and a spot representing benzamide was present. Since this bioconversion was observed it suggests that a nitrile hydratase was present in the reaction. These exact results were produced, on the TLC plate, for the nitrile hydratase assay performed with the cell lysate (Fig. 3.6). This suggests that a soluble nitrilase hydratase was present after transformed-induced *E. coli* BL21 (DE3) cells were lysed.

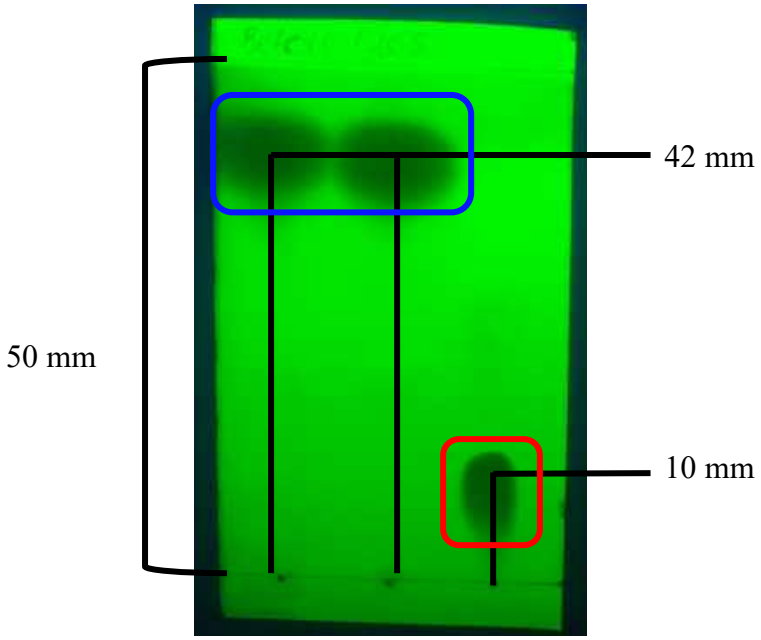

Figure 3.5: Products of Nitrile Hydratase Assay from Whole Cells, on a TLC Plate Under UV Light. The solvent, 40 % ethyl acetate/hexane, travelled 50 mm up the TLC plate. **Spot 1** represents benzonitrile (Blue) with an R_f = 0.84 as it travelled 42 mm. **Spot 2** represents benzonitrile (Blue) with an R_f = 0.84 which travelled 42 mm. **Spot 3** represents benzamide (Red) with an R_f = 0.20 which travelled 10 mm.

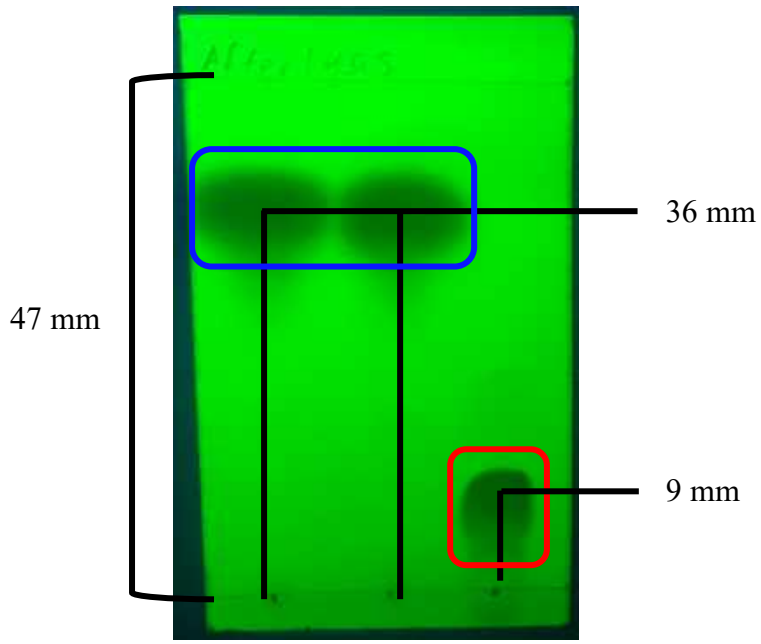

Figure 3.6: Products of Nitrile Hydratase Assay from Cell Lysate, on a TLC Plate Under UV Light. The solvent, 40 % ethyl acetate/hexane, travelled 47 mm up the TLC plate. **Spot 1** represents benzonitrile (Blue) with an R_f = 0.77 as it travelled 36 mm. **Spot 2** represents benzonitrile (Blue) with an R_f = 0.77 which travelled 36 mm. **Spot 3** represents benzamide (Red) with an R_f = 0.19 which travelled 9 mm.

3.4.2.2 Chemical Analytical Data for Benzamide

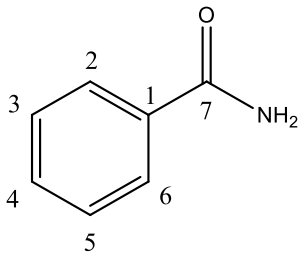

Rf = 0.19 (40 % Ethyl Acetate/Hexane); **Mp =** 126 – 128 °C; **IR(v_{max}/cm^{-1}):** 3363, 3163 (N–H_2); 1656 (C=O); 3065 (**Ar**C–H); 1577 (**Ar**C=C); **^{1}H NMR (400 MHz, DMSO-d_6):** δ 8.04 (s, 1H, NH), 7.93 – 7.81 (m, 2H,H2,H6), 7.56 – 7.49 (m, 1H, H4), 7.48 – 7.34 (m, 3H, H3,H5, NH); **^{13}C NMR (101 MHz, DMSO-d_6):** δ 168.51 (C7), 134.62 (C1), 131.73 (C4), 128.68 (C3&C5), 127.90 (C2&C6). **HRMS *m/z*:** calculated for C_7H_7NO: 121.14, found: [M+H]: 122.0777.

3.4.3 Benzonitrile Conversion

A total of 100 µL of cell lysate containing a nitrile hydratase and benzonitrile was used with 18 mL of Tris buffer (7.6 pH) for the nitrile hydratase assay. Since the resulting TLC plates (Fig. 3.5 & Fig. 3.6), NMR spectra (Fig. B1 & B2, Appendix B), and the FT-IR spectrum (Fig. B3, Appendix B) exhibit no presence of benzonitrile after the nitrile hydratase activity assay it suggests that 100 % of benzonitrile was converted. During the assay, 960 µmol of benzonitrile was present and was bio-converted to 960 µmol benzamide by a nitrile hydratase in 30 minutes. Therefore, at the end of the reaction, 960 µmol of benzamide was present. Every gram of wet cell paste produces ~ 2 mL of cell lysate after cell lysis. Since 100 µL of the cell-free extract produced 960 µmol of benzamide in 30 minutes then ~38.4 mmol of benzamide would be produced from 1.0 g of wet cell paste in an hour. Therefore, 1 kg of wet cell paste will afford ~38.4 mol/kg/h (*w/w*) at which a molecular mass of 121.14 g/mol would give a productivity of 4.65 kg/kg/h (*w/w*). In addition, a minimum of 32 U of the enzyme was required to catalyse the conversion of 1 µmol per minute. In order to determine the specific activity of the enzyme further tests, such as HPLC are required.

3.4.3.1 HPLC-MS/MS

The specific activity of the nitrile hydratase enzyme, encoded on the plasmids of the transformed-induced *E. coli* BL21(DE3), was determined using HPLC. Both columns presented unsuccessful results in the separation of benzamide from benzonitrile. Benzamide was identified at a peak of ~ 122 g/mol and benzonitrile at ~ 104 g/mol. Two peaks were present on the spectrum (Fig. B4, Appendix B) containing both compounds; this is due to splitting and not separation of the compounds as both the molar mass for both compounds were present in both peaks.

3.4.4 Protein Quantification

After lysis, the cell lysate was subject to protein quantification by an Invitrogen 2.0 Fluorometer Qubit™. The concentration (mg/mL) of total cellular proteins were detected (Table 3.2). There was an ~ 0.14 mg/mL increase in the concentration of total soluble proteins including a nitrile hydratase, present in the cell lysate from transformed-induced *E. coli*

BL21(DE3) compared to both untransformed-uninduced *E. coli* BL21(DE3) and transformed-uninduced *E. coli* BL21(DE3).

Table 3.2: Total Soluble Protein Concentration in *Escherichia coli* BL21(DE3)

Bacteria	Contain Plasmids	Induced	Total Soluble Protein Concentration
***E. coli* BL21 (DE3)**	No	No	1.89 mg/mL
	Yes	No	1.9 mg/mL
	Yes	Yes	2.13 mg/mL

3.5 DISCUSSION

During biomass production, all fermentations were stopped a few hours into the stationary phase and before the death phase. This is done to ensure that the maximum number of cells can be harvested and utilised. *E. coli* has the ability to grow over a range of ~ 40 °C (20 – 37 °C) (Farewell & Neidhardt, 1998). However, this bacterium has an optimum growth temperature of 37 °C. The untransformed-uninduced *E. coli* BL21(DE3) culture was grown for 16 hours as the stationary phase was reached faster than the other cultures as it was subjected to a constant temperature of 37 °C whereas the other cultures were lowered to 25 °C. The change in temperature is implemented to ensure correct folding of the protein which is important when attempting to produce soluble proteins (San-Miguel *et al.*, 2013). Since, two-construct systems whereby cells contain two plasmids, has been found to have a slower growth rate than those with one plasmid (Pei *et al.*, 2014), future studies should culture untransformed-uninduced *E. coli* BL21(DE3) which is initially grown at 37 °C and the temperature should be reduced to 25 °C when an OD_{600} = ~ 0.3 is reached. This should be conducted in order to determine if there is a significant effect on the growth rate depending on the presence of plasmids.

No significant effect was observed on the growth rate, after induction with 0.1mM IPTG and 0.1mM $CoCl_2$. These results are consistent with recent studies conducted by Han and co-workers (2020), whereby green fluorescent protein (GFP) was inserted on the expression plasmid in order to view expression. Acceptable concentrations of $CoCl_2$ are required to be less than 0.5mM. When increased, the concentration reached a toxic level which inhibited cell growth and gene expression as GFP expression was suppressed. Additionally, Han and co-workers (2020) observed that the highest expression levels occurred when cells were induced

at an OD_{600} = ~ 0.6. Therefore, future studies should attempt at inducing plasmids containing the nitrile hydratase gene at this level of cell density in order to optimise expression levels.

If the enzyme of interest is produced without the presence of an inducer, the expression is considered to be "leaky" (Briand *et al.*, 2016). In this study, leaky expression was not observed when testing for the presence of the enzyme in an uninduced culture hosting the plasmids. If leaky expression does occur it can be avoided if 1 % of glucose is added to the culture medium or if the plasmid codes for a T7 phage lysozyme, such as pLysS or pLysE, in an *E. coli* BL21strain (Grossman *et al.*, 1998; Stano & Patel, 2004). This will reduce the instability of the plasmid (Kang & Hoang, 2007).

In order to confirm the presence of a nitrile hydratase enzyme benzonitrile was used as the substrate during the nitrile hydratase activity assay as benzonitrile is expected to be hydrolysed into its corresponding amide (Asano *et al.*, 1982). If no enzyme was present then no reaction would take place and benzonitrile will still be present with no other observable spots. Before lysing the cells, nitrile hydratase activity assay was performed to confirm nitrile hydratase activity to ensure the plasmids and the method of induction and cell culturing were effective. Only the substrate was detected from both untransformed-uninduced *E. coli* BL21(DE3) and transformed-uninduced *E. coli* BL21(DE3) reactions. This is due to an absence of induction and an absence of the nitrile hydratase gene. However, transformed-induced *E. coli* BL21(DE3) formed a spot with the same R_f range as the amide in the positive control. An R_f of 0.3 for benzamide was determined by Maity and co-workers (2018). However, in this study, the R_f indices for amides in all TLC plates differed by 0.1. This may be due to the difference in the ratio of the mobile phase solvents. Maity and co-workers (2018) used 30 % ethyl acetate with 70 % hexane, making the mobile phase less polar than the solvent used here (40 % ethyl acetate and 60 % hexane). Therefore, the less polar the mobile phase, the higher the R_f value will be for amides.

After lysis, the same assay was run to ensure the protein of interest was soluble and present in the supernatant and not the pellet. The same results were observed for the nitrile hydratase activity assay both before and after lysis. When the compound formed was confirmed to be benzamide, it would indicate that a soluble nitrile hydratase enzyme had been successfully produced from the transformed-induced *E. coli* BL21(DE3) culture.

In order to confirm benzamide as the synthesised compound, the temperature at which benzamide melts at atmospheric pressure was established. The range from initial melting to the completely melted product was recorded as 126 – 128 °C. This shows a 3 °C range which is considered short, depicting a purer compound than a longer range (Allen, 1942). This is the same range was observed by Sathe and co-workers (2018) as well as Kuwabara and co-workers (2018). However, other researchers, such as You and co-workers (2017) and Hamed & Ali (2020) obtained a melting point range of 125-127 °C for benzamide while a higher melting point (127-129 °C) was observed by Srinivas and co-workers (2015). These differences can be attributed to the purity of each benzamide compound acquired, as well as the instrument used to determine the melting point.

The benzamide produced by transformed-induced *E. coli* BL21(DE3) shows a spectrum where the required amide bond types fell within the expected range (Gable, 2006). The N–H_2 bonds are portrayed as a scissoring peak with each point at 3363 and 3136 cm^{-1}. This is the expected range for peaks from an N–H bond in an amide (Poeschl & Mountford, 2014; Saha & Desiraju, 2018). The aromatic (C–H) bonds were located next to the N–H region, as a small peak at 3065 cm^{-1}. Aromatic C–H bonds and C–H bonds for non-aromatic compounds have a peak in different regions on the spectrum due to hybridisation (Gable, 2006). Therefore, the aromatic structure was confirmed in the compound. The aromatic C=C bonds had one peak, at 1577 cm^{-1}, next to the C=O bond which had a sharp peak at 1656 cm^{-1}. All the required bonds for benzamide were present and fell within the correct regions according to Gable (2019) and work conducted by Poeschl & Mountford (2014). These results establish the presence of an aromatic amide as the product.

Nuclear magnetic resonance spectroscopy aids in the confirmation, identification, purity and molecular structure of an organic compound. Both TLC and FT-IR spectroscopy indicate that the synthesised product, by transformed-induced *E. coli* BL21(DE3), is benzamide. The synthesised product had a ^1H NMR spectrum showing split peaks for the H atoms in the NH_2 group. Sathe and co-workers (2018) also obtained a split in NH_2 protons whereby one was found downfield of the peaks and the other upfield. This is due to the restricted rotation of the C–N amide bond (Quintanilla-Licea *et al.*, 2002). The first NH proton was observed as a singlet, more downfield that of the other peaks, in the 8.04 ppm region. This is due to the electronegativity of the N atom de-shielding H by reducing the electron density around the nucleus. Therefore, the nucleus has an increased chemical shift. Two protons (H2 and H6)

appeared as a multiplet with a chemical shift of 7.93 – 7.81 ppm. Another multiplet occurred representing one proton (H4) with a chemical shift of 7.56 – 7.49 ppm. The last three protons (H3, H5 and NH) appeared as a multiplet with a chemical shift of 7.48 – 7.34 ppm. These multiplets are due to the signal interference of neighbouring protons (Diehl, 2008). Therefore, ^{1}H NMR showed that a total of seven protons were present. These results agree with the NMR results, performed using the same solvent and frequency, by Fu and co-workers (2016) as well as Shimokawa and co-workers (2016).

The ^{13}C NMR spectrum shows the carbon from the carbonyl group (C7) of benzamide with a chemical shift of 168.51 ppm. This down-field location is due to the de-shielding effect of the electronegative O atom. This carbonyl group location agrees with the range (160 – 220 ppm) where carbonyls are generally located, (Diehl, 2008). The shorter peak with a chemical shift of 134.62 ppm represents one carbon (C1). The next carbon (C4), also with a short peak in the para-position of the carbonyl group, was depicted with a chemical shift of 131.73 ppm. The peak with a chemical shift of 127.90 ppm represents two carbons (C3 and C5) as they share the same environment. This is due to the tall height of the peak compared to shorter peaks. This also occurs for the last two carbons (C2 and C6) which have a chemical shift of 128.68 ppm. Therefore, ^{13}C NMR showed that a total of seven carbons were present and the chemical shifts correspond with the work done by Scott (1972). Furthermore, the three DMSO-d_6 solvent peaks present have a chemical shift of 40.46, 40.26, 40.05, 39.84, 39.63, 39.42 and 39.21 ppm. This corresponds to the work performed by Fu and co-workers (2016) which used the same NMR frequency and the same solvent. This confirms that benzamide was synthesised during the nitrile hydratase assay suggesting that a nitrile hydratase enzyme was successfully expressed.

HRMS uses an electric and magnetic field is to determine the molecular weight (mass) of a compound (Baghel *et al.*, 2017). This is done when the mass spectrometer generates ionised particles of the compound. Benzamide has a molar mass of 121.14. After ionisation, the mass was expected to be ~ 122.0, in positive mode. In this study mass of 122.0777 was observed which is the expected mass of benzamide.

During the conversion of benzonitrile to benzamide, approximately, 6 g of wet cell paste was produced in a 1.2 L, in a bioreactor in 24 hours. Therefore, large quantities of benzamide can be produced and extracted for commercial use. The minimum enzyme activity (32 U) expresses the minimum number of μmols, of the substrate, is converted per minute (Farrell & Taylor, 2005). During HRMS, the standard of benzamide and benzonitrile was detected at a mass of

122.0520 g/mol and 103.9535 g/mol, respectively. When testing the sample, benzonitrile required formic acid to aid in ionisation in order to read an expected mass of ~104 g/mol instead of 103 g/mol. In the HRMS spectrum, peak splitting occurred during the separation of benzonitrile and benzamide whereby two peaks were observed and contained both compounds. This can be due to several factors such as the different strengths of the injected solvent and the mobile phase, incorrect pore sizes in the column for the compound, a blocked or plugged frit which will distort the flow, a channel or a void existing in the stationary phase of the column and an overloading of the column (Bidlingmeyer, 2001). Due to a limited selection of columns, this experiment could not be repeated. In future, various columns such as the 4.6 x 250 mm or a Luna C18 column manufactured by Phenomenex can be utilised as Frederick (2013) as well as Kamble and co-workers (2012) have successfully separated these compounds using these columns.

In terms of the total protein concentration, determined by using a fluorescent dye that binds to any present proteins. The untransformed-uninduced control *E. coli* BL21(DE3) had a protein concentration (1.89 mg/mL) similar to that of transformed-uninduced *E. coli* BL21(DE3) (1.90 mg/mL). This is expected since this culture was not induced and did not show any leaky expression as no nitrile hydratase was present as deduced from previous tests. However, transformed-induced *E. coli* BL21(DE3) had an increase in the concentration of total proteins (2.13 mg/mL). This 0.14 mg/mL increase in protein can be partially attributed to cobalt-containing nitrile hydratase as the confirmation of benzamide proves that expression of nitrile hydratase was successful. In addition, the increase in protein is also caused by naturally occurring enzymes on the *lac* operon, β-galactosidase, lactose permease and thiogalactoside transacetylase. Therefore, the heterologous expression of nitrile hydratase was successful.

3.6 CONCLUSION

Transformed-induced *E. coli* BL21 (DE3) hosting plasmids coding for the *R. rhodochrous* ATCC BAA-870 nitrile hydratase gene and induced with IPTG and $CoCl_2$, was found to successfully produce a nitrile hydratase. This was confirmed by performing an enzyme assay with benzonitrile as the substrate and using TLC plates, melting point, NMR spectroscopy, HRMS and FT-IR spectroscopy to confirm the presence of benzamide formed by a nitrile hydratase. A 100 % conversion of benzonitrile was observed after 30 minutes. Therefore, 960 µmol was converted to 960 µmol of benzamide by a nitrile hydratase. This provides a minimum

enzyme activity of 32 U. Furthermore, no leaky expression was observed as there was no conversion of benzonitrile to benzamide observed in the enzyme essay when *E. coli* BL21(DE3) cells transformed with the nitrile hydratase plasmids but not induced with IPTG were utilized. This study may represent a suitable method of heterologous expression and production of nitrile hydratase for potential commercialisation.

3.7 RECOMMENDATIONS

In future, optimisation of nitrile hydratase expression should be explored to increase the yield of the enzyme at an efficient rate. It may be necessary to perform protein purification for commercial enzyme sales. A more robust HPLC approach may be able to provide a better insight into the specific activity of the heterologously expressed enzyme. Furthermore, testing the enzyme on various nitrile substrates to determine the substrate range of the enzyme should be conducted.

CHAPTER 4:

SUMMARY

The enzymes of importance in this paper are nitrilase and nitrile hydratase. Each enzyme provides a different pathway when hydrolysing nitriles in bacterial cells. This occurs as part of a detoxification pathway due to the toxic cyano functional group of nitriles. Nitrilase degrades the nitrile into a carboxylic acid whereas nitrile hydratase degrades the nitrile to an amide. The resulting compounds prove to be very useful in the chemical and pharmaceutical industries. The goal of this project was to successfully produce nitrile hydrolysing enzymes encoded by the bacterium, *Rhodococcus rhodochrous*. Each enzyme produced were encoded by genes naturally located in *R. rhodochrous* strains isolated from Gauteng, South Africa.

During nitrilase production, *R. rhodochrous* A29, A99 and ATCC BAA-870 were utilised. The aim was to culture these cells in a bioreactor and induce nitrilase using the cost-effective DMF compound. The growth rates of the control and DMF induced cells were compared and statistical analyses show that there was no significant difference in growth rates after the addition of 0.5 % (*v/v*) DMF. This suggests that a concentration of 0.5 % DMF in the culture, had no significant effect on the growth rate of the bacteria. This is a beneficial property of using DMF as an inducer in the future. Next, an activity assay was performed in order to determine if nitrilase was induced. Benzonitrile was used as the substrate and therefore benzoic acid was the expected product if nitrilase expression occurred. Several analytical chemistry tests were done to determine whether benzoic acid was produced. TLC plates were run, FT-IR and NMR spectroscopy were performed. TLC plates showed that a 100 % conversion of benzonitrile occurred in all three strains after DMF induction. The FT-IR spectroscopy spectra showed that an aromatic structure with a carboxylic functional group was present in the product of all three strains. In order to determine how many carbons and hydrogens were present in the compound, NMR spectroscopy was performed. A total of six hydrogens and seven carbons were found for the compound thereby confirming the presence of benzoic acid. In addition, the melting point for each product was within the correct range for benzoic acid. Since no benzonitrile was present in the products, 100 % of the substrate was converted to benzoic acid. A minimum enzyme activity of 32 U was calculated for the reaction and a total productivity of benzoic acid ~ 2.34 kg/kg/h (*w/w*) was determined.

During nitrile hydratase production, *E. coli* BL21 (DE3) hosting the plasmids encoding nitrile hydratase, from *R. rhodochrous* ATCC BAA-870, was used. The cells were also cultured and induced in a bioreactor. IPTG was used as an inducer and $CoCl_2$ was added as a metal source for the cobalt-containing nitrile hydratase enzyme. Controls of untransformed-uninduced *E. coli* BL21 (DE3) and transformed-uninduced *E. coli* BL21 (DE3) containing the nitrile hydratase gene were also cultured separately in the bioreactor. Activity assays were performed with benzonitrile as the substrate. TLC plates were run and the controls showed no conversion of benzonitrile which indicates no leaky expression of the enzyme. The transformed-induced culture converted benzonitrile to benzamide. In order to confirm that benzamide was produced, FT-IR spectroscopy was performed to confirm the presence of an aromatic compound with an amide as the functional group. Next, NMR spectroscopy was performed to confirm the structure of benzamide by determining the number of carbons and protons present in the compound. A total of seven carbons and seven hydrogens were present which is expected for benzamide. The melting point and molecular mass (as determined by HRMS) also fell within the correct range for a benzamide compound. HPLC-MS/MS was unsuccessful due to complications with the columns. Since no benzonitrile was present in the enzyme assay product, 100 % was converted to benzamide. A minimum enzyme activity of 32 U was determined for the reaction with a productivity of ~ 4.65 kg/kg/h (*w/w*).

From this work, it can be deduced that DMF is a suitable inducer for nitrilase in *R. rhodochrous* strains which host the nitrilase enzyme. It has more advantages compared to other inducers as firstly, it is not metabolised during induction and secondly it is obtained at a cheaper price than ε-Caprolactam. The production of nitrilase with a cost-effective inducer is beneficial when utilising this enzyme for the bioconversion of nitriles to their corresponding carboxylic acid which has a multitude of beneficial applications in pharmaceutical and industrial sectors. Subsequently, a two-construct system for the heterologous production of nitrile hydratase was successful. Therefore, the use of an *E. coli* host allows for efficient mass production of this enzyme compared to using the native host. This is beneficial as the bioconversion of nitriles to their corresponding amide has numerous pharmaceutical and industrial applications. In addition, this work is proof *R. rhodochrous* strains isolated from South African have the ability to produce nitrile hydrolysing enzymes of high catalytic potential.

REFERENCE

Aiba, S., Tsunekawa, H., & Imanaka, T. (1982). New Approach to Tryptophan Production by *Escherichia coli*: Genetic Manipulation of Composite Plasmids In Vitro. *Applied Environmental Microbiology*, *43*(2), 289-297.

Allen, E. (1942). The Melting Point of Impure Organic Compounds. *Journal of Chemical Education, 19*(6), 278.

Alteri, C. J., & Mobley, H. L. (2012). *Escherichia coli* Physiology and Metabolism Dictates Adaptation to Diverse Host Microenvironments. *Current Opinion in Microbiology*, *15*(1), 3-9.

Alvarez, H. M. (2019). Biology of *Rhodococcus*, *Microbiology Monographs, 2*. Cham, Switzerland: Springer International Publishing.

Angelini, L. M. L., Silva, A. R. M. D., Rocco, L. D. F. C., & Milagre, C. D. D. F. (2015). A High-Throughput Screening Assay for Distinguishing Nitrile Hydratases from Nitrilases. *Brazilian Journal of Microbiology*, *46*(1), 113-116.

Armstrong, R. N. (1987). Enzyme-Catalyzed Detoxication Reactions: Mechanisms and Stereochemistry. *Critical Reviews in Biochemistry*, *22*(1), 39-88.

Asano, Y., Fujishiro, K., Tani, Y., & Yamada, H. (1982). Aliphatic Nitrile Hydratase from *Arthrobacter* sp. J-1 Purification and Characterization. *Agricultural and Biological Chemistry, 46*(5), 1165-1174.

Ashby, R. E., & Stacey, K. A. (1984). Stability of a Plasmid F Trim in Populations of a Recombination-Deficient Strain of *Escherichia coli* in Continuous Culture. *Antonie van Leeuwenhoek*, *50*(2), 125-134.

Asif, M. (2016). Pharmacological Potential of Benzamide Analogues and their Uses in Medicinal Chemistry. *Modern Chemistry and Applications*, *4*, 194.

Assidi, M., Dufort, I., Ali, A., Hamel, M., Algriany, O., Dielemann, S., & Sirard, M. A. (2008). Identification of Potential Markers of Oocyte Competence Expressed in Bovine

Cumulus Cells Matured with Follicle-Stimulating Hormone and/or Phorbol Myristate Acetate in Vitro. *Biology of Reproduction*, *79*(2), 209-222.

Badoei-Dalfard, A., Karami, Z., & Ramezani-pour, N. (2016). Bench Scale Production of Nicotinic Acid Using a Newly Isolated *Stenotrophomonas maltophilia* AC21 Producing Highly-Inducible and Versatile Nitrilase. *Journal of Molecular Catalysis B: Enzymatic*, *133*, S552-S559.

Baghel, U. S., Singh, A., Singh, D., & Sinha, M. (2017). Application of Mass Spectroscopy in Pharmaceutical and Biomedical Analysis. *Spectroscopic Analyses: Developments and Applications*, 105.

Barati, B., Moghadam, M., Rahmati, A., Tangestaninejad, S., Mirkhani, V., & Mohammadpoor-Baltork, I. (2013). Ruthenium Hydride Catalyzed Direct Oxidation of Alcohols to Carboxylic Acids Via Transfer Hydrogenation: Styrene Oxide as Oxygen Source. *Synlett*, *24*(1), 90-96.

Bauer, M., Griengl, H., & Steiner, W. (1999). Parameters Influencing Stability and Activity of a S-Hydroxynitrile Lyase from *Hevea Brasiliensis* in Two-Phase Systems. *Enzyme and Microbial Technology*, *24*(8-9), 514-522.

Betts, S., & King, J. (1999). There's a Right Way and a Wrong Way: In Vivo and In Vitro Folding, Misfolding and Subunit Assembly of the P22 Tailspike. *Structure*, *7*(6), R131-R139.

Bhalla, T. C., Miura, A., Wakamoto, A., Ohba, Y., & Furuhashi, K. (1992). Asymmetric Hydrolysis of α-Aminonitriles to Optically Active Amino Acids by a Nitrilase of *Rhodococcus rhodochrous* PA-34. *Applied Microbiology and Biotechnology*, *37*(2), 184-190.

Bidlingmeyer, B. (2001). Liquid Chromatography Problem Solving and Troubleshooting. *Journal of Chromatographic Science*, *39*(5), 215-215.

Bittner, M., & Vapnek, D. (1981). Versatile Cloning Vectors Derived from the Runaway-Replication Plasmid pKN402. *Gene*, *15*(4), 319-329.

Blackwell, J. R., & Horgan, R. (1991). A novel Strategy for Production of a Highly Expressed Recombinant Protein in an Active Form. *FEBS letters*, *295*(1-3), 10-12.

Brady, D., Beeton, A., Zeevaart, J., Kgaje, C., Van Rantwijk, F., & Sheldon, R. A. (2004). Characterisation of Nitrilase and Nitrile Hydratase Biocatalytic Systems. *Applied Microbiology and Biotechnology*, *64*(1), 76-85.

Briand, L., Marcion, G., Kriznik, A., Heydel, J. M., Artur, Y., Garrido, C., Seigneuric, R., & Neiers, F. (2016). A Self-Inducible Heterologous Protein Expression System in *Escherichia coli*. *Scientific Reports*, *6*, 33037.

Bromley-Challenor, K. C. A., Caggiano, N., & Knapp, J. S. (2000). Bacterial Growth on *N, N*-Dimethylformamide: Implications for the Biotreatment of Industrial Wastewater. *Journal of Industrial Microbiology and Biotechnology*, *25*(1), 8-16.

Brown, T. A. (1995). *Gene Cloning and DNA Analysis: An Introduction, 3.* Manchester, UK: Chapman & Hall.

Brown, T. A. (2006). *Gene Cloning and DNA Analysis: An Introduction, 5.* Oxford, UK: Blackwell Publishing.

Buckland, B. C., Drew, S. W., Connors, N. C., Chartrain, M. M., Lee, C., Salmon, P. M., Gbewonyo, K., Zhou, W., Gailliot, P., Singhvi, R., & Olewinski Jr, R. C. (1999). Microbial Conversion of Indene to Indandiol: A Key Intermediate in the Synthesis of Crixivan. *Metabolic Engineering*, *1*(1), 63-74.

Busch, H., Hagedoorn, P. L., & Hanefeld, U. (2019). *Rhodococcus* as a Versatile Biocatalyst in Organic Synthesis. *International Journal of Molecular Sciences*, *20*(19), 4787.

Campbell, N. A., Reece, J. B., Urry, L. A., Cain, M. L. Wasserman, S. A., Minorsky, P. V., & Jackson, R. B. (2014). The Genetic Basis of Life. *Biology: A Global Approach*, *10*, 452. London, U.K: Pearson Education.

Cao, D., Wu, H., Li, Q., Sun, Y., Liu, T., Fei, J., Zhao, Y., Wu, S., Hu, X., & Li, N. (2015). Expression of Recombinant Human Lysozyme in Egg Whites of Transgenic Hens. *PLoS One*, *10*(2).

Carlson, L. A. (2005). Nicotinic acid: The Broad-Spectrum Lipid Drug. A 50th Anniversary Review. *Journal of Internal Medicine*, *258*(2), 94-114.

Carrier, M. J., Nugent, M. E., Tacon, W. C. A., & Primrose, S. B. (1983). High Expression of Cloned Genes in *E. coli* and its Consequences. *Trends in Biotechnology*, *1*(4), 109-113.

Carroll, W. L. (1993). Introduction to Recombinant-DNA Technology. *The American Journal of Clinical Nutrition*, *58*(2), 249S-258S.

Çatak, J. (2019). Determination of Niacin Profiles in Some Animal and Plant Based Foods by High Performance Liquid Chromatography: Association with Healthy Nutrition. *Journal of Animal Science and Technology*, *61*(3), 138.

Charsley, E. L., Laye, P. G., Palakollu, V., Rooney, J. J., & Joseph, B. (2006). DSC Studies on Organic Melting Point Temperature Standards. *Thermochimica Acta*, *446*(1-2), 29-32.

Chartrain, M., Jackey, B., Taylor, C., Sandford, V., Gbewonyo, K., Lister, L., Dimichele, L., Hirsch, C., Heimbuch, B., Maxwell, C., & Pascoe, D. (1998). Bioconversion of Indene to *Cis*-(1*S*, 2*R*) Indandiol and *Trans*-(1*R*, 2*R*) Indandiol by *Rhodococcus* Species. *Journal of Fermentation and Bioengineering*, *86*(6), 550-558.

Chatterjee, J., & Meighen, E. A. (1995). Biotechnological Applications of Bacterial Bioluminescence (*lux*) Genes. *Photochemistry and Photobiology*, *62*(4), 641-650.

Chen, B. S., Otten, L. G., Resch, V., Muyzer, G., & Hanefeld, U. (2013). Draft Genome Sequence of *Rhodococcus rhodochrous* Strain ATCC 17895. *Standards in Genomic Sciences*, *9*(1), 175-184.

Chhiba-Govindjee, V. P., Mathiba, K., van der Westhuyzen, C. W., Steenkamp, P., Rashamuse, J. K., Stoychev, S., Bode, M.L. & Brady, D. (2018). Dimethylformamide is a Novel Nitrilase Inducer in *Rhodococcus rhodochrous*. *Applied Microbiology and Biotechnology*, *102*(23), 10055-10065.

Costes, D., Rotčnkovs, G., Wehtje, E., & Adlercreutz, P. (2001). Stability and Stabilization of Hydroxynitrile Lyase in Organic Solvents. *Biocatalysis and Biotransformation*, *19*(2), 119-130.

Crater, J. S., & Lievense, J. C. (2018). Scale-Up of Industrial Microbial Processes. FEMS *Microbiology Letters*, *365*(13), 138.

Curragh, H., Flynn, O., Larkin, M. J., Stafford, T. M., Hamilton, J. T., & Harper, D. B. (1994). Haloalkane Degradation and Assimilation by *Rhodococcus rhodochrous* NCIMB 13064. *Microbiology*, *140*(6), 1433-1442.

Czarnetzki, B. M., Thiele, T., & Rosenbach, T. (1990). Immunoreactive Leukotrienes in Nettle Plants (*Urtica urens*). *International Archives of Allergy and Immunology*, *91*(1), 43-46.

De Carvalho, C. C. (2017). Whole Cell Biocatalysts: Essential Workers from Nature to the Industry. *Microbial Biotechnology*, *10*(2), 250-263.

De Regil, R., & Sandoval, G. (2013). Biocatalysis for Biobased Chemicals. *Biomolecules*, *3*(4), 812-847.

Del Olmo, A., Calzada, J., & Nuñez, M. (2017). Benzoic Acid and its Derivatives as Naturally Occurring Compounds in Foods and as Additives: Uses, Exposure, and Controversy. *Critical Reviews in Food Science and Nutrition*, *57*(14), 3084-3103.

Dent, S. (2006). Purity and Identification of Solids Using Melting Points. Department of Chemistry, Portland State University.

Devasahayam, M. (2007). Factors Affecting the Expression of Recombinant Glycoproteins. *Indian Journal of Medical Research*, *126*(1), 22-28.

Diehl, B. (2008). Principles in NMR Spectroscopy. *NMR Spectroscopy in Pharmaceutical Analysis*. *1*, 1-41. Oxford, UK: Elsevier.

Endo, T., & Watanabe, I. (1989). Nitrile Hydratase of *Rhodococcus* Sp. N-774 Purification and Amino Acid Sequences. *FEBS Letters*, *243*(1), 61-64.

Epishina, M. A., Kulikov, A. S., Ignat'ev, N. V., Schulte, M., & Makhova, N. N. (2015). Nucleophilic Aromatic Cine-Substitution of Hydrogen: The Ionic Liquid-Promoted von Richter Reaction. *Mendeleev Communications*, *1*(25), 41-43.

Ercan, D., & Demirci, A. (2016). Recent Advances for the Production and Recovery Methods of Lysozyme. *Critical Reviews in Biotechnology*, *36*(6), 1078-1088.

Fahnert, B., Lilie, H., & Neubauer, P. (2004). Inclusion Bodies: Formation and Utilisation. In *Physiological Stress Responses in Bioprocesses*, 93-142. Heidelberg, Germany: Springer.

Fakruddin, M., Mazumdar, R. M., Mannan, K. S. B., Chowdhury, A., & Hossain, M. N. (2012). Critical Factors Affecting the Success of Cloning, Expression, and Mass Production of Enzymes by Recombinant *E. coli. ISRN Biotechnology*, *2013*.

Fan, Q. R., & Hendrickson, W. A. (2005). Structure of Human Follicle-Stimulating Hormone in Complex with its Receptor. *Nature*, *433*(7023), 269-277.

Farewell, A., & Neidhardt, F. C. (1998). Effect of Temperature on *In Vivo* Protein Synthetic Capacity in *Escherichia coli*. *Journal of Bacteriology*, *180*(17), 4704-4710.

Farrell, S. O., & Taylor, L. E. (2005). *Experiments in Biochemistry: A Hands-On Approach*. *2*. California: USA: Thomson Brooks/Cole.

Finnerty, W. R. (1992). The Biology and Genetics of the Genus *Rhodococcus*. *Annual Review of Microbiology*, *46*(1), 193-218.

Fisk, H., Xu, Y., Westley, C., Turner, N. J., Micklefield, J., & Goodacre, R. (2017). From Multistep Enzyme Monitoring to Whole-Cell Biotransformations: Development of Real-Time Ultraviolet Resonance Raman Spectroscopy. *Analytical Chemistry*, *89*(22), 12527-12532.

Fleming, A. (1929). On the Antibacterial Action of Cultures of a Penicillium, with Special Reference to Their Use in the Isolation of *B. influenzae*. *British Journal of Experimental Pathology*, *10*(3), 226.

Foerstner, K. U., Doerks, T., Muller, J., Raes, J., & Bork, P. (2008). A Nitrile Hydratase in the Eukaryote *Monosiga brevicollis*. *PloS one*, *3*(12).

Frederick, J. (2013). Genetic Characterization of *Rhodococcus rhodochrous* ATCC BAA-870 with Emphasis on Nitrile Hydrolysing Enzymes. Doctoral Dissertation, University of Cape Town.

Frederick, J., Brady, D., & Dirr, H. (2006). Characterisation of the Nitrile Biocatalytic Activity of *Rhodococcus rhodochrous* ATCC BAA-870. Masters Dissertation, University of Cape Town.

Fricker, R. A., Green, E. L., Jenkins, S. I., & Griffin, S. M. (2018). The Influence of Nicotinamide on Health and Disease in the Central Nervous System. *International Journal of Tryptophan Research*, *11*, 1-11.

Fried, B., & Sherma, B. (1999). Thin-Layer Chromatography, Revised and Expanded. Chromatographic Science Series. New York, USA: CRC Press.

Fu, R., Yang, Y., Zhang, J., Shao, J., Xia, X., Ma, Y., & Yuan, R. (2016). Direct Oxidative Amidation of Aldehydes with Amines Catalyzed by Heteropolyanion-Based Ionic Liquids Under Solvent-Free Conditions via a Dual-Catalysis Process. *Organic & Biomolecular Chemistry*, *14*(5), 1784-1793.

Gable, K. P. (2019). Spectral Interpretation. Infrared Spectroscopy: Identifying Functional Groups. USA: Oregon State University.

Glazer, A. N., & Nikaido, H. (2007). *Microbial Biotechnology: Fundamentals of Applied Microbiology*. New York, USA: Cambridge University Press.

Glick, B. R., & Whitney, G. K. (1987). Factors Affecting the Expression of Foreign Proteins in *Escherichia coli*. *Journal of Industrial Microbiology*, *1*(5), 277-282.

Gomes, A. R., Byregowda, S. M., Veeregowda, B. M., & Balamurugan, V. (2016). An Overview of Heterologous Expression Host Systems for the Production of Recombinant Proteins. *Advances in animal and Veterinary Sciences*, *4*(7), 346-356

Goodfellow, M., & Alderson, G. (1977). The Actinomycete-Genus *Rhodococcus*: A Home for the '*Rhodochrous'* Complex. *Microbiology*, *100*(1), 99-122.

Grossman, T. H., Kawasaki, E. S., Punreddy, S. R., & Osburne, M. S. (1998). Spontaneous Camp-Dependent Derepression of Gene Expression in Stationary Phase Plays a Role in Recombinant Expression Instability. *Gene*, *209*(1-2), 95-103.

Hamed, A. S., & Ali, E. M. (2020). Cu (II)–Metformin Immobilized on Graphene Oxide: An Efficient and Recyclable Catalyst for the Beckmann Rearrangement. *Research on Chemical Intermediates*, *46*(1), 701-714.

Han, L., Cui, W., Lin, Q., Chen, Q., Suo, F., Ma, K., Wang, Y., Hao, W., Cheng, Z. & Zhou, Z. (2020). Efficient Overproduction of Active Nitrile Hydratase by Coupling Expression Induction and Enzyme Maturation via Programming a Controllable Cobalt-Responsive Gene Circuit. *Frontiers in Bioengineering and Biotechnology*, *8*, 193.

Hausjell, J., Weissensteiner, J., Molitor, C., Halbwirth, H., & Spadiut, O. (2018). *E. coli* HMS174 (DE3) is a Sustainable Alternative to BL21 (DE3). *Microbial Cell Factories*, *17*(1), 169.

He, Y. C., Wu, Y. D., Pan, X. H., & Ma, C. L. (2014). Biosynthesis of Terephthalic Acid, Isophthalic Acid and Their Derivatives from the Corresponding Dinitriles by Tetrachloroterephthalonitrile-Induced *Rhodococcus* sp. *Biotechnology Letters, 36*(2), 341-347.

Heinemann, U., Engels, D., Bürger, S., Kiziak, C., Mattes, R., & Stolz, A. (2003). Cloning of a Nitrilase Gene from the Cyanobacterium *Synechocystis* Sp. Strain PCC6803 and Heterologous Expression and Characterization of the Encoded Protein. *Applied Environmental Microbiology*, *69*(8), 4359-4366.

Heinrich, R., Meléndez-Hevia, E., & Cabezas, H. (2002). Optimization of Kinetic Parameters of Enzymes. *Biochemistry and Molecular Biology Education*, *30*(3), 184-188.

Hoffman, C. S., & Wright, A. (1985). Fusions of Secreted Proteins to Alkaline Phosphatase: An Approach for Studying Protein Secretion. *Proceedings of the National Academy of Sciences*, *82*(15), 5107-5111.

Hook, R. H., & Robinson, W. G. (1964). Ricinine Nitrilase II. Purification and Properties. *Journal of Biological Chemistry*, *239*(12), 4263-4267.

Hoseini, S. S., & Sauer, M. G. (2015). Molecular Cloning Using Polymerase Chain Reaction, an Educational Guide for Cellular Engineering. *Journal of Biological Engineering*, *9*(1), 2.

Howden, A. J., & Preston, G. M. (2009). Nitrilase Enzymes and Their Role in Plant-Microbe Interactions. *Microbial Biotechnology*, *2*(4), 441–45.1

Huang, W., Jia, J., Cummings, J., Nelson, M., Schneider, G., & Lindqvist, Y. (1997). Crystal Structure of Nitrile Hydratase Reveals a Novel Iron Centre in a Novel Fold. *Structure*, *5*(5), 691-699.

Kamal, A., Kumar, M. S., Kumar, C. G., & Shaik, T. B. (2011). Bioconversion of Acrylonitrile to Acrylic Acid by *Rhodococcus ruber* strain AKSH-84. *Journal of Microbiology and Biotechnology*, *21*(1), 37-42.

Kamble, A. L., Banoth, L., Meena, V. S., Singh, A., Chisti, Y., & Banerjee, U. C. (2013). Nitrile hydratase of *Rhodococcus erythropolis*: Characterization of the Enzyme and the Use of Whole Cells for Biotransformation of Nitriles. *3 Biotechnology*, *3*(4), 319-330.

Kang, Y., Son, M. S., & Hoang, T. T. (2007). One Step Engineering of T7-Expression Strains for Protein Production: Increasing the Host-Range of the T7-Expression System. *Protein Expression and Purification*, *55*(2), 325-333.

Kato, Y., Nakamura, K., Sakiyama, H., Mayhew, S. G., & Asano, Y. (2000). Novel Heme-Containing Lyase, Phenylacetaldoxime Dehydratase from *Bacillus* Sp. Strain Oxb-1: Purification, Characterization, and Molecular Cloning of the Gene. *Biochemistry*, *39*(4), 800-809.

Kaul, P., & Asano, Y. (2012). Strategies for Discovery and Improvement of Enzyme Function: State of the Art and Opportunities. *Microbial Biotechnology*, *5*(1), 18-33.

Khan, S., Ullah, M. W., Siddique, R., Nabi, G., Manan, S., Yousaf, M., & Hou, H. (2016). Role of Recombinant DNA Technology to Improve Life. *International Journal of Genomics*, *2016*.

Kim, S., Jeong, H., Kim, E. Y., Kim, J. F., Lee, S. Y., & Yoon, S. H. (2017). Genomic and Transcriptomic Landscape of *Escherichia coli* BL21 (DE3). *Nucleic Acids Research*, *45*(9), 5285-5293.

King, J. M. H., DiGrazia, P. M., Applegate, B., Burlage, R., Sanseverino, J., Dunbar, P., Larimer, F., & Sayler, G. A. (1990). Rapid, Sensitive Bioluminescent Reporter

Technology for Naphthalene Exposure and Biodegradation. *Science*, *249*(4970), 778-781.

Kis, Á. E., Laczi, K., Zsíros, S., Kós, P., Tengölics, R., Bounedjoum, N., Kovács, T., Rákhely, G., & Perei, K. (2017). Characterization of the *Rhodococcus* sp. MK1 Strain and its Pilot Application for Bioremediation of Diesel Oil-Contaminated Soil. *Acta Microbiologica et Immunologica Hungarica*, *64*(4), 463-482.

Kobayashi, M., Nagasawa, T., & Yamada, H. (1989). Nitrilase of *Rhodococcus rhodochrous* J1: Purification and Characterization. *European Journal of Biochemistry*, *182*(2), 349-356.

Kobayashi, M., Nagasawa, T., & Yamada, H. (1992). Enzymatic Synthesis of Acrylamide: A Success Story not yet Over. *Trends in Biotechnology*, *10*, 402-408.

Kuwabara, J., Sawada, Y., & Yoshimatsu, M. (2018). Nitrile Hydration Reaction Using Copper Iodide/Cesium Carbonate/DBU in Nitromethane–Water. *Synlett*, *29*(15), 2061-2065.

Larentis, A. L., Nicolau, J. F. M. Q., dos Santos Esteves, G., Vareschini, D. T., de Almeida, F. V. R., dos Reis, M. G., Galler, R. & Medeiros, M. A. (2014). Evaluation of Pre-Induction Temperature, Cell Growth at Induction and IPTG Concentration on the Expression of a Leptospiral Protein in *E. coli* Using Shaking Flasks and Microbioreactor. *BMC Research Notes*, *7*(1), 671.

Larkin, M. J., Kulakov, L. A., & Allen, C. C. (2006). Biodegradation by Members of the Genus *Rhodococcus*: Biochemistry, Physiology, and Genetic Adaptation. *Advances in Applied Microbiology*, *59*, 1-29.

Lavrov, K. V., Shemyakina, A. O., Grechishnikova, E. G., Novikov, A. D., Kalinina, T. I., & Yanenko, A. S. (2019). In Vivo Metal Selectivity of Metal-Dependent Biosynthesis of Cobalt-Type Nitrile Hydratase in *Rhodococcus* Bacteria: A New Look at the Nitrile Hydratase Maturation Mechanism?. *Metallomics*, *11*(6), 1162-1171.

Layh, N., Hirrlinger, B., Stolz, A. & Knackmuss, H.J. (1997). Enrichment Strategies for Nitrile-Hydrolysing Bacteria. *Applied Microbiology and Biotechnology*. *47*, 668-674.

Leonhartsberger, S. (2006). *E. coli* Expression System Efficiently Secretes Recombinant Proteins into Culture Broth. *BioProcess International*, *4*(4), 64-66.

Li, L. X., Zhang, Y. L., Zhou, L., Chen, J. M., Fu, X., Ye, C. L., Wu, J. X., Liu, R. Y., & Huang, W. (2013). Antitumor Efficacy of a Recombinant Adenovirus Encoding Endostatin Combined with an E1B55KD-Deficient Adenovirus in Gastric Cancer Cells. *Journal of Translational Medicine*, *11*(1), 257.

Lin, B., & Tao, Y. (2017). Whole-Cell Biocatalysts by Design. *Microbial Cell Factories*, *16*(1), 106.

Lodish, H., Berk, A., Zipursky, S. L., Matsudaira, P., Baltimore, D., & Darnell, J. (2000). *Molecular cell biology, 4*. New York, USA: W. H. Freeman.

Madigan, M. T., & Martinko. J. M. (2006). *Brock Biology of Microorganisms*, *11*. New Jersey, USA: Pearson Prentice Hall.

Maity, R., Naskar, S., & Das, I. (2018). Copper (II)-Catalyzed Reactions of α-Keto Thioesters with Azides via C–C and C–S Bond Cleavages: Synthesis of N-Acylureas and Amides. *The Journal of Organic Chemistry*, *83*(4), 2114-2124.

Majidzadeh, M., & Fatahi-Bafghi, M. (2018). Current Taxonomy of *Rhodococcus* species and Their Role in Infections. *European Journal of Clinical Microbiology & Infectious Diseases*, *37*(11), 2045-2062.

Makino, T., Skretas, G., & Georgiou, G. (2011). Strain Engineering for Improved Expression of Recombinant Proteins in Bacteria. *Microbial Cell Factories*, *10*(1), 32.

Mandenius, C. F. (2016). *Bioreactors: Design, Operation and Novel Applications*. Germany: John Wiley & Sons.

Martinkova, L., & Křen, V. (2002). Nitrile-and Amide-Converting Microbial Enzymes: Stereo-, Regio-and Chemoselectivity. *Biocatalysis and Biotransformation*, *20*(2), 73-93.

Mascharak, P. K. (2002). Structural and Functional Models of Nitrile Hydratase. *Coordination Chemistry Reviews*, *225*(1-2), 201-214.

Mathew, C. D., Nagasawa, T., Kobayashi, M., & Yamada, H. (1988). Nitrilase-Catalyzed Production of Nicotinic Acid From 3-Cyanopyridine in *Rhodococcus Rhodochrous* J1. *Applied Environmental Microbiology.*, *54*(4), 1030-1032.

Matsusaki, Y., Yamaguchi, T., Tada, N., Miura, T., & Itoh, A. (2012). Aerobic Photooxidative Cleavage of Vicinal Diols to Carboxylic Acids Using 2-Chloroanthraquinone. *Synlett*, *23*(14), 2059-2062.

Miller, J. M., & Conn, E. E. (1980). Metabolism of Hydrogen Cyanide by Higher Plants. *Plant Physiology*, *65*(6), 1199-1202.

Mollaoglu, A. D., Ozyurt, I., & Severcan, F. (2018). Applications of Infrared Spectroscopy and Microscopy in Diagnosis of Obesity. *In Infrared Spectroscopy-Principles, Advances, and Applications*. London, U.K: IntechOpen.

Nagasawa, T., & Yamada, H. (1989). Microbial Transformations of Nitriles. *Trends in Biotechnology*, *7*(6), 153-158.

Nagasawa, T., Kobayashi, M., & Yamada, H. (1988a). Optimum Culture Conditions for the Production of Benzonitrilase by *Rhodococcus rhodochrous* J1. *Archives of Microbiology*, *150*(1), 89-94.

Nagasawa, T., Mathew, C. D., Mauger, J., & Yamada, H. (1988b). Nitrile Hydratase-Catalyzed Production of Nicotinamide from 3-Cyanopyridine in *Rhodococcus rhodochrous* J1. *Applied Environmental Microbiology*, *54*(7), 1766-1769.

Nagasawa, T., Nakamura, T., & Yamada, H. (1990). ε-Caprolactam, A New Powerful Inducer for the Formation of *Rhodococcus rhodochrous* J1 Nitrilase. *Archives of Microbiology*, *155*(1), 13-17.

Nagasawa, T., Ryuno, K., & Yamada, H. (1989). Superiority of *Pseudomonas chlororaphis* B23 Nitrile Hydratase as a Catalyst for the Enzymatic Production of Acrylamide. *Experientia*, *45*(11-12), 1066-1070.

Nagasawa, T., Shimizu, H., & Yamada, H. (1993). The Superiority of the Third-Generation Catalyst, *Rhodococcus rhodochrous* J1 Nitrile Hydratase, for Industrial Production of Acrylamide. *Applied Microbiology and Biotechnology*, *40*(2-3), 189-195.

Nagasawa, T., Takeuchi, K., & Yamada, H. (1991a). Characterization of a New Cobalt-Containing Nitrile Hydratase Purified from Urea-Induced Cells of *Rhodococcus rhodochrous* J1. *European Journal of Biochemistry*, *196*(3), 581-589.

Nagasawa, T., Takeuchi, K., Nardi-Dei, V., Mihara, Y., & Yamada, H. (1991b). Optimum Culture Conditions for the Production of Cobalt-Containing Nitrile Hydratase by *Rhodococcus rhodochrous* J1. *Applied Microbiology and Biotechnology*, *34*(6), 783-788.

Nageshwar, Y. V. D., Sheelu, G., Shambhu, R. R., Muluka, H., Mehdi, N., Malik, M. S., & Kamal, A. (2011). Optimization of Nitrilase Production from *Alcaligenes faecalis* MTCC 10757 (IICT-A3): Effect of Inducers on Substrate Specificity. *Bioprocess and Biosystems Engineering, 34(*5), 515-523.

Namkoong, W., Hwang, E. Y., Park, J. S., & Choi, J. Y. (2002). Bioremediation of Diesel-Contaminated Soil with Composting. *Environmental Pollution*, *119*(1), 23-31.

Nichols, L. (2017). Extraction. *Organic Chemistry Laboratory Techniques, 2*. Chemistry LibreTexts.

Nikishin, G. I., Sokova, L. L., & Kapustina, N. I. (2009). Oxidation of Alkanols Into "Symmetric" Esters with the System Ce (SO4) 2—LiBr. *Russian Chemical Bulletin*, *2*(58), 303-308.

Nojiri, M., Nakayama, H., Odaka, M., Yohda, M., Takio, K., & Endo, I. (2000). Cobalt-Substituted Fe-Type Nitrile Hydratase of *Rhodococcus* sp. N-771. *FEBS Letters*, *465*(2-3), 173-177.

Novak, P., Vikić-Topić, D., Meić, Z., Sekušak, S., & Sabljić, A. (1995). Investigation of Hydrogen Bond Structure in Benzoic Acid Solutions. *Journal of Molecular Structure*, *356*(2), 131-141.

O'Reilly, C., & Turner, P. D. (2003). The Nitrilase Family of CN Hydrolysing Enzymes–A Comparative Study. *Journal of Applied Microbiology*, *95*(6), 1161-1174.

Obom, K. M., Magno, A., & Cummings, P. J. (2013). Operation of a Benchtop Bioreactor. *Journal of Visualized Experiments*, (79), e50582.

Osbon, Y., & Kumar, M. (2019). Biocatalysis and Strategies for Enzyme Improvement. *Biophysical Chemistry*, *60*, 1-16.

Pace, H. C., & Brenner, C. (2001). The Nitrilase Superfamily: Classification, Structure and Function. *Genome Biology*, *2*(1), 1-1.

Pace, H. C., Hodawadekar, S. C., Draganescu, A., Huang, J., Bieganowski, P., Pekarsky, Y., Croce, C.M., & Brenner, C. (2000). Crystal Structure of the Worm Nitfhit Rosetta Stone Protein Reveals A Nit Tetramer Binding Two Fhit Dimers. *Current Biology*, *10*(15), 907-917.

Pei, X., Yang, L., Xu, G., Wang, Q., & Wu, J. (2014). Discovery of a New Fe-Type Nitrile Hydratase Efficiently Hydrating Aliphatic and Aromatic Nitriles by Genome Mining. *Journal of Molecular Catalysis B: Enzymatic*, *99*, 26-33.

Pierce, J., & Gutteridge, S. (1985). Large-scale Preparation of Ribulosebisphosphate Carboxylase from a Recombinant System in *Escherichia coli* Characterized by Extreme Plasmid Instability. *Applied Environmental Microbiology*, *49*(5), 1094-1100.

Pitt, J. J. (2009). Principles and Applications of Liquid Chromatography-Mass Spectrometry in Clinical Biochemistry. *The Clinical Biochemist Reviews*, *30*(1), 19.

Poeschl, A., & Mountford, D. M. (2014). A Facile Manganese Dioxide Mediated Oxidation of Primary Benzylamines to Benzamides. *Organic & Biomolecular Chemistry*, *12*(36), 7150-7158.

Prasad, S., & Bhalla, T. C. (2010). Nitrile Hydratases (NHases): At the Interface of Academia and Industry. *Biotechnology Advances*, *28*(6), 725-741.

Prasad, S., Misra, A., Jangir, V. P., Awasthi, A., Raj, J., & Bhalla, T. C. (2007). A Propionitrile-Induced Nitrilase of *Rhodococcus* Sp. NDB 1165 and its Application in Nicotinic Acid Synthesis. *World Journal of Microbiology and Biotechnology*, *23*(3), 345-353.

Priefert, H., O'Brien, X. M., Lessard, P. A., Dexter, A. F., Choi, E. E., Tomic, S., Nagpal, G., Cho, J.J., Agosto, M., Yang, L., & Treadway, S. L. (2004). Indene Bioconversion by a Toluene Inducible Dioxygenase of *Rhodococcus* Sp. I24. *Applied Microbiology and Biotechnology*, *65*(2), 168-176.

Quintanilla-Licea, R., Colunga-Valladares, J. F., Caballero-Quintero, A., Rodríguez-Padilla, C., Tamez-Guerra, R., Gómez-Flores, R., & Waksman, N. (2002). NMR Detection of Isomers Arising from Restricted Rotation of the CN Amide Bond of N-Formyl-o-toluidine and N, N'-bis-Formyl-o-tolidine. *Molecules*, *7*(8), 662-673.

Rai, M., & Padh, H. (2001). Expression systems for production of heterologous proteins. *Current Science*, 1121-1128.

Rapheeha, O. K. L., Roux-van der Merwe, M. P., Badenhorst, J., Chhiba, V., Bode, M. L., Mathiba, K., & Brady, D. (2017). Hydrolysis of Nitriles by Soil Bacteria: Variation with Soil Origin. *Journal of Applied Microbiology*, *122*(3), 686-697.

Ringquist, S., Shinedling, S., Barrick, D., Green, L., Binkley, J., Stormo, G. D., & Gold, L. (1992). Translation Initiation in *Escherichia coli*: Sequences Within the Ribosome-Binding Site. *Molecular Microbiology*, *6*(9), 1219-1229.

Ripp, S., Nivens, D. E., Ahn, Y., Werner, C., Jarrell, J., Easter, J. P., Cox, C.D., Burlage, R. S. & Sayler, G. S. (2000). Controlled Field Release of a Bioluminescent Genetically Engineered Microorganism for Bioremediation Process Monitoring and Control. *Environmental Science & Technology*, *34*(5), 846-853.

Robinson, W. G., & Hook, R. H. (1964). Ricinine Nitrilase I. Reaction Product and Substrate Specificity. *Journal of Biological Chemistry*, *239*(12), 4257-4262.

Rosano, G. L., & Ceccarelli, E. A. (2014). Recombinant Protein Expression in *Escherichia coli*: Advances and Challenges. *Frontiers in Microbiology*, *5*, 172.

Saeki, H., Akira, M., Furuhashi, K., Averhoff, B., & Gottschalk, G. (1999). Degradation of Trichloroethene by a Linear-Plasmid-Encoded Alkene Monooxygenase in *Rhodococcus corallinus* (*Nocardia corallina*) B-276. *Microbiology*, *145*(7), 1721-1730.

Saha, S., & Desiraju, G. R. (2018). Acid-Amide Supramolecular Synthon in Cocrystals: From Spectroscopic Detection to Property Engineering. *Journal of the American Chemical Society*, *140*(20), 6361-6373.

Saleh, H. E. D. M., & Koller, M. (2018). Introductory Chapter: Principles of Green Chemistry. *Green Chemistry*. Rijeka, Croatia: IntechOpen.

Samuelsson, B., & Funk, C. D. (1989). Enzymes Involved in the Biosynthesis of Leukotriene B4. *Journal of Biological Chemistry*, *264*(33), 19469-19472.

San-Miguel, T., Pérez-Bermúdez, P., & Gavidia, I. (2013). Production of Soluble Eukaryotic Recombinant Proteins in *E. coli* is Favoured in Early Log-Phase Cultures Induced at Low Temperature. *Springerplus*, *2*(1), 89.

Sankhian, U. D., Kumar, H., Chand, D., Kumar, D., & Bhalla, T. C. (2003). Nitrile Hydratase of *Rhodococcus rhodochrous* NHB-2: Optimization of Conditions for Production of Enzyme and Conversion of Acrylonitrile to Acrylamide. *Asian Journal of Microbiology, Biotechnology and Environmental Sciences*, *5*, 217-223.

Sathe, P. A., Karpe, A. S., Parab, A. A., Parade, B. S., Vadagaonkar, K. S., & Chaskar, A. C. (2018). Tandem Synthesis of Aromatic Amides from Styrenes in Water. *Tetrahedron Letters*, *59*(29), 2820-2823.

Sayler, G. S., Cox, C. D., Burlage, R., Ripp, S., Nivens, D. E., Werner, C., Ahn, Y., & Matrubutham, U. (1999). Field Application of a Genetically Engineered Microorganism for Polycyclic Aromatic Hydrocarbon Bioremediation Process Monitoring and Control. In *Novel Approaches for Bioremediation of Organic Pollution*, 241-254.

Schmid, K. (2020). Nitrile Hydratase Enantioselectivity as a Function of Genetic Diversity and Directed Evolution. Masters Dissertation, University of the Witwatersrand.

Schumann, W., & Ferreira, L. C. S. (2004). Production of Recombinant Proteins in *Escherichia coli*. *Genetics and Molecular Biology*, *27*(3), 442-453.

Scott, K. N. (1972). Carbon-13 Nuclear Magnetic Resonance of Biologically Important Aromatic Acids. I. Chemical Shifts of Benzoic Acid and Derivatives. *Journal of the American Chemical Society, 94(24)*, 8564-8568.

Sharma, N. N., Sharma, M., & Bhalla, T. C. (2011). An Improved Nitrilase-Mediated Bioprocess for Synthesis of Nicotinic Acid from 3-Cyanopyridine with Hyper-induced

Nocardia globerula NHB-2. *Journal of Industrial Microbiology and Biotechnology*, *38*(9), 1235-1243.

Sharma, N. N., Sharma, M., Kumar, H., & Bhalla, T. C. (2006). *Nocardia globerula* NHB-2: Bench Scale Production of Nicotinic Acid. *Process Biochemistry*, *41*(9), 2078-2081.

Shimokawa, S., Kawagoe, Y., Moriyama, K., & Togo, H. (2016). Direct Transformation of Ethylarenes into Primary Aromatic Amides with N-Bromosuccinimide and I2–Aqueous NH3. *Organic Letters*, *18*(4), 784-787.

Singh, R., Pandey, D., Dhariwal, S., Sood, P., & Chand, D. (2018). Bioconversion of Acrylonitrile Using Nitrile Hydratase Activity of *Bacillus* Sp. APB-6. *3 Biotechnology*, *8*(5), 225.

Srinivas Kotha, S., Badigenchala, S., & Sekar, G. (2015). Iron-Catalyzed Direct Synthesis of Amides from Methylarenes. *Advanced Synthesis & Catalysis*, *357*(7), 1437-1445.

Stano, N. M., & Patel, S. S. (2004). T7 Lysozyme Represses T7 RNA Polymerase Transcription by Destabilizing the Open Complex During Initiation. *Journal of Biological Chemistry*, *279*(16), 16136-16143.

Sugiura, Y., Kuwahara, J., Nagasawa, T., & Yamada, H. (1987). Nitrile Hydratase: The First Non-Heme Iron Enzyme with a Typical Low-Spin Iron (III)-Active Center. *Journal of the American Chemical Society*, *109*(19), 5848-5850.

Swartz, J. R. (2001). Advances in *Escherichia coli* Production of Therapeutic Proteins. *Current Opinion in Biotechnology*, *12*(2), 195-201.

Swaving, J., & de Bont, J. A. (1998). Microbial Transformation of Epoxides. *Enzyme and Microbial Technology*, *22*(1), 19-26.

Takaichi, S., Ishidsu, J. I., Seki, T., & Fukada, S. (1990). Carotenoid Pigments from *Rhodococcus rhodochrous* RNMS1: Two Monocyclic Carotenoids, A Carotenoid Monoglycoside and Carotenoid Glycoside Monoesters. *Agricultural and Biological chemistry*, *54*(8), 1931-1937.

Tao, J. A., Lin, G. Q., & Liese, A. (2009). *Biocatalysis for the Pharmaceutical Industry: Discovery, Development, and Manufacturing*. Singapore: John Wiley & Sons.

Thimann, K. V., & Mahadevan, S. (1964). Nitrilase: I. Occurrence, Preparation, and General Properties of the Enzyme. *Archives of Biochemistry and Biophysics*, *105*(1), 133-141.

Tokmakov, A. A., Kurotani, A., Takagi, T., Toyama, M., Shirouzu, M., Fukami, Y., & Yokoyama, S. (2012). Multiple Post-Translational Modifications Affect Heterologous Protein Synthesis. *Journal of Biological Chemistry*, *287*(32), 27106-27116.

Touhara, K., & Prestwich, G. D. (1993). Juvenile Hormone Epoxide Hydrolase. Photoaffinity Labeling, Purification, and Characterization from Tobacco Hornworm Eggs. *Journal of Biological Chemistry*, *268*(26), 19604-19609.

Truppo, M. D. (2017). Biocatalysis in the Pharmaceutical Industry: The Need for Speed. *ACS Medicinal Chemistry Letters*, *8*(5), 476-480.

Tsukamoto, J., Haebel, S., Valenca, G. P., Peter, M. G., & Franco, T. T. (2008). Enzymatic Direct Synthesis of Acrylic Acid Esters of Mono-And Disaccharides. *Journal of Chemical Technology & Biotechnology: International Research in Process, Environmental & Clean Technology*, *83*(11), 1486-1492.

Turner, N. J., & Truppo, M. D. (2013). Biocatalysis Enters a New Era. *Current Opinion in Chemical Biology*, *2*(17), 212-214.

Ullmann, A. (2001). *Escherichia coli* Lactose Operon. *Encyclopaedia of Life Sciences*. Chichester, U.K: John Wiley & Sons.

Van der Werf, M. J., Overkamp, K. M., & de Bont, J. A. (1998). Limonene-1, 2-epoxide Hydrolase from *Rhodococcus erythropolis* DCL14 Belongs to a Novel Class of Epoxide Hydrolases. *Journal of Bacteriology*, *180*(19), 5052-5057.

Vejvoda, V., Kubáč, D., Davidová, A., Kaplan, O., Šulc, M., Šveda, O., Chaloupková, R. & Martínková, L. (2010). Purification and Characterization of Nitrilase from *Fusarium solani* IMI196840. *Process Biochemistry*, *45*(7), 1115-1120.

Waegeman, H., & De Mey, M. (2012). Increasing Recombinant Protein Production in *E. Coli* by an Alternative Method to Reduce Acetate. In *Advances in Applied Biotechnology*, 127-144.

Watanabe, I., Satoh, Y., & Enomoto, K. (1987a). Screening, Isolation and Taxonomical Properties of Microorganisms Having Acrylonitrile-Hydrating Activity. *Agricultural and Biological Chemistry*, *51*(12), 3193-3199.

Watanabe, I., Satoh, Y., Enomoto, K., Seki, S., & Sakashita, K. (1987b). Optimal Conditions for Cultivation of *Rhodococcus* Sp. N-774 and for Conversion of Acrylonitrile to Acrylamide by Resting Cells. *Agricultural and Biological Chemistry*, *51*(12), 3201-3206.

Widdel, F. (2007). Theory and Measurement of Bacterial Growth. *Grundpraktikum Mikrobiologie*, *4*(11), 1-1. Universität Bremen.

Yalkowsky, S. H., Krzyzaniak, J. F., & Myrdal, P. B. (1994). Relationships Between Melting Point and Boiling Point of Organic Compounds. *Industrial & Engineering Chemistry Research*, *33*(7), 1872-1877.

Yamada, H., & Kobayashi, M. (1996). Nitrile Hydratase and its Application to Industrial Production of Acrylamide. *Bioscience, Biotechnology, and Biochemistry*, *60*(9), 1391-1400.

Yanagawa, R., & Honda, E. I. I. C. H. I. (1976). Presence of Pili in Species of Human and Animal Parasites and Pathogens of the Genus *Corynebacterium*. *Infection and Immunity*, *13*(4), 1293-1295.

Yildirim, N., & Mackey, M. C. (2003). Feedback Regulation in the Lactose Operon: A Mathematical Modelling Study and Comparison with Experimental Data. *Biophysical Journal*, *84*(5), 2841-2851.

You, T., Wang, Z., Chen, J., & Xia, Y. (2017). Transfer Hydro-Dehalogenation of Organic Halides Catalyzed by Ruthenium (II) Complex. *The Journal of Organic Chemistry*, *82*(3), 1340-1346.

Yuan, Y. C., Kamaraj, R., Bruneau, C., Labasque, T., Roisnel, T., & Gramage-Doria, R. (2017). Unmasking Amides: Ruthenium-Catalyzed Protodecarbonylation of N-Substituted Phthalimide Derivatives. *Organic Letters*, *19*(23), 6404-6407.

Yusuf, F., Chaubey, A., Jamwal, U., & Parshad, R. (2013). A New Isolate from *Fusarium proliferatum* (AUF-2) For Efficient Nitrilase Production. *Applied Biochemistry and Biotechnology*, *171*(4), 1022-1031.

Zhang, J., Tarbet, E. B., Toro, H., & Tang, D. C. C. (2011). Adenovirus-Vectored Drug–Vaccine Duo as a Potential Driver for Conferring Mass Protection Against Infectious Diseases. *Expert Review of Vaccines*, *10*(11), 1539-1552.

Zopf, W. (1891). Über Ausscheidung von Fettfarbstoffen Lipochromen Seitens Gewisser Spaltpilze. *Berichte der Deutschen Botanischen Gesellschaft*, *9*, 22-28.

APPENDIX A

Table A2.1: Absorbance (OD_{600}) of DMF Uninduced *Rhodococcus rhodochrous*

Time (Hours)	ATCC BAA-870	A29	A99
0	2.124	2.364	2.694
12	2.235	2.457	2.739
24	2.307	2.595	2.928
36	3.352	3.168	3.460
48	3.975	3.905	4.100
60	4.245	4.155	6.240
72	4.590	4.332	6.496

Table A2.2: Absorbance (OD_{600}) of DMF Induced *Rhodococcus rhodochrous*

Time (Hours)	ATCC BAA-870	A29	A99
0	1.578	1.350	2.352
12	2.037	1.728	2.682
24	2.168	2.288	2.932
36	3.368	3.395	4.390
48	4.182	4.086	4.926
60	4.984	4.914	5.904
72	5.292	5.096	6.040

NMR SPECTRA

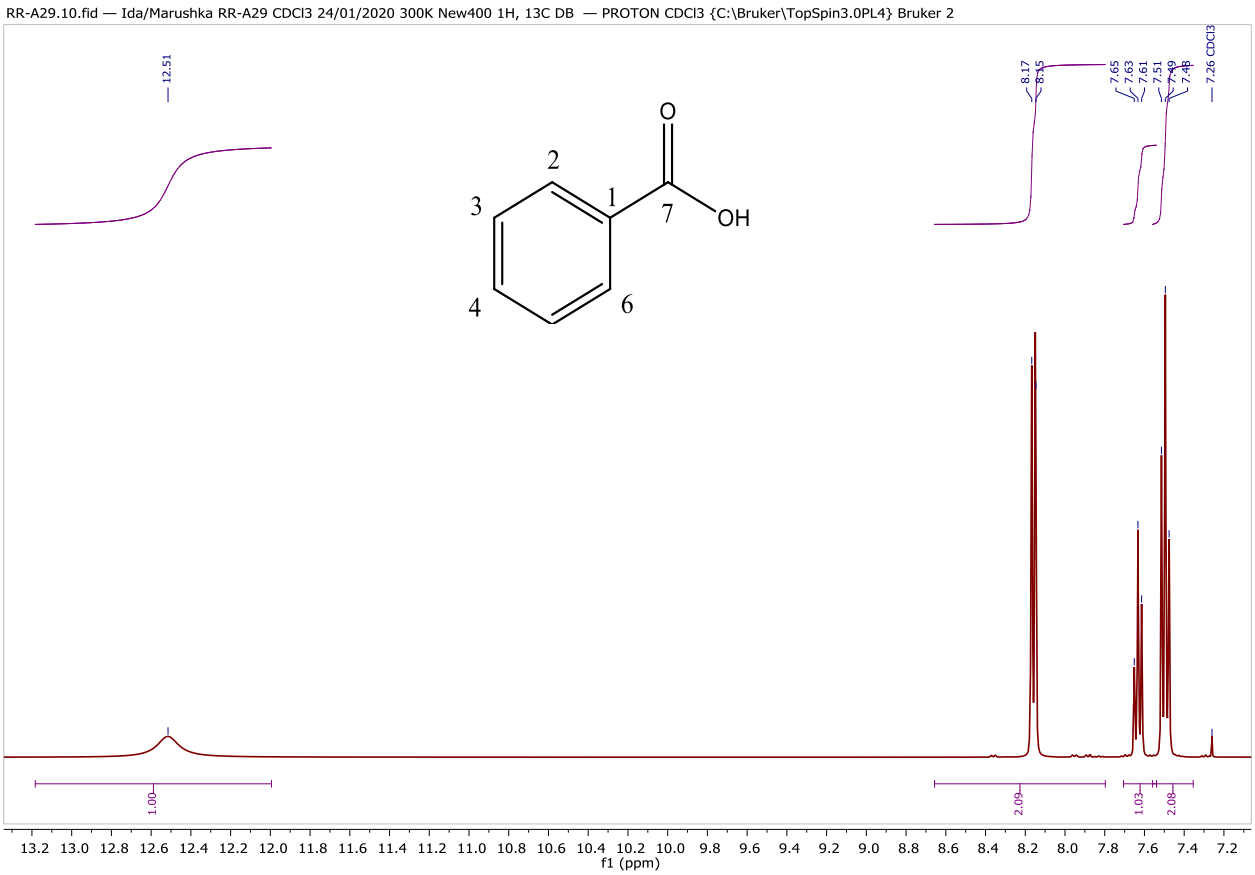

Figure A1: ^{1}H NMR Spectrum for Benzoic Acid Bio-converted by a Nitrilase Produced by *Rhodococcus rhodochrous* A29

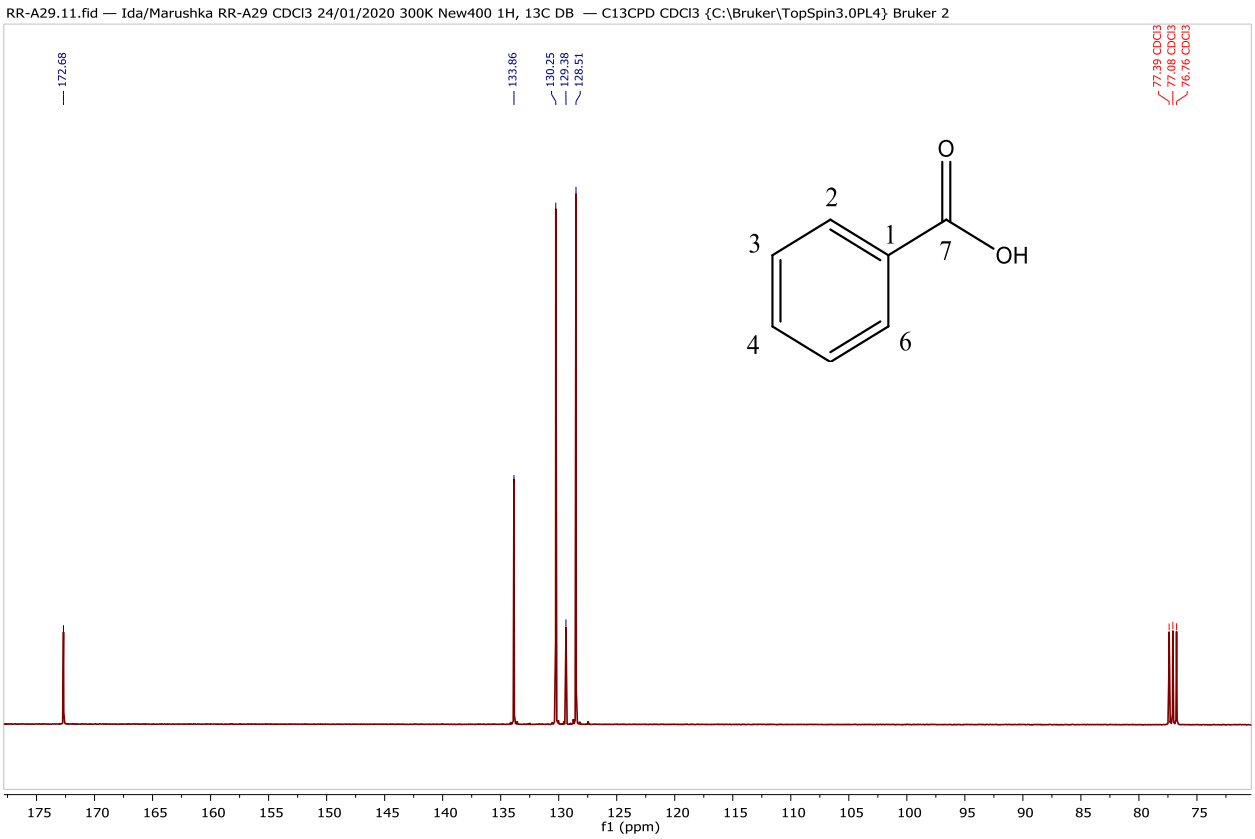

Figure A2: ^{13}C NMR Spectrum for Benzoic Acid Bio-converted by a Nitrilase Produced by *Rhodococcus rhodochrous* A29

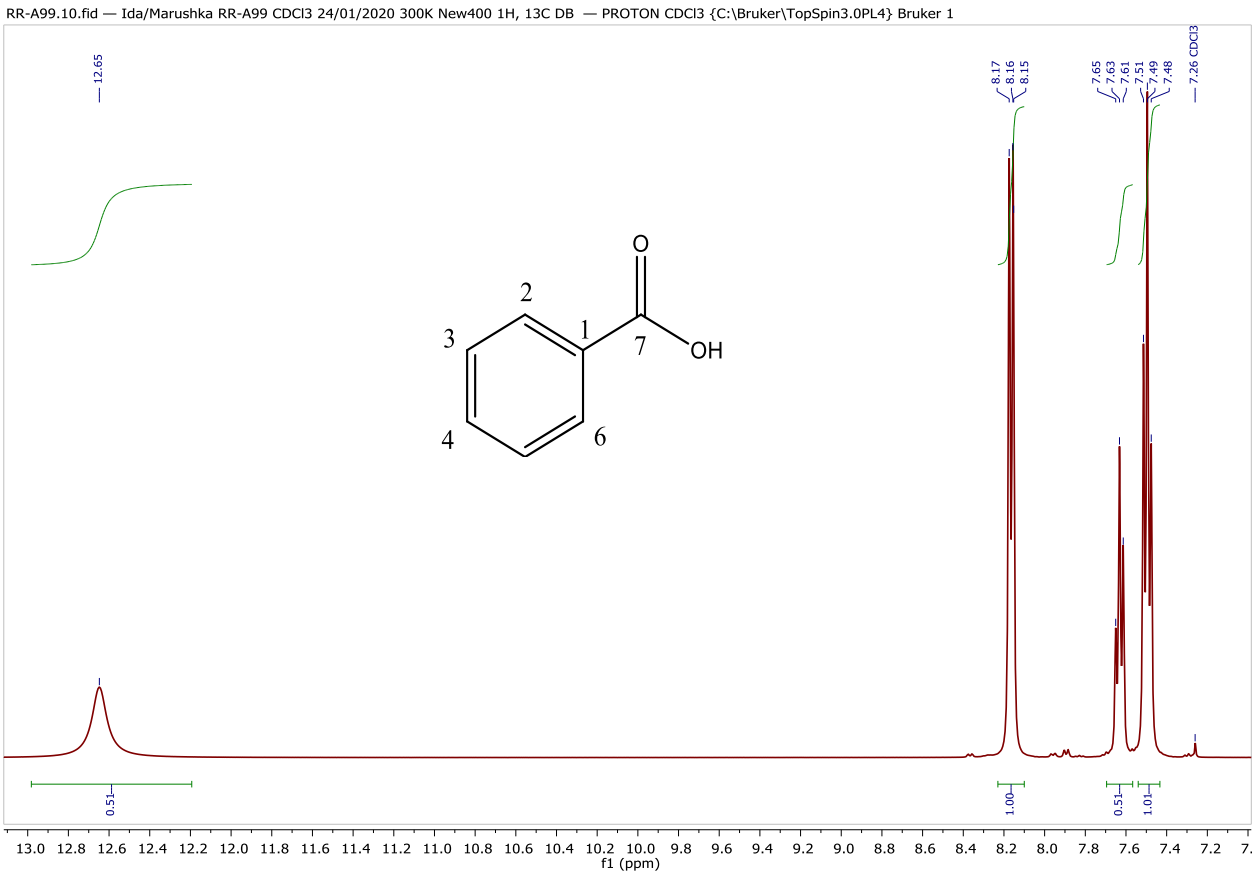

Figure A3: ^{1}H NMR Spectrum for Benzoic Acid Bio-converted by a Nitrilase Produced by *Rhodococcus rhodochrous* A99

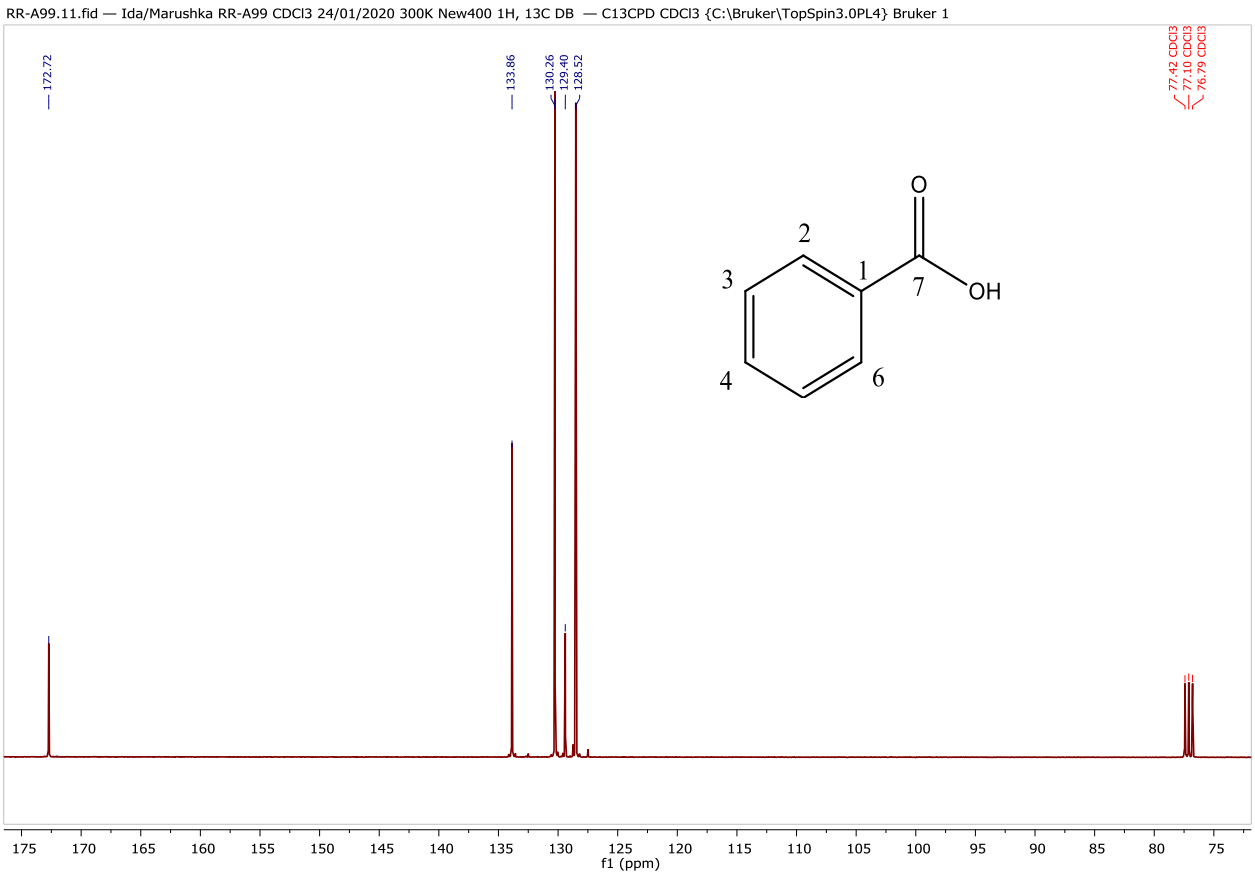

Figure A4: ^{13}C NMR Spectrum for Benzoic Acid Bio-converted by a Nitrilase Produced by *Rhodococcus rhodochrous* A99

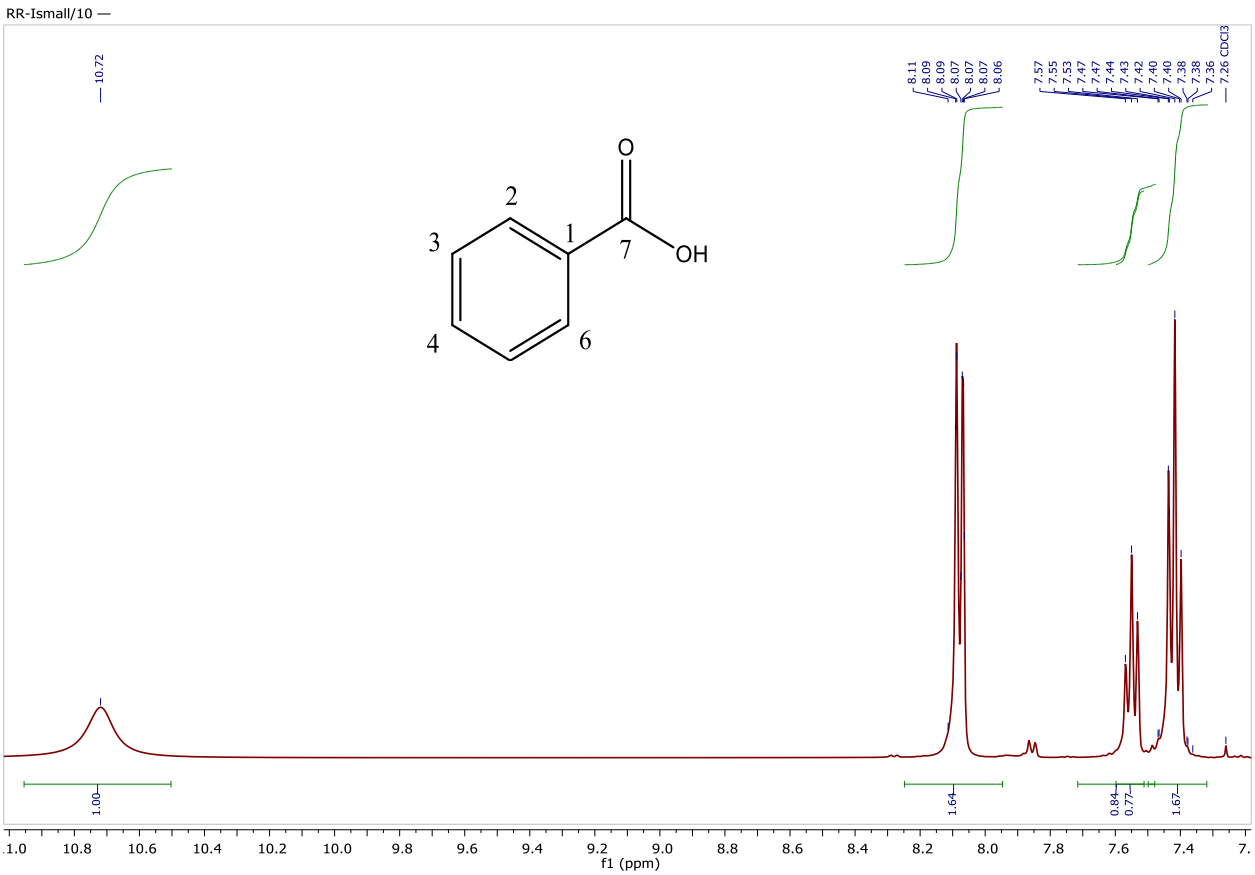

Figure A5: ^{1}H NMR Spectrum for Benzoic Acid Bio-converted by a Nitrilase Produced by *Rhodococcus rhodochrous* ATCC BAA-870

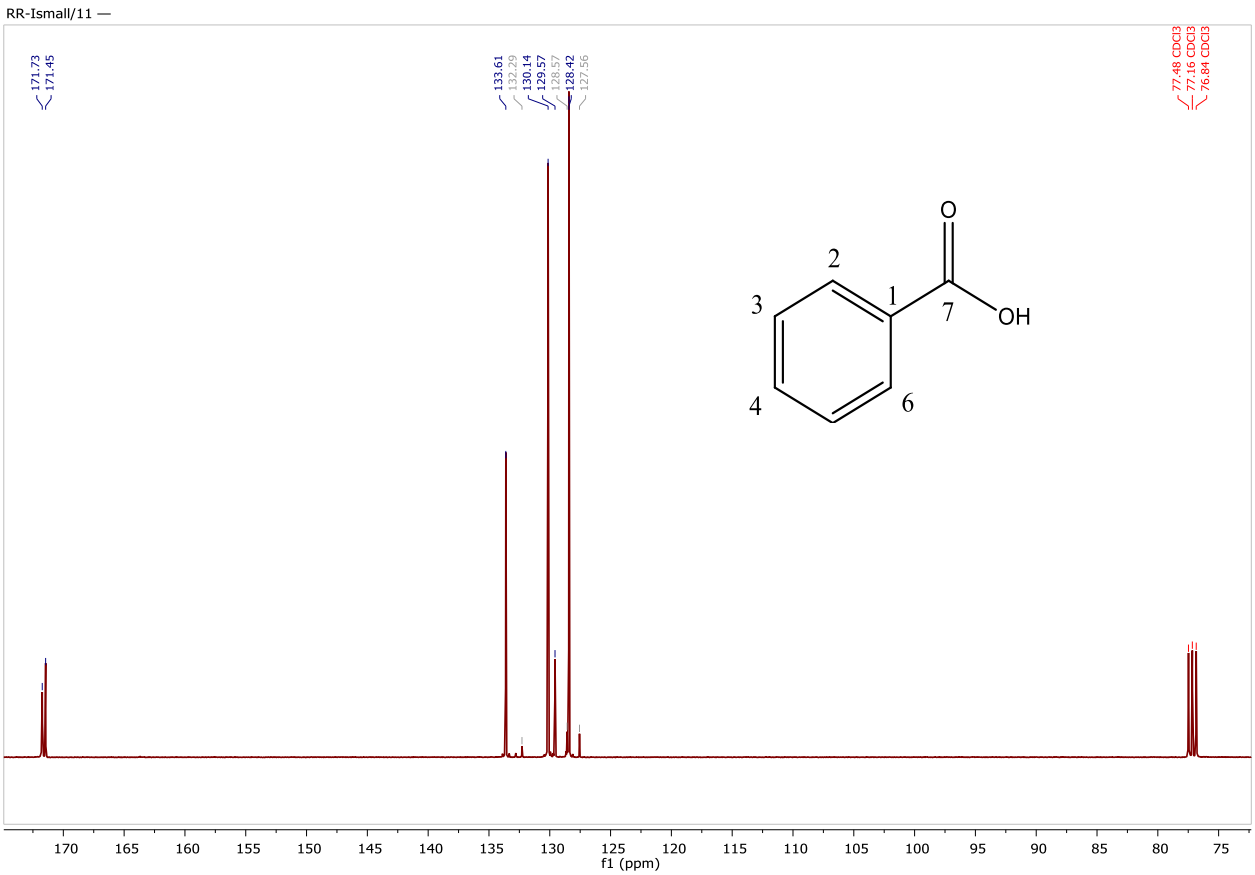

Figure A6: ^{13}C NMR Spectrum for Benzoic Acid Bio-converted by a Nitrilase Produced by *Rhodococcus rhodochrous* ATCC BAA-870

FT-IR INTERFEROGRAM

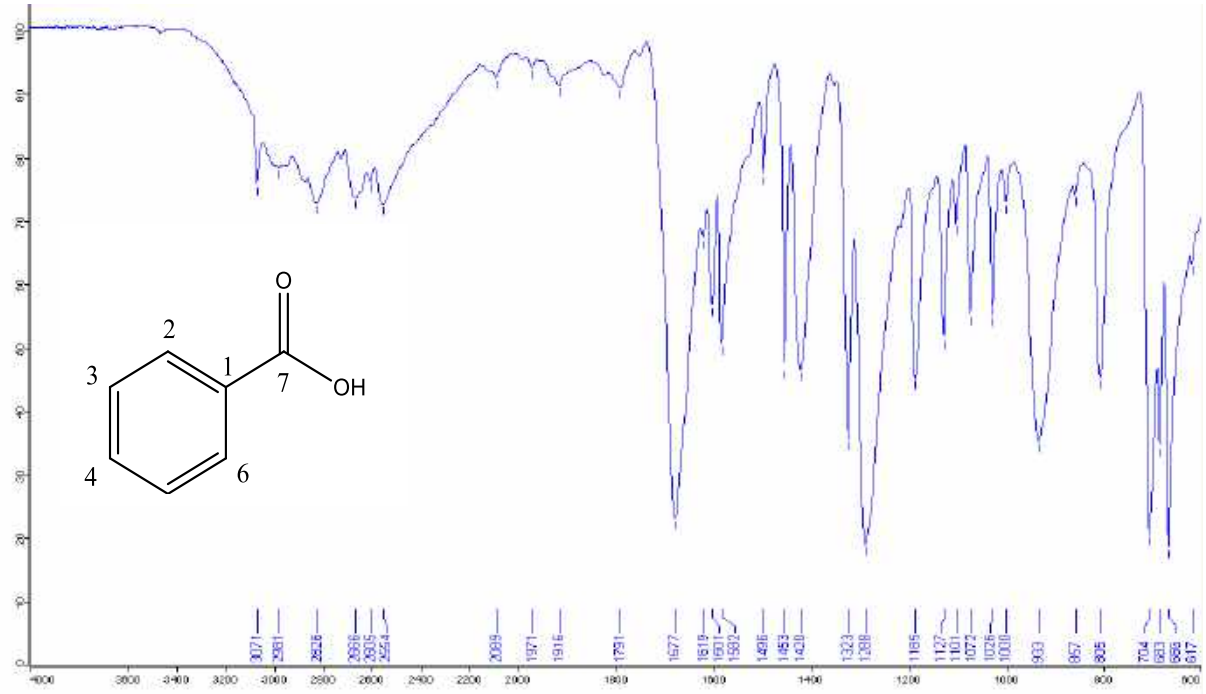

Figure A7: FT-IR Spectrum for Benzoic Acid Bio-converted by a Nitrilase Produced by *Rhodococcus rhodochrous* A29

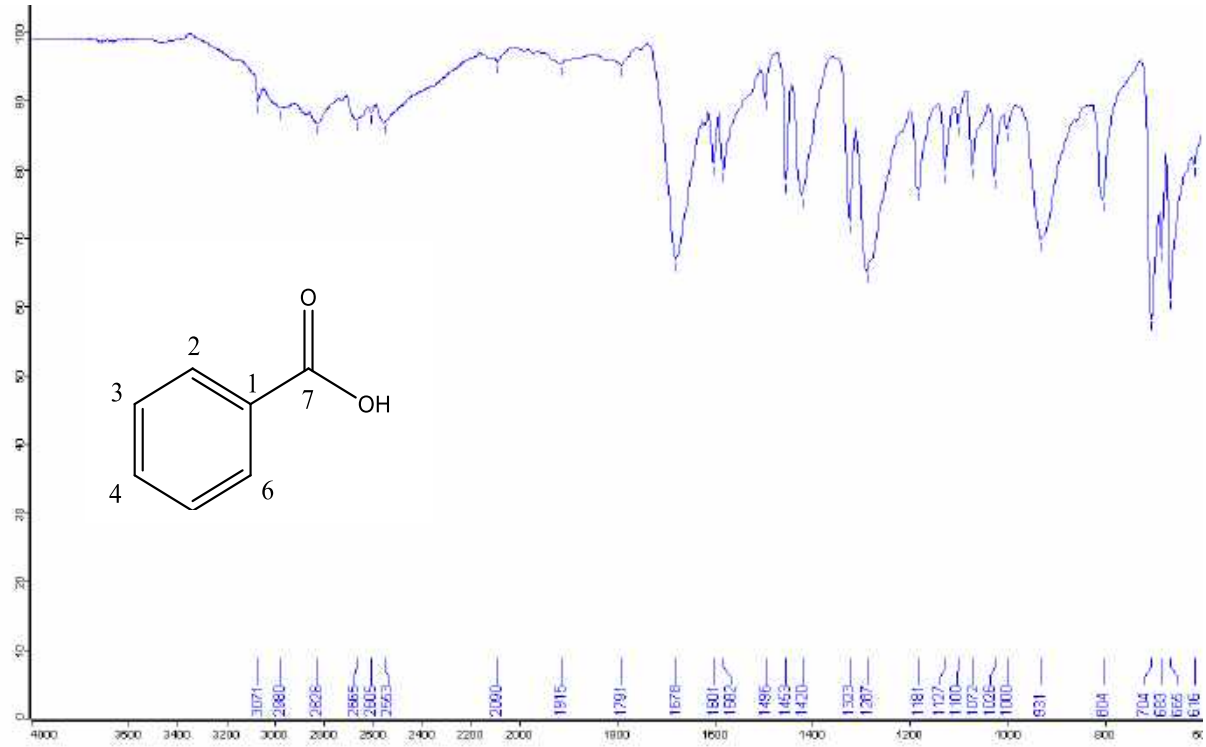

Figure A8: FT-IR Spectrum for Benzoic Acid Bio-converted by a Nitrilase Produced by *Rhodococcus rhodochrous* A99

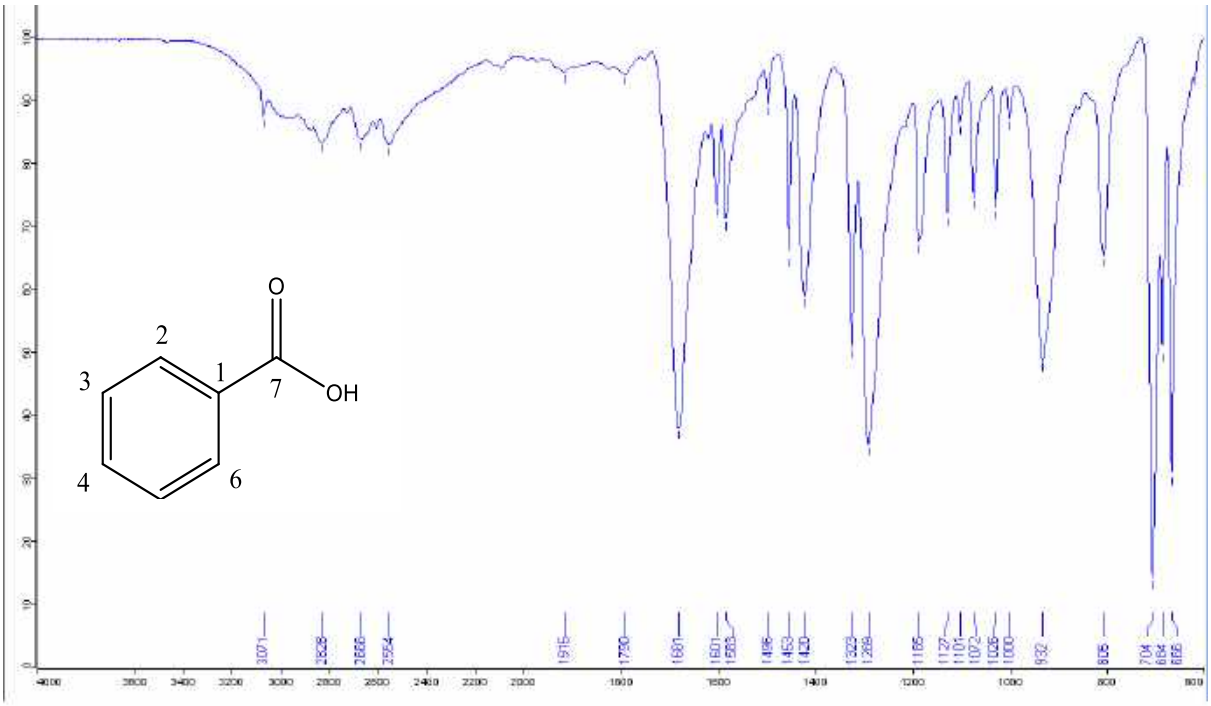

Figure A9: FT-IR Spectrum for Benzoic Acid Bio-converted by a Nitrilase Produced by *Rhodococcus rhodochrous* ATCC BAA-870

APPENDIX B

Table B1: Absorbance (OD_{600}) of *Escherichia coli* Cells Grown in a Bioreactor.

Time (Hours)	*E. coli*	Uninduced NHase *E. coli*	Induced NHase *E. coli*
0	0.326	0.237	0.201
1	0.415	0.356	0.278
2	0.867	0.411	0.336
4	1.512	0.507	0.378
5	2.433	0.698	0.427
6	3.66	0.788	0.519
7	3.89	0.895	0.635
8	4.075	1.156	0.798
9	4.49	1.408	1.174
10	4.602	1.917	1.698
11	4.638	2.457	2.187
12	4.692	2.956	2.724
13	4.704	3.488	3.032
14	4.758	3.73	3.5
15	4.794	4.435	3.985
16	4.86	5.034	4.572
17	-	5.355	5.005
18	-	5.565	5.145
19	-	5.568	5.328
20	-	5.664	5.424
21	-	5.68	5.48
22	-	5.704	5.608
23	-	5.841	5.634
24	-	5.895	5.661

NMR SPECTRA

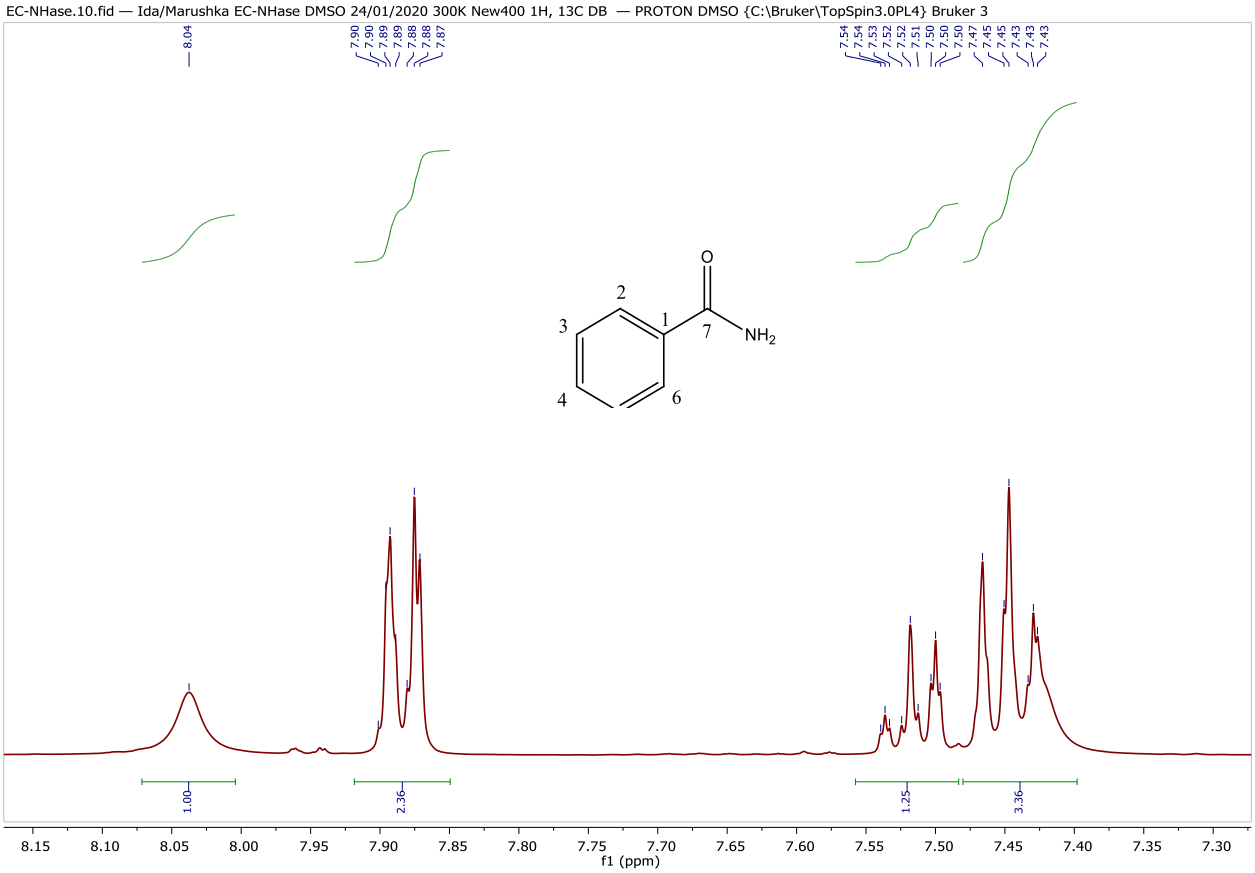

Figure B1: ^{1}H NMR Spectrum for Benzamide Bio-converted by a Nitrile Hydratase.

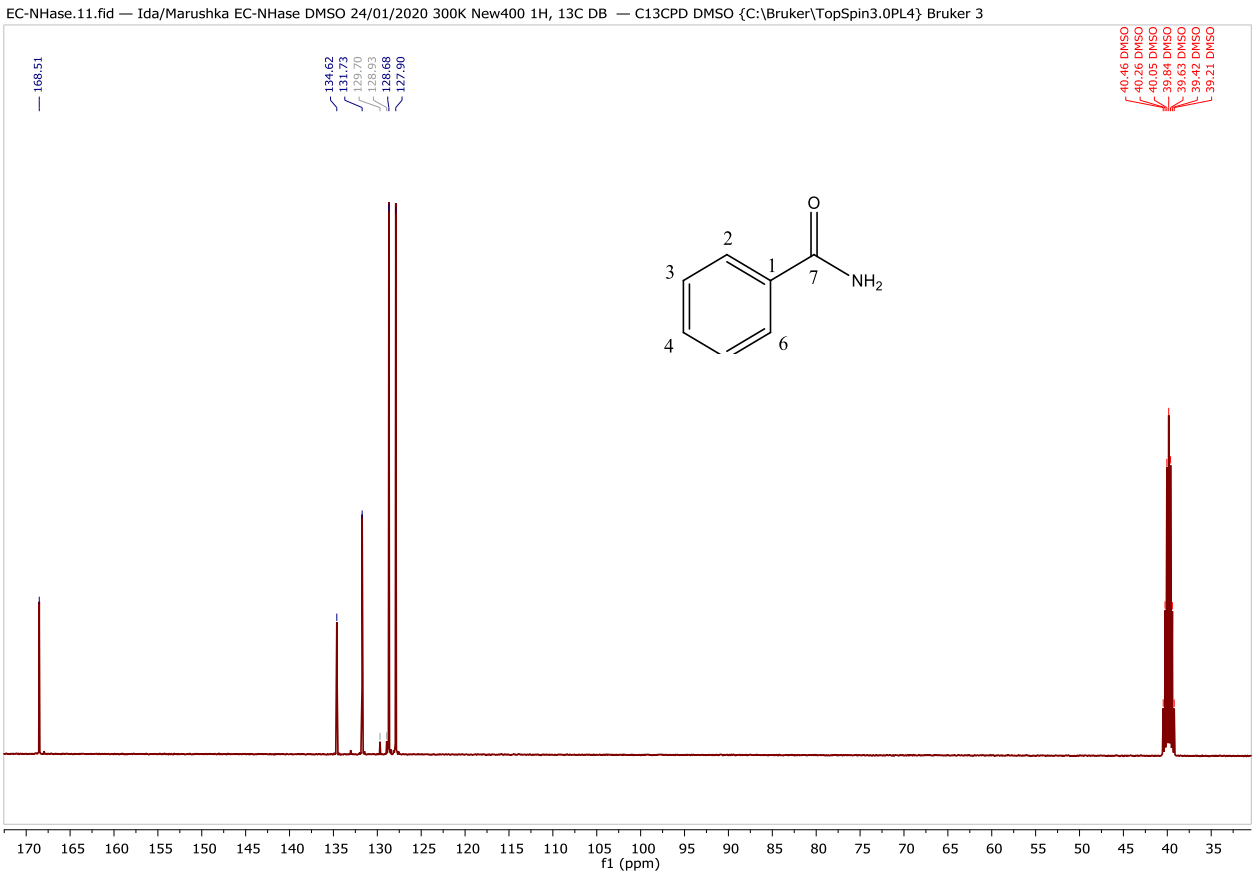

Figure B2: ^{13}C NMR Spectrum for Benzamide Bio-converted by a Nitrile Hydratase.

FT-IR INTERFEROGRAM

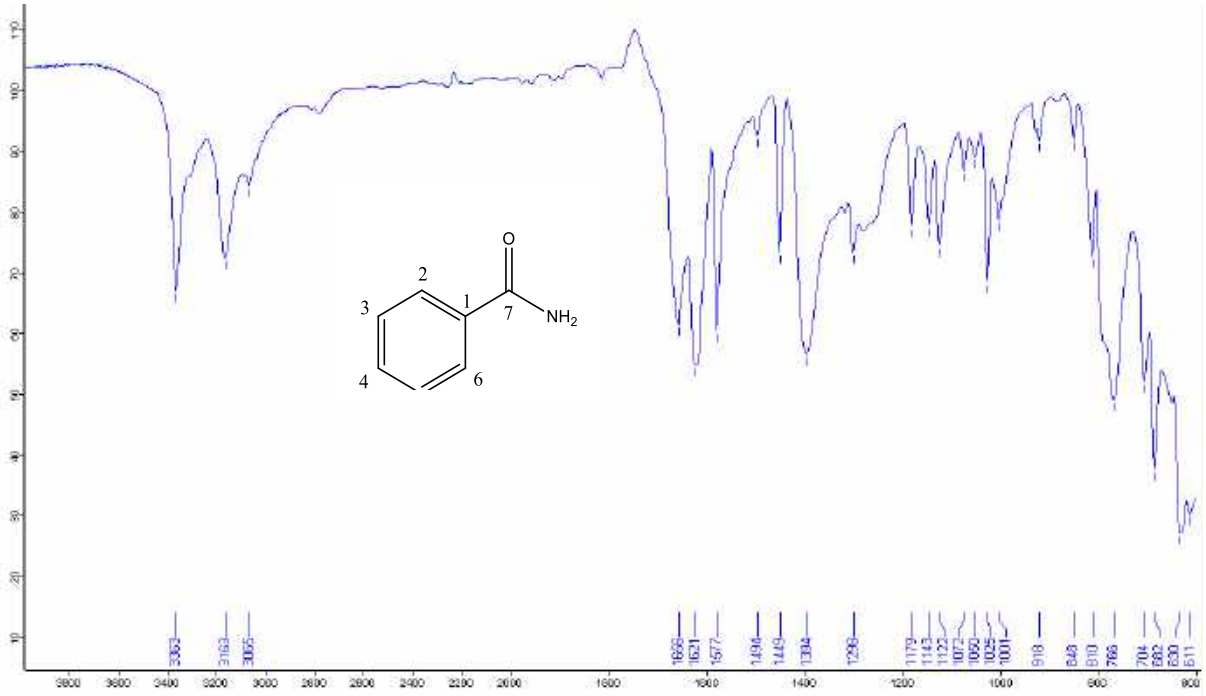

Figure B3: FT-IR Spectrum for Benzamide Bio-converted by a Nitrile Hydratase.

HPLC-MS/MS SPECTRA

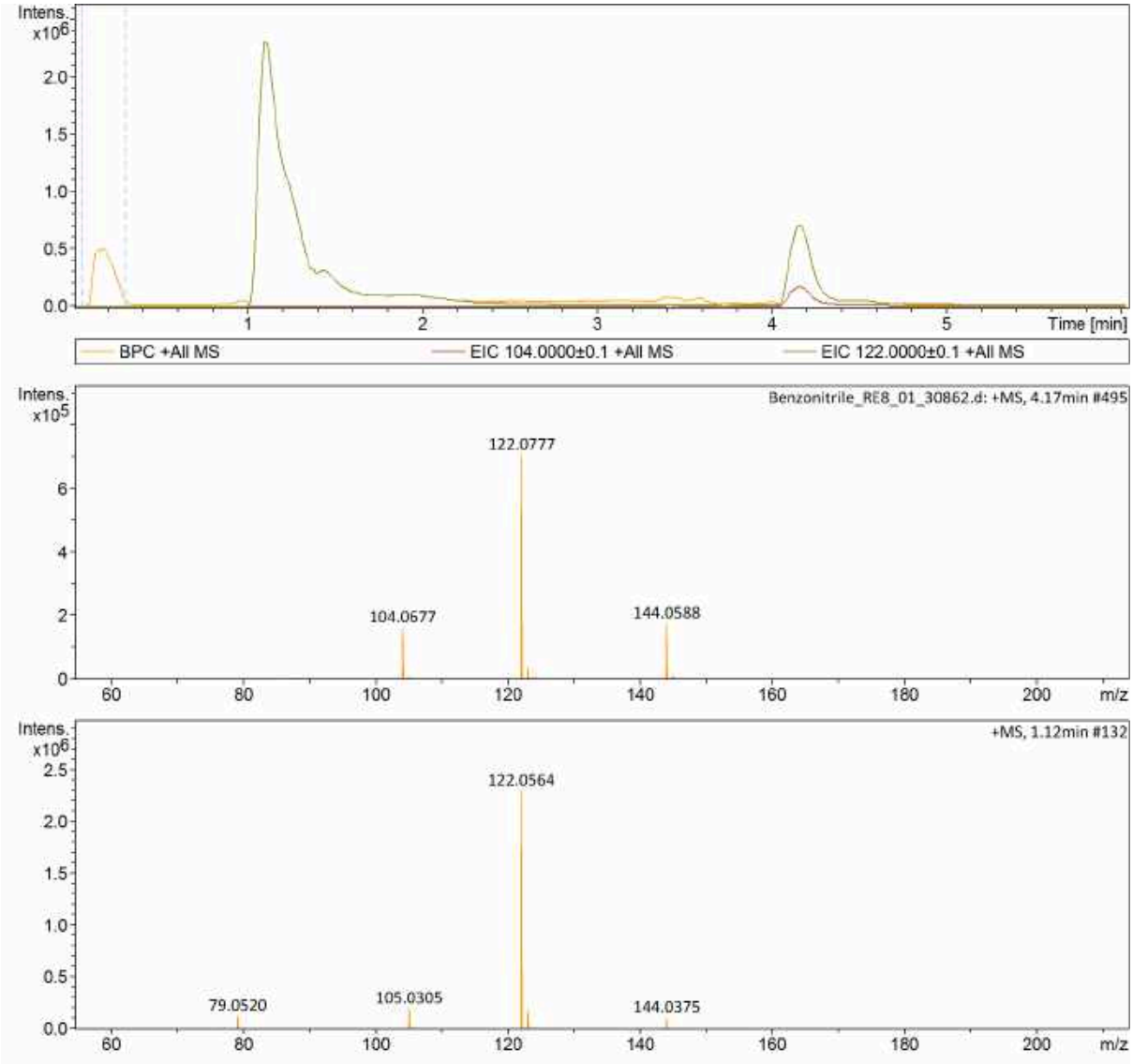

Figure B4: HPLC-MS/MS Spectra for Sample Containing Benzonitrile and Benzamide from a Nitrile Hydratase Enzyme Assay.